HEAT PIPE COOLED INJECTION LANCES - EXPERIMENTAL INVESTIGATION AND MATHEMATICAL MODELING

by

NING JIN

Department of Mining and Metallurgical Engineering
McGill University
Montreal, Canada

August 11, 1997

A Thesis Submitted to the Faculty of Graduate Studies and Research
in Partial Fulfillment of the Requirements
for the Degree of Doctor of Philosophy

Dedicated to my wife, Yanbai Wu, and our daughter, Lisa

ABSTRACT

Heat pipes have been investigated, developed and applied in many industrial fields since their inception in 1964. However, the area of heat pipe technology is still a new topic in the metallurgical industry. This study focused on applying heat pipes as cooling devices to protect injection lances in pyrometallurgical operations.

Even though patents were recently granted for a heat pipe gas injection technique (annular heat pipe gas injection lance or tuyere), a number of problems were encountered when applying the concept in an industrial setting. Some fundamental issues were yet to be explored. Thus, further investigation was needed to address these issues and to provide scientific explanations.

The fundamental study showed that a thermosyphon cannot be used in high temperature applications even in the vertical position because of the uneven coverage of working fluid on the evaporator. It was also shown that a variable-conductance heat pipe cannot work properly for a long period time if the melting point of its working fluid is higher than the environment temperature on the inert gas section. In addition, forced convection cooling of the condenser section provides the possibility of operating the heat pipe at the lowest temperature under various conditions. It was also demonstrated that the superheat in the liquid pool of working fluid can be reduced dramatically by employing a temperature stabilizer in the pool. Finally, a very important discovery arising from this fundamental study is that of the mass balance of working fluid on large scale annular heat pipe cooled injection lances. It has been clearly shown that annular heat pipe cooled injection lances as had been proposed prior to the current study cannot be scaled up without violating the mass balance of working fluid.

A new generation of heat pipe cooled injection lances has been developed based on all the improvements made in this fundamental study. This new generation of heat pipe cooled injection lances is capable of being scaled up for industrial applications without encountering the mass imbalance of working fluid and other problems. Steelmaking, copper converting, and silver refining experiments featuring the heat pipe cooled injection lance in vertical and several inclined positions have been carried out. When compared with

water-cooled lances for oxygen injection, this kind of lance has many advantages such as reduced operating cost, enhanced energy efficiency, greater control and flexibility, and it is safer to operate.

Finally, a mathematical model for this new generation of heat pipe cooled injection lance was formulated and tested.

RESUME

Les caloducs ont été étudiés, développés et utilisés dans de nombreux domaines industriels depuis leur invention en 1964. Cependant, ils restent toujours peu employés dans le domaine de la métallurgie. Il s'agit ici d'étudier la possibilité d'utiliser les caloducs comme moyen de refroidissement pour protéger les lances d'injection dans les opérations pyrométallurgiques.

Bien que des brevets aient été récemment proposés pour une technique d'injection de gaz utilisant les caloducs (lance ou tuyère d'injection de gaz munie d'un caloduc en anneau), de nombreuses barrières se sont présentées lors de l'application industrielle. Quelques points fondamentaux restaient à éclaicir. Ainsi, une étude plus poussée était nécessaire pour permettre une telle utilisation industrielle et pour fournir des explications scientifiques.

L'étude théorique a montré que le syphon thermique ne peut pas être utilisé dans des applications à hautes températures, même en position verticale, et ce à cause d'une couverture non uniforme de l'évaporateur par le fluide utilisé. Il a aussi été montré qu'un caloduc à conductivité variable ne peut pas fonctionner correctement pendant un temps long si la température de fusion du fluide utilisé est supérieure à celle de la section de gaz inerte environnante. De plus, une convection forcée de refroidissement appliquée au condenseur permet d'utiliser la caloduc à une température plus basse dans de nombreuses conditions opératoires. Il a aussi été démontré que le surplus de chaleur dans le réservoir de liquide de refroidissement peut être extrêmement réduit par utilisation d'un stabilisateur de température dans ce réservoir. Enfin, une découverte importante émanant de cette étude fondamentale porte sur le bilan de masse relatif au fluide de refroidissement pour des lances d'injection de grande taille refroidies par des caloducs annulaires. Il a clairement été montré que ce type de lances comme proposées avant la présente étude ne peuvent pas être utilisées pour de grandes tailles tout en respectant le bilan de masse relatif au fluide de refroidissement.

Une nouvelle génération de lances refroidies par caloducs a été developpée à partir des améliorations apportées par cette étude fondamentale. Cette nouvelle génération peut

être réalisée à grande échelle en vue d'utilisations industrielles, tout en respectant le bilan de masse relatif au fluide de refroidissement et en solutionnant les autres problèmes. Des expériences sur la fabrication d'acier, la conversion de cuivre et l'affinage de l'argent ont été réalisées pour caractériser les lances refroidies par caloducs, et ce, en position verticale et pour d'autres inclinaisons. Par comparaison avec des lances à oxygène refroidies par eau, ce type de lance présente de nombreux avantages; réduction des coûts d'opération, augmentation du rendement énergétique, meilleur contrôle, plus grande flexibilité et augmentation la sécurité de travail.

Enfin, un modèle mathématique pour cette nouvelle génération de caloducs a été proposé et testé.

ACKNOWLEDGMENTS

I would like to express my sincere gratitude to my thesis supervisor, Professor Frank Mucciardi, for his guidance, encouragement and support through the whole course of this work. His kind, mature, unique, scientific approach, and hard work have been of themselves an example which I have tried and will emulate in the future.

The pleasant and friendly international environment created by my fellow graduate students along with their knowledge and skills are deeply appreciated. I would like to thank Jonathan Kay, Mahmood Meratian, Musbah Mahfoud, and Thomas Letermann for their assistance and support. Special thanks are due to Walter Greenland, and Martin Knoepfel for their patience and enormous help in the fabrication of heat pipes, and to Robert Paquette for his enormous assistance in conducting the tests. I would also like to thank Arnaud Tronche for translating the abstract to French.

Last, but not least, I would like to express my sincere gratitude to my wife, Yanbai Wu, and our daughter, Lisa, for their love, encouragement, and patience. I am also much indebted to my parents, parents-in-law, and friends for their understanding, and continuous support.

TABLE OF CONTENTS

LIST OF FIGURES

LIST OF TABLES

CHAPTER 1

INTRODUCTION

In the extractive metallurgical industry, oxidation is one of major mechanisms whereby impurities are removed from a melt by oxidizing the impurities into a gaseous phase or into a lighter liquid phase. Thus, oxygen is used extensively in a number of smelting and refining processes in both ferrous and non-ferrous industries. Meanwhile, to achieve proper efficiencies in these processes, oxygen needs to be released or injected either in the melt or close to it by means of lances or tuyeres.

Through the history of the pyrometallurgical industry, the development of oxygen injection lances and tuyeres constitutes a successful metallurgical innovation in that different cooling methods have been implemented to prolong the lives of the lances and tuyeres, to improve the efficiencies of the processes, and to insure the safety of the operations. The present project is primarily concerned with the development and implementation of an alternative yet novel cooling method - heat pipe to protect injection lances and tuyeres used in the pyrometallurgical industry.

Basically, there are three means to introduce oxygen into a melt. They are top-blowing, side-blowing, and bottom-blowing. During the last half century, much attention has been paid to top-blowing lances because of their simplicity in implementation and maintenance, and their safety features. In this project, the focus is on top-blowing injection lances.

Generally, all top-blowing injection lances can be divided into two main categories, consumable lances and non-consumable lances. Consumable lances are also referred to as

non-cooled lances, while non-consumable lances are used to indicate lances which are cooled usually by water or air.

Although both consumable and non-consumable injection lances have been used in a number of smelting and refining processes for quite a few decades, each of them has some drawbacks which have caused some great concerns. The problems associated with consumable lances are high materials cost and unknown operating conditions. On the other hand, the problems associated with water-cooled lances, the most important of non-consumable lances, are related to safety and environmental concerns. Therefore, a new type of top-blowing injection lance that is less costly and safer to operate would be of benefit to the extractive industry.

In this project, the cooling method chosen for protecting top-blowing lances is based on heat pipe technology. Generally, the heat pipe is a device which can transport a large amount of heat energy from one area to another by vaporizing and condensing working fluid in a sealed chamber. It can operate under any orientation by employing capillary, gravitational, or other forces to recycle the working fluid with a very high thermal conductivity without requirement for any external power.

As a cooling device, the heat pipe is very efficient. For instance, when a heat pipe with water as working fluid operates at 100°C, the heat transfer coefficient at the inner surface of the pipe shell can be more than 10,000 W/m^2-°C, the heat flux on the pipe shell can be in excess of 1 MW/m^2, and the equivalent axial thermal conductivity of the heat pipe can be 100 to 1,000 times higher than that of pure copper. Overall, the heat transport capacity of the heat pipe with water as working fluid is comparable to that of a forced convection system with water as the cooling medium.

In the metallurgical industry, the heat pipe as a cooling device not only has great cooling capacity to protect lances and tuyeres, but also has a big advantage over the conventional forced convection method with water as the cooling medium. A heat pipe cooled injection lance is much safer than a conventional water-cooled system because only a small amount of working fluid is used, and depending on the choice of working fluid it may be compatible with the pyrometallurgical environment. Furthermore, heat pipe technology can also be used to protect submerged lances and tuyeres by using forced convection cooling methods thus rendering these equivalent to conventional water-cooled systems.

Although the heat pipe was invented more than three decades ago, little attention was paid to using this technology to protect top-blowing injection lances until the late 1980's. In 1994, a patent was granted to Noranda Inc. for a new method of cooling injection lances and tuyeres based on heat pipe technology. However, satisfactory results

have yet to be attained in plant trials because some fundamental issues are still unexplored, and several key scientific assumptions have yet to be substantiated. Therefore, further study is required to both identify and resolve the issues that to date have impeded the implementation of the heat pipe cooled injection lance.

Thus, the overall aims of this investigation were:

- to identify the problems associated with the patented heat pipe cooled injection lances and tuyeres, and to develop and test possible solutions;
- to improve the performance of the heat pipes, and heat pipe cooled injection lances by applying forced convection cooling on their condensers;
- to investigate the superheats in the liquid pools of gravity-assisted heat pipes, and to develop and test a method which can reduce these superheats significantly;
- to examine patented heat pipe cooled injection lances - annular heat pipes with forced convection applied on the inner pipe, to identify potential problems, and to develop and test possible solutions;
- to design, fabricate, and test a new generation of heat pipe cooled injection lances in different pyrometallurgical processes;
- to formulate and test a mathematical model for the new generation of heat pipe cooled injection lances with empirical data.

To fulfill the above objectives, the present investigation was divided into five parts. A literature review is first presented in Chapter 2. The current status of both oxygen injection technology and heat pipe technology is described. Chapter 3 deals with heat pipe design criteria, and practical considerations.

Problems associated with vertical thermosyphons and gravity-assisted heat pipes are identified and detailed in Chapter 4. Explanations of the phenomena along with possible solutions are presented and discussed in the same chapter. Forced convection cooling applied on the condenser is also presented in Chapter 4. Superheats in the liquid pool of gravity-assisted heat pipes are investigated in Chapter 5. Problems associated with the patented heat pipe cooled injection lances are identified, and some possible solutions are presented and discussed in Chapter 6. The concepts, design considerations, and results of several smelting and converting tests are presented and discussed in Chapter 7.

A mathematical model for simulating the performance of heat pipe cooled injection lances is developed in Chapter 8. The results are evaluated by comparing them to experimental data.

The general conclusions of this research are drawn in Chapter 9. Finally, the statement of originality of this work and the contributions of this thesis to knowledge are outlined.

CHAPTER 2

LITERATURE REVIEW

A literature review of injection technology in metallurgy, top-blowing lancing technology in metallurgy, overall heat pipe technology, and development of heat pipe cooled injection technology is presented in this chapter.

2.1 Injection Technology in Metallurgy

In the extractive metallurgical industry, oxygen has been used extensively in many smelting and refining processes in order to remove impurities. To achieve proper efficiencies in these processes, oxygen needs to be released either in the melt or close to it by means of a piece of pipe which is called a lance or a tuyere depending on the orientation and position of the pipe.

Inevitably, corrosion, erosion, and oxidation occur on the tips and bodies of lances or tuyeres, which in turn lead to the failure of the lances and tuyeres. Corrosion, erosion, and oxidation occur because oxygen, the primary metals, a number of impurities, and the oxide phases all coexist in the vicinity of the lances and tuyeres. Moreover, the lances and tuyeres are exposed to the pyrometallurgical environments which include elevated temperatures typically associated with smelting and refining processes. Therefore, the life of the lances and tuyeres is an important issue in many smelting and refining processes.

Since corrosion, erosion, and oxidation are all temperature dependent, the lower the operating temperatures of lances or tuyeres are, the longer the lives of the lances or tuyeres will be. Therefore, applying cooling to the lances or tuyeres to slow down the reactions of corrosion, erosion, and oxidation is one of the most effective ways to prolong their lives.

In the extractive metallurgical industry, applying cooling to lances and tuyeres has been common practice for a number of decades. Basically, there are four types of injection lances and tuyeres which have been employed in the modern metallurgical industry. They are non-cooled lances and tuyeres, water-cooled lances and tuyeres, shrouded tuyeres and lances, and air-cooled lances and tuyeres. A brief review of each category follows.

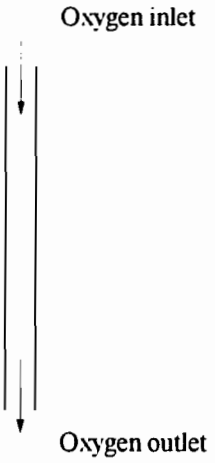

Figure 2.1 Schematic diagram of a non-cooled lance

2.1.1 Non-Cooled Lances and Tuyeres

A non-cooled lance or tuyere, as shown in Figure 2.1, is simply a piece of pipe with no additional cooling applied besides the cooling effect provided by the reagents (air, oxygen enriched air, or oxygen).

The non-cooled lances and tuyeres are the easiest ones to design and fabrication, and often are the safest ones in operation. They are suitable for both non-submerged and submerged operating modes. However, intensive heat and high concentrations of liquid oxides make the operating environment of the unit very severe. The life of this kind of

lance or tuyere is usually short. In some cases, the life is so short that using non-cooled lances and tuyeres is no longer economically or operationally feasible.

Non-cooled lances and tuyeres can be found in all ferrous and non-ferrous industries[1]. However, they are more popular in the non-ferrous industry.

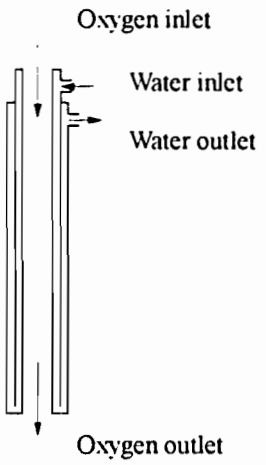

Figure 2.2 Schematic diagram of a water-cooled lance

2.1.2 Water-Cooled Lances and Tuyeres

Water-cooled lances and tuyeres have been used quite extensively because of their unique ability to withstand elevated temperatures. In particular, the combination of water and copper is one of the most effective means of cooling a system. This cooling method has not only been employed to cool the lances and tuyeres, it has also been adopted to cool many of the other facilities in the pyrometallurgical industry.

Basically, the water-cooled lance or tuyere consists of three concentric pipes, as shown in Figure 2.2. The central pipe is for introducing oxygen, the inner annular passage is for the inlet of water, and the outer annular passage is for the outlet of water. The water cools the entire lance or tuyere to protect the tip and body of the lance or tuyere.

Although water-cooling forced convection is one of the most effective means of cooling a system, its cooling capability is still limited. It is still possible for the water-cooled lance or tuyere to be damaged. Given the incompatibility between liquid metals and water, the application of this method is restricted to non-submerged, top-blowing lances. Nonetheless, safety is still the biggest concern for water-cooled, top-blowing lances[2].

Up to now, the single largest implementation of water-cooled lances is in the BOF steelmaking process. Water-cooled lances have made the BOF process viable.

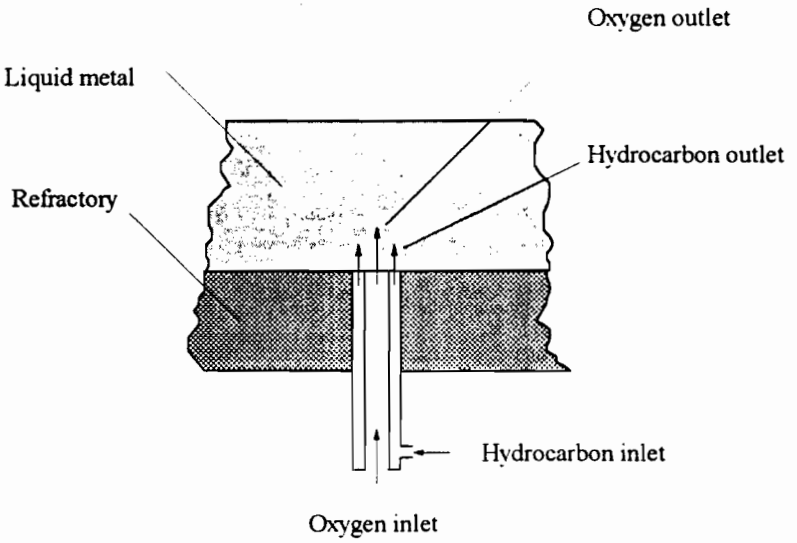

Figure 2.3 Schematic diagram of a shrouded tuyere

2.1.3 Shrouded Tuyeres and Lances

Shrouded tuyeres have permitted the bottom and side injection of oxygen by shrouding the oxygen with a hydrocarbon to protect the adjacent refractory and the tip of the tuyere[3-6].

As shown in Figure 2.3, a shrouded tuyere consists of two concentric pipes. The central pipe is for introducing oxygen, and the annular passage defined by the two pipes is used for blowing a hydrocarbon gas (e.g. natural gas). It was reasoned that by shrouding the skin of the oxygen jet with a hydrocarbon gas which cracks (endothermic reaction) upon entering the melt heat generation in the vicinity of the tuyere is minimized. Moreover, the reducing conditions offered by the dissociated hydrocarbon also minimize the concentration of metal oxides in the vicinity of the tip. This reduces the corrosion of the tip and leads to a longer lifetime. Also, since the oxygen reagent is separated from the molten metal by the hydrocarbon gas, the oxygen travels for some distance from the tip of the tuyere before reacting with the melt. Thus, the tuyere is protected.

Shrouded tuyeres and lances are usually used for submerged oxygen injection

systems. Initially, the idea of shrouded tuyeres was proposed for the steelmaking industry. Shrouded tuyeres have made possible the Q/BOP process of steelmaking. Since then, the concept has been adopted in several non-ferrous smelting and refining processes. Meanwhile, the concept of injecting oxygen by shrouding it with a hydrocarbon has also been used to protect submerged top-blowing lances in several other processes.

2.1.4 Air-Cooled Lances and Tuyeres

Air-cooled lances and tuyeres can be designed in many different ways[7, 8]. One of the best known air-cooled lancing systems is the Sirosmelt lance.

Basically, a Sirosmelt lance consists of one regular pipe or two concentric pipes with helical fins attached on the inner surface of the outer pipe. This kind of lance is claimed non-consumable and constructed of steel pipe. It is mainly used as an immersed top-blowing lance in the smelting of copper sulphide concentrates to elemental copper. By the manner of its operation, the lance is coated by solid slag before immersion into the bath. The solid slag layer protects the steel from attack by the liquid slag top layer.

The development of the Sirosmelt lancing system has been reviewed in a paper which describes the first ten years of Sirosmelt[9]. In 1981, Sirosmelt technology was licensed to the Ausmelt Corp. with a subsequent change in name. So far, the Ausmelt lancing system can only be found in the non-ferrous industry[10].

2.2 Top-Blowing Lancing Technology in Metallurgy

Top-blowing lancing systems with specific emphasis on the BOF process in steelmaking and the Mitsubishi process in coppermaking are reviewed in order to illustrate where and how current top-blowing lancing technology is implemented in the pyrometallurgical industry.

2.2.1 BOF Process in the Steelmaking Industry

The basic oxygen furnace process (BOF/BOP), originally known as LD steelmaking, has been used commercially since the 1950's, because of its low capital cost, low labor cost, high productivity, excellent ability to produce low carbon steels, and relative insensitivity to scrap price and quality. It was the development of large tonnage oxygen, as well as water-cooled top-blowing lances which made the BOF process possible.

The BOF is a cylindrical vessel with its upper portion forming an open top cone

with a taphole in one side above the junction of the barrel and cone. Oxygen is blown from the top using a long water-cooled lance lowered well into the furnace. About 600 m^3 (STP) of high purity oxygen per ton of final product is required within a span of about 20 minutes. Oxygen is blown into the charge at a supersonic speed exceeding Mach 2. Figure 2.4 shows a schematic diagram of a typical BOF furnace.

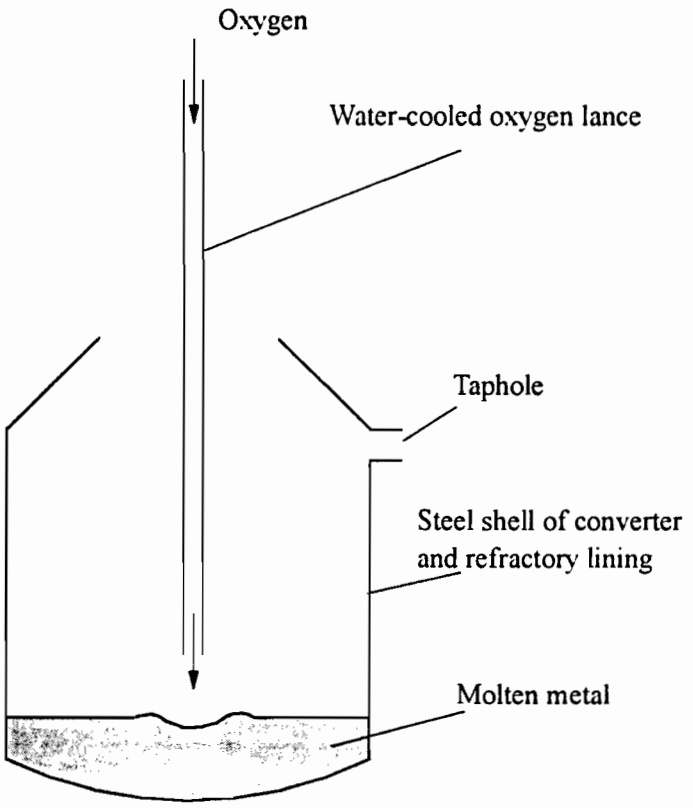

Figure 2.4 Schematic diagram of a BOF furnace

The BOF oxygen injection lance for top blowing, in all likelihood, is the most dominant of lances in both the non-ferrous and the ferrous industries. Its shear size and oxidizing potential, coupled with the extreme thermal conditions under which it operates, make the BOF oxygen lance a strong contender for this distinction.

The vast majority of integrated steelmaking concerns now use the basic oxygen process to produce steel. Of these, many have adopted the top-blowing route (i.e., BOF

lance) for oxygen injection. Because of the extreme temperatures and heat fluxes, it is essential to cool the BOF lance with a relatively large flow rate of water (e.g. 5,000 litres/minute) that is pumped within a cooling jacket. Without the coolant, the lance tip would be destroyed within a matter of seconds. Safety is the most important consideration when using water-cooled lances[1,2]. Leakage of water from a damaged tip can, in some circumstances, result in a serious explosion. In designing such systems, water consumption and treatment are important issues that warrant attention.

2.2.2 Mitsubishi Process in the Coppermaking Industry

In the Mitsubishi continuous copper smelting process, three furnaces are employed in the process design: the S-furnace, the SH-furnace, and the C-furnace. The S-furnace is for smelting in which dried concentrates react with pulverized fluxes, C-slag and coal, and oxygen enriched air. The SH-furnace is for separation in which matte and slag are separated. And the C-furnace is for converting in which copper matte is converted to blister copper[11, 12]. The smelting furnace and the converting furnace are both continuous bath smelting processes. These furnaces are circular in design, and feature a number of non-cooled consumable top-blowing lances, with the lance tips about 50 cm above the bath surface. Figure 2.5 is a schematic diagram of the Mitsubishi continuous smelter.

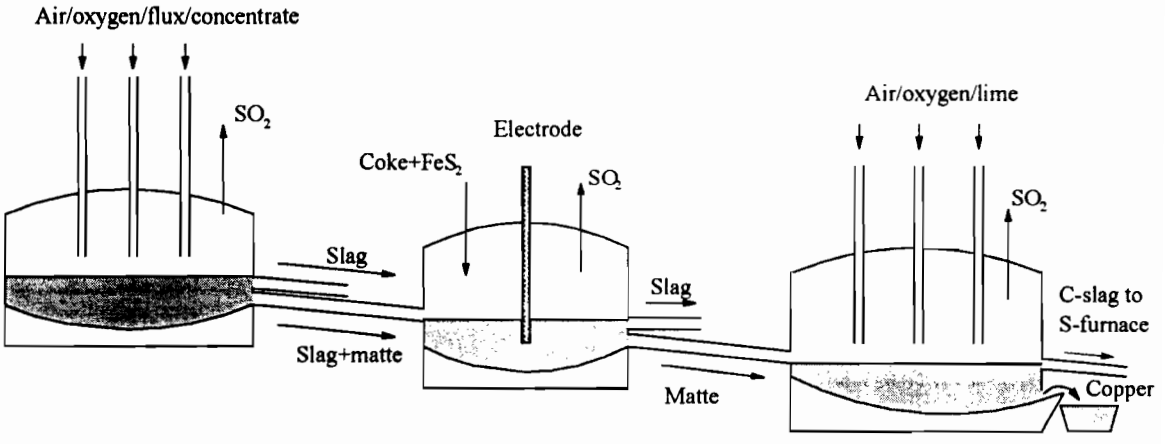

Figure 2.5 Schematic diagram of the Mitsubishi continuous smelter

To get away from the lance material problems as other processes have, the Mitsubishi process was designed initially to use water-cooled, non-submerged lances to blow the air onto the melt. However, because of safety concerns, only consumable, non-submerged, top-blowing lances are employed. Obviously, the lives of these lances are relatively short. Prolonging the lives of the lances has had high priority on the agenda of improving the Mitsubishi process since the process was invented.

Presently, the Mitsubishi process uses stainless steel non-submerged lances to blow oxygen enriched air onto the pool of liquids.

2.3 Heat Pipe Technology

The heat pipe is a device which can transport a large amount of heat energy from one area to another by means of vaporizing and condensing of a working fluid in a sealed chamber. It can operate under any orientation by employing capillary, gravitational, and/or other forces to recycle the working fluid with an effective, overall, very high thermal conductivity without requirement for external power[13-16].

2.3.1 Evolution of Heat Pipes

Of the many different types of heat transport systems, the heat pipe is one of the most efficient heat transport systems known today. While the heat pipe was originally invented in 1944[17], the idea was dormant until it was reinvented in 1964[18]. The initial formulation of the heat pipe concept can be traced to the patents of A.M. Perkins and J. Perkins in the mid-1800's.

The Perkins Tube had been used for over a hundred years as a superconductor of heat energy on steam boilers and other applications since it was invented in 1836 by Jacob Perkins (UK Patent No. 7059). It was a closed tube containing a small quantity of water. The ratio of the amount of water in liquid phase to the capacity of the tube was *x:1800* at operating pressure x bar. The high heat transport ability of the tube was achieved by employing the phase change of water. In a more general sense, the concept of the Perkins Tube is the same as that of a thermosyphon.

The thermosyphon, like a heat pipe is a device which can transport a large amount of heat energy from one point to another by means of vaporizing and condensing of a working fluid in a sealed chamber. It operates with an orientation whereby the heat source section is lower than the heat sink section and thus employs the gravitational forces to

recycle the working fluid. In general, a thermosyphon has a very high thermal conductivity and it does not require any external power to operate.

Typically, a thermosyphon consists of only two components: a container and a working fluid. When heat is introduced to one section which is referred to as the 'evaporator section', the working fluid in that region starts to vaporize. Driven by a pressure differential the vapor moves to a colder section which is referred to as the 'condenser section' and condenses there. The condensed phase of the working fluid flows back by gravity to the evaporator to complete a cycle.

The possible benefits of such a device are great. Because the gas and liquid phases are close to thermodynamic equilibrium within the pipe, the working fluid (comprising both the liquid and gas phases) operates at near isothermal conditions. Heat transfer arises as a result of the relatively small pressure gradient that is established between the heat source section and the heat sink section. The counter current flow of vapor and liquid uses the latent heat of vaporization to perform net heat transfer from the heat source to the heat sink. Since enormous quantities of heat can be transported by a near-isothermal substance across relatively small pressure gradients, a thermosyphon has been termed a 'superconductor' of heat.

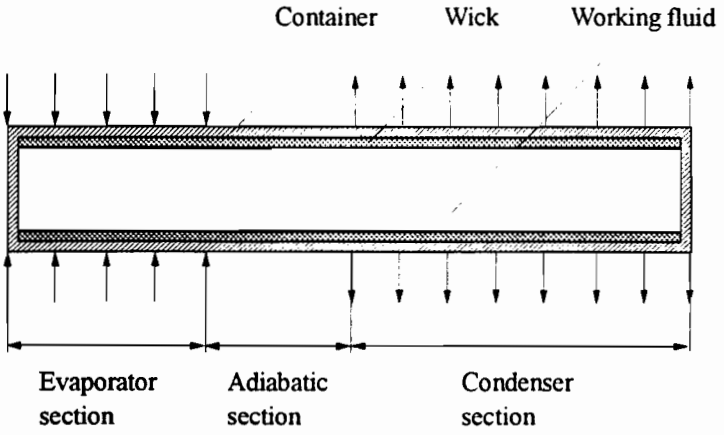

Figure 2.6 Schematic diagram of a basic heat pipe

The concept of the heat pipe was first introduced by Gaugler, an engineer of the General Motors Corporation in the U.S. Patent No 2350348 in 1944. The novelty of this

invention was that it made it possible for a thermosyphon to work under the unusual orientation of the heat source section being higher than the heat sink section without the requirement of any external power. The concept of this invention is to employ capillary forces against the gravitational force to move and recycle the working fluid in the liquid state from a lower heat sink section to a higher heat source section. However, during the time that the patent was valid the idea didn't attract much attention.

In 1963, the heat pipe was reinvented by Grover, a scientist at the Los Alamos National Laboratory in New Mexico, and awarded as U.S. Patent No. 3,229,759. In 1964, Grover, Cotter, and Erickson of Los Alamos National Laboratory described heat transfer experiments with three structures of unique internal construction, which they referred to as a 'heat pipe', as shown in Figure 2.6.

2.3.2 Basic Concept of Heat Pipes

Heat pipes evolved from thermosyphons. Whereas a thermosyphon comprises two components, a heat pipe typically consists of three components: a container, an inner lining porous material, and a working fluid. When heat is introduced to one section which is referred to as the 'evaporator section', the working fluid in that region starts to vaporize. Driven by pressure differential, the vapor moves to a colder section which is referred to as the 'condenser section' and condenses in it. Subsequently, as a result of capillary forces, the gravitational force, and/or other forces, the working fluid flows back to evaporator to complete the cycle.

The ideal gas law in thermodynamics can be used to explain why the vapor can be and should be driven from the evaporator to condenser. The Hagen-Poisuille equation for laminar flow and the Fanning equation for turbulent flow can be used for calculation. In a basic heat pipe, the capillary force is responsible for moving and recycling the working fluid from the condenser to the evaporator.

With the counter current flows of the vapor and liquid, heat pipes can function as passive heat transfer devices.

2.3.3 Heat Transport Limitations of Heat Pipes

Generally, there are five heat transport limitations for heat pipes. They are: capillary limit, viscous limit, sonic limit, entrainment limit, and boiling limit. Considerable progress has been made in the study of these operating limits in last three decades. It is very important to make sure in the design stage that the heat pipe will operate below all the heat transport limits.

Capillary limit

The capillary limit is the highest heat transport rate that can be sustained by the capillary pressure in a heat pipe wick. Higher than that the capillary force is no longer able to pump enough working fluid to cover the entire evaporator. Operating a heat pipe above its capillary limit will result in a dry out region with no working fluid wetting the inner surface. Because no working fluid wetting the surface means no cooling applied on that region, the dry out region on an evaporator tends to be heated up to the heat environment temperature. Thus, the dry out region is often called a hot-spot. For relatively low temperature applications of the heat pipe, a dry out region usually results in a lower than the optimum heat transport ability of the heat pipe. For relatively high temperature applications, a dry out region often results in the disintegration of the pipe shell in a short time. Therefore, heat pipes especially those operating in high temperature environments should operate below the capillary limit.

A capillary limit was proposed by Chun[19] in 1972. Since then, it has become standard text book content[13-16]. Predicting permeability of wick structure is one active area of research[13, 20]. Predicting vapor pressure drop and pressure recovery is another active area[21, 22].

Viscous limit

The viscous limit is the highest heat transport rate that can be sustained in a heat pipe for a specific vapor viscosity at the evaporator end of the heat pipe.

The viscous limit is only important at low temperature. A two dimensional analysis was carried out, and an equation for the viscous limit was worked by Busse[23].

The viscous limit usually governs heat pipes when the system pressure is very low. Within a normal range of operating temperature the viscous limit is not an issue.

Sonic limit

The sonic limit is the highest possible heat transport rate that can be sustained in a heat pipe for a specific vapor temperature at the evaporator end of the heat pipe.

The sonic limit was studied at the early stages of development of heat pipe technology[24, 25]. A compressive analysis of the sonic limit was given by Busse[23]. A simplified frictionless sonic limit was presented by Silverstein[26].

When the sonic limit is attained the heat transport rate is limited for the given temperature (pressure). Usually, hitting the sonic limit does not necessarily mean that the heat pipe will be damaged. In this case, the system pressure of the heat pipe will increase, which will bring the sonic limit up at the same time. The sonic limit is usually hit at the start-up stage.

Entrainment limit

The entrainment limit is the highest possible heat transport rate that the vapor flowing through a heat pipe at a sufficiently high velocity does not cause the entrainment of its counter current flowing liquid. The entrainment limit is often referred to as the counter current flooding limit in a vapor-liquid flow system.

The entrainment limit has its origin in the interfacial interaction between vapor and liquid flows. When the relative velocity between the vapor and liquid is sufficiently large, the interface becomes unstable and the destabilizing effects appear in the form of a wave at the interface. As the velocity increases, the wave action, together with the interfacial shear force, may become sufficient to overcome the liquid surface-tension force, and liquid droplets are thus sheared from the surface and entrained into the vapor by the vapor flow.

The entrainment phenomenon is an early signal of an unstable flow condition that can develop into the highest level of system instability and can be caused even by a very small disturbance or perturbation. This thus leads to the partial or total stoppage of liquid flow or dry out. The phenomenon is generally characterized by the Weber number that compares the vapor inertial force to the liquid surface tension force.

The entrainment limit in heat pipes was presented by Tien and Chung[27] for conventional gravity-assisted and rotating heat pipes. More information about the entrainment limit is available[28, 29].

Boiling limit

The boiling limit is the highest possible heat transport rate that can be sustained in a heat pipe for a specific vapor temperature at the evaporator section of the heat pipe. It is limited by film boiling of working fluid.

Although the boiling limit for liquids is well established[30], the boiling limit for liquid metals has only been studied recently. Two of the available boiling limits for liquid metals were presented by Caswell and Balzhieser[31], and Ratiani and Shekriladze[32].

2.3.4 Types of Heat Pipes

Generally, heat pipes can be classified as basic heat pipes, variable-conductance heat pipes, and rotating heat pipes.

Basic heat pipes

Basic heat pipes refer to heat pipes with the original design, which means that the pipes are cylindrical in shape and horizontal in position[18], and they have three components (pipe shell, wick, and working fluid) and three sections (evaporator, adiabatic, and condenser sections).

Basic heat pipes can work fairly well for most applications. However, when liquid metals are employed as working fluids the heat pipes pose the problem of starting up from a frozen state. This leads to the development of variable-conductance heat pipes.

Gravity-assisted heat pipes

For the terrestrial applications of heat pipes, gravity-assisted heat pipes deviate from basic heat pipes by virtue of their orientations. For any orientation that the evaporator is lower than the condenser, in the other words, that gravity assists the condensed working fluid to returned from the condenser to the evaporator, the heat pipe is referred to as a gravity-assisted heat pipe, as shown in Figure 2.7.

The gravity-assisted wicked heat pipe has become increasingly popular in terrestrial applications because of its high heat-transfer performance and less stringent requirement on the wick structure[33, 37].

Heat-pipe startup characteristics are of interest because the heat-pipe working fluid inventory that forms a pool in the lowest part of the evaporator section behaves differently from the working fluid in basic heat pipes. Slugging of the working fluid is a unique character, which may occur during startup[34]. Great attention has been paid to the heat transportation limits of gravity-assisted heat pipes[35-38], and their applications[39, 40].

Gravity-assisted heat pipes have been used for a variety of terrestrial applications, such as heat recovery, energy conservation, and solar energy utilization.

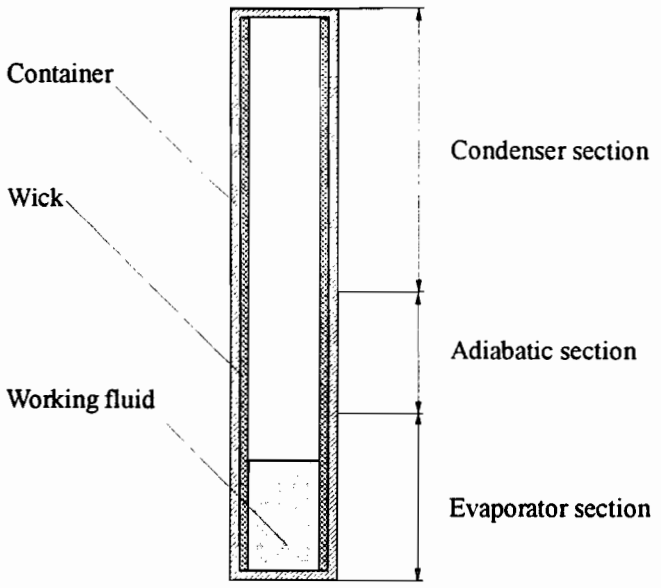

Figure 2.7 Schematic diagram of a gravity-assisted heat pipe

Variable-conductance heat pipes

Variable-conductance heat pipes are the most versatile modification of the basic heat pipe. This type of heat pipe not only has the three sections - evaporator, adiabatic, and condenser sections as the basic heat pipe has, but it also has one more section - the inert gas section. If the volume ratio between the inert gas section and all the other sections is big enough, the variable-conductance heat pipe is capable of maintaining a near constant temperature at the evaporator, adiabatic, and condenser sections, independent of the amount of heat energy being transported by the pipe.

The concept of variable-conductance heat pipe was first examined by Wyatt during experiments on non-condensable gas generation within sodium-stainless steel heat pipes[41]. The schematic of a variable-conductance heat pipe shown in Figure 2.8 is of the passively controlled type.

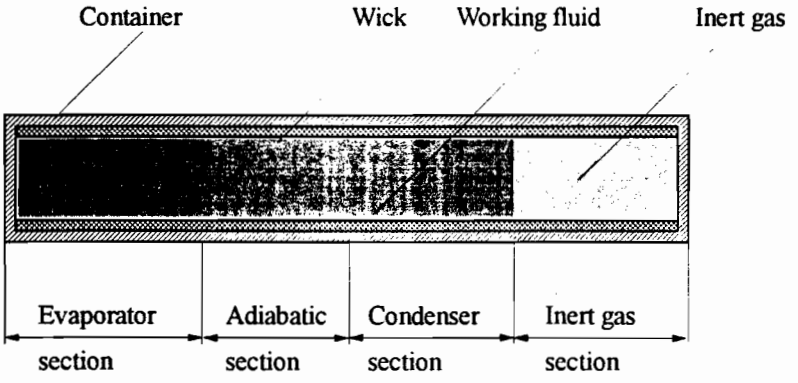

Figure 2.8 Schematic diagram of a variable-conductance heat pipe

Typically, variable-conductance heat pipes are referred to as heat pipes with a modified design. This means that the heat pipes are still cylindrical in shape, but have four components (pipe shell, wick structure, working fluid, and inert gas) and four sections (evaporator, adiabatic, condenser, and inert gas sections). Variable-Conductance Heat Pipes (VCHP) are often referred to as gas-loaded heat pipes or gas buffered heat pipes.

Liquid metal heat pipes have exhibited difficulties starting up from a frozen-state. Inert gas loading is a possible solution to the frozen-state startup problem[42-45].

Rotating heat pipes

The rotating heat pipe, as envisaged by Gray[46], is a two-phase thermosyphon in which the condensate is returned to the evaporator by means of centrifugal force, as shown in Figure 2.9. The rotating heat pipe consists of a sealed hollow shaft, having a slight internal taper along its axial length, and containing a fixed amount of working fluid. The rotating heat pipe, like the basic heat pipe, is divided into three sections: the evaporator, adiabatic, and condenser regions. However, rotation about the axis will cause a centrifugal acceleration with a component along the wall of the pipe. The corresponding force will cause the condensed working fluid to flow along the wall back to the evaporator section.

Polasek reported experiments on cooling an a/c motor incorporating a rotating heat pipe in a hollow shaft[47].

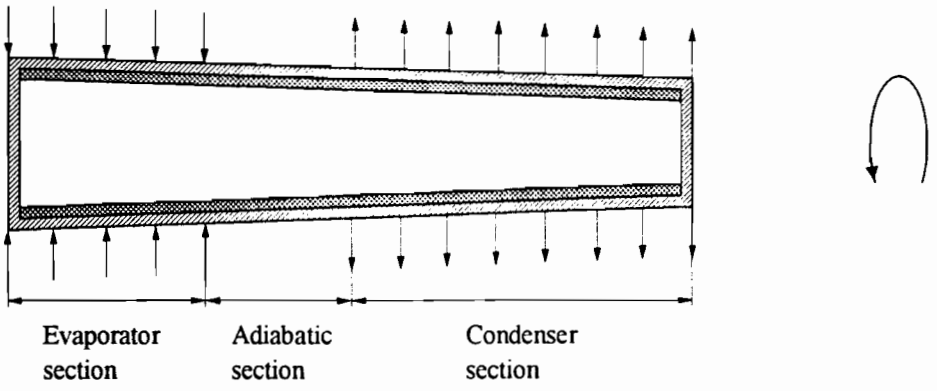

Figure 2.9 Schematic diagram of a rotating heat pipe

2.3.5 Applications of Heat Pipes

Initially, heat pipes were invented for space application in 1964. Shortly there after they were considered for many terrestrial applications because of their unique properties. The applications have increased dramatically since the late 1960's. The following narrative is one way to classify the applications for heat pipes.

Cooling device

As cooling devices heat pipes can provide an isothermal environment for the components needed to be cooled.

As discussed by Veltkamp[48], et. al. an air-cooled sodium heat pipe has been used to cool the Thermionic Energy Converter (TEC). An important advantage of air-cooling as compared to water-cooling was given. Heat pipes are not only used to cool electronic systems[49], they can also be used to remove huge amount of heat energy from a nuclear reactor[50] or other sizable equipment[51-54].

Heat exchanger

Using heat pipes as heat exchangers is another important area. It was reported that several tests had been carried with an unique design of a 15-kW gas-fired liquid-metal heat pipe[55]. Many heat pipe heat exchangers were reviewed by Terpstra and Van Veen[56].

Temperature control

Temperature control is an important aspect of the application of heat pipes, especially for variable conductance heat pipes[57].

As discussed by Ralph and Chaffey a heat pipe was used to control irradiation experiments[58]. Heat pipes can also be employed to provide an appropriate operating temperature to insure the maximum output from the sodium/sulfur battery[59].

Generally, variable conductance heat pipes can provide better control of temperature because the operating temperature does not vary much with the input of heat on the evaporator.

Applications in the metallurgical industry

Given that heat pipes are such effective cooling systems and so many components for pyrometallurgical equipment need to be cooled, the pyrometallurgical industry should be one of those industries which would be involved in the development and implementation of heat pipe technology. Unfortunately, it has not yet happened in the pyrometallurgical industry. Nevertheless, there have been a few reports and proposals on the applications of heat pipe technology in metallurgy.

Heat pipes have been used to alleviate many problems in both plastic injection molding and alloy die-casting[60-62]. Heat pipe core pins can aid in local cooling in injection molding. The heat pipe may be used to even out temperature gradients in the die by inserting it into the main body of the die, without connecting it to water cooling circuits. Probably the most important application is in assisting heat transfer between the die face and the water cooling path in areas where hot spots are likely to occur.

One proposal was made for cooling rolls used in the hot rolling of steel products with heat pipes[63]. Another proposal is for cooling of arc furnace electrodes with heat pipes[64]. Up to now, no further report regarding these two proposals has been published.

One of most important applications of heat pipe technology in the pyro-

metallurgical industry is the cooling of top-blowing lances. This aspect will be discussed in Section 2.4[65].

2.3.6 Mathematical Modeling of Heat Pipes

The wide interest of considering heat pipes for many terrestrial and space applications has stimulated the development of numerous transient heat pipe and steady-state models, which employ a variety of simplifying assumptions. During the last three decades, heat pipe technology has developed significantly. Based on the better understanding of heat pipes, the models describe the real systems more and more accurately which makes the results predicted by the models more and more reliable and useful.

Of the transient analysis models, the one proposed by Cotter was one of the first to study the dynamics of heat pipe startup[66]. One and two-dimensional transient models have been developed over a long period of time[67, 68]. Like the transient analysis models, the steady-state models can be built up based on a variety of simplifying assumptions[69, 70].

Modeling the operation of a heat pipe can be performed at many levels of sophistication. At the highest level are full 2-dimensional models that account for axial and radial diffusion at the gas/vapor interface, as well as natural convection and wall conduction effects. A number of authors have put forward complex numerical and analytical models that account for all of these effects[70-74]. However, in many cases it is not necessary to implement full-blown models that, by their very nature, are time intensive and relatively complex. For initial design calculations and analysis of fluctuations in macroscopic boundary conditions, excellent predictive results may be obtained by using a one-dimensional model[13, 75].

2.4 Development of Heat Pipe Cooled Injection Lancing Technology

This section describes the concepts, designs, experimental work, pilot plant trials, and mathematical modeling that were undertaken by other researches prior to the current research project described in this thesis.

2.4.1 Introduction

The heat pipe cooled injection lance or tuyere was developed by Noranda Inc. in collaboration with McGill University. Prior to this research, a United States Patent was granted to Noranda Inc. for its application of 'self-cooling lance or tuyere' in 1994[65] and

a Canadian Patent in 1996; two Masters theses were completed on investigating and developing this technology at McGill University; and four pilot plant trials were conducted on the Mitsubishi Copper Smelter at Kidd Metallurgical Division, Timmins, Ontario.

Basically, a heat pipe cooled injection lance is an annular heat pipe with the inner pipe serving as a conduit for the oxygen reagent. The advantages of the heat pipe cooled injection lance are effective cooling ability and a reduction in safety concerns.

In reality, the annular heat pipe was first proposed by Faghri in 1986[76], and was called the double-walled concentric heat pipe. The double-walled heat pipe consists of two concentric pipes of unequal diameter attached by means of end caps, creating an annular vapor space between the two pipes. Wick structures are placed on both the inner surface of the outer pipe and the outer surface of the inner pipe. The space inside the inner pipe is open to the surroundings. However, the double-walled concentric heat pipe was only introduced for its diversity of geometry from the basic heat pipe. The advantage of the double-walled concentric heat pipe over the conventional heat pipe, if there is any, is insignificant. Meanwhile, there was not any specific application for it at the time when it was proposed.

2.4.2 Concept

The concept of heat pipe cooled injection technology was clearly described in the abstract of the United State Patent 5,310,166 as follows. 'A self-cooling lance or tuyere for the conveying of gases, liquids or solids into a metallurgical bath comprises a heat pipe or thermosyphon made of two tubular members adapted to be immersed in a furnace environment at one end, such tubular members defining a closed annular chamber there between for containing a working substance (fluid) adapted to evaporate in the region of the heat pipe which is in the furnace environment and flow toward the end which is out of the hot environment where it condenses and flows back to the evaporator region. Means are provided for introducing the gases, liquids or solids to be conveyed into the bath through the inner tubular member of the lance.'

Regardless of the claims in the patent, the key concept is to shroud a consumable lance with a heat pipe, as shown in Figure 2.10. Naturally, this kind of heat pipe cooled injection lance falls into the category of annular heat pipe. Since such a heat pipe cooled injection lance can operate at temperatures much lower than a consumable lance can, the corrosion, erosion, and oxidation that occur on the tip and body of the heat pipe cooled injection lance may be much slower than that of the consumable lance. Thus, the heat pipe cooled injection lance may have longer life than the consumable lance has.

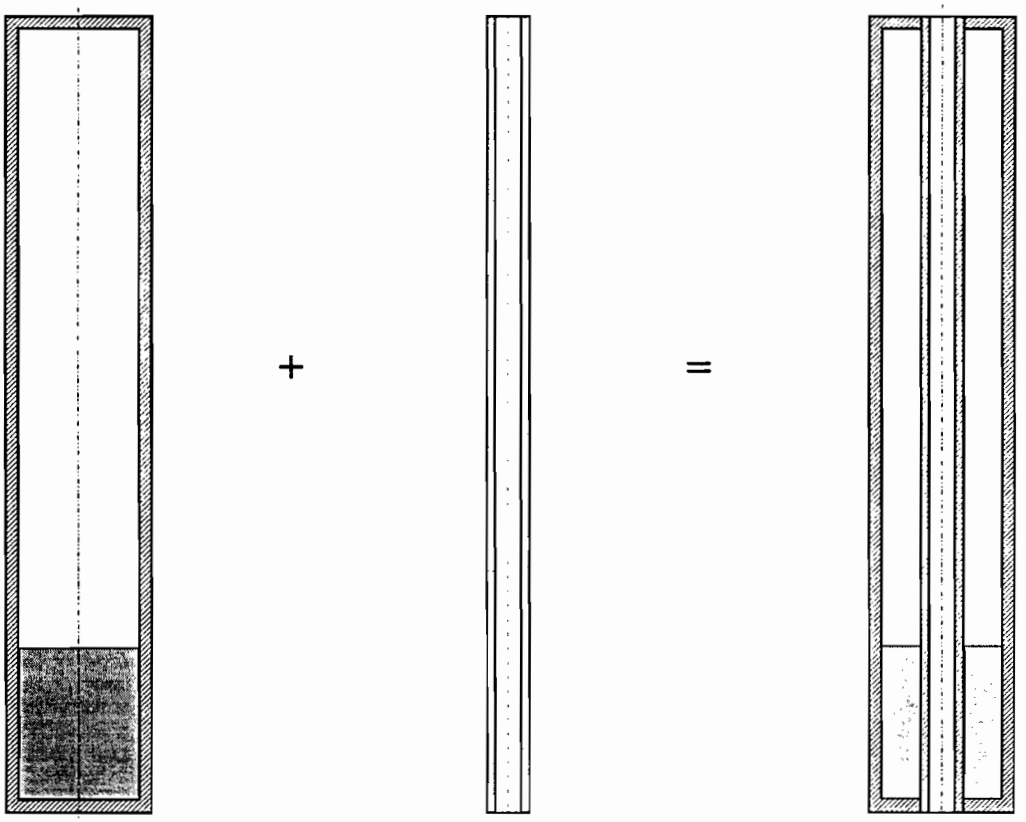

Figure 2.10 The concept of heat pipe cooled injection lances

When compared to a non-consumable cooled lance, the heat pipe cooled injection lance as described in the patent features several advantages. With this invention, it is no longer necessary to pump coolant all the way down to the lance tip. In fact, the conventional cooling circuit is replaced by a circuit based on heat pipe technology for energy extraction. In the annular space of a heat pipe cooled injection lance, the working fluid operates at near isothermal conditions, because the gas and liquid phases of the working fluid are in equilibrium. Heat transport arises as a result of the relatively small pressure gradient that is established between the condenser and the evaporator. The counter current flow of vapor and liquid uses the latent heat of vaporization to perform net heat transfer from the heat source to the heat sink. Since enormous quantities of heat can be transported by a near-isothermal substance across extremely small pressure gradients, the axial thermal conductivity of the heat pipe can be a few orders of magnitude higher than that of the best pure metal.

2.4.3 Design Criteria

Several criteria related to the configuring and operating of heat pipes were used to form the patented idea of cooling top-blowing lances with heat pipe technology. These are described in the following.

The first criterion relates to the configuration of the patented heat pipe cooled injection lance. The patented lance is constructed by fitting a central conduit through a heat pipe to carry the reagent. Thus, it should be called an annular heat pipe cooled injection lance. In an annular heat pipe cooled injection lance of this type, the working fluid is contained within the outer annulus and is recycled by the gravitational force from the condenser to the evaporator while the inner core is hollow and serves as a conduit for the reagent gas, which is pumped down the pipe core.

The second criterion relates to inert gas loading in a heat pipe. Usually, a heat pipe has three zones (an evaporator, a condenser , and an adiabatic zone). However, it is often desirable to have another zone, an inert gas zone. A heat pipe containing inert gas is called a variable-conductance heat pipe. Such heat pipes are considered to have advantages over conventional heat pipes for control under varying operating conditions. The inert gas section operates as a buffer, expanding and contracting in response to the fluctuating pressures caused by varying heat loads. The inert gas remains segregated in the inert gas zone because of the strong convective effect of the migrating vapor and, if applicable, because of the buoyancy of the inert gas relative to that of the working fluid vapor. Based on the analysis mentioned above, the concept of a variable-conductance heat pipe was proposed and used in the patented annular heat pipe cooled injection lances. Thus, the unit should have been called a variable-conductance, annular, heat pipe cooled, injection lance.

The third criterion relates to the cooling method. The initial design of the patented lance was proposed for a vertical top-blowing lance. Due to the fact that the lower part of top-blowing lance was exposed to a high temperature environment, and the higher part of the lance was out of the high temperature environment, gravity was deemed sufficient to return the working fluid from the condenser to the evaporator. Therefore, it was judged unnecessary to employ a wick structure in the lance. Thus, a wick was never used in actual practice. Gravitational force was responsible for recycling the working fluid from the condenser to the evaporator. Based on this fact, the patented variable-conductance annular heat pipe cooled injection lance for top-blowing really was, in fact, a wickless, variable-conductance, annular, heat pipe cooled, injection lance.

The last criterion relates to the cooling method applied on the condenser side. For a high temperature application of this type, only radiation and natural convection were employed in the first generation of the heat pipe cooled injection lance. Thus, a more

accurate description of the patented lance could have been a self-cooled, wickless, variable-conductance, annular, heat pipe cooled, injection lance.

2.4.4 Investigation and Development

Development of self-cooled, wickless, variable-conductance, annular, heat pipe cooled, injection lances started in 1990. Up to 1994, the project consisted of two stages as outlined below.

Experimental investigation

During the first stage, 1990-1991, the concept of the heat pipe injection lance was tested in the laboratory by Botos[77]. A transparent heat pipe was constructed and studied. Subsequently, a self-cooled, wickless, variable-conductance, annular heat pipe with sodium as working substance was fabricated at McGill, and tested at the Noranda Technology Center (NTC). One thing which was noted was that during the tests at NTC the amount of heat transported between the evaporator and condenser of the heat pipe apparently violated the conservation of energy criterion, if one assumed that the evaporator and condenser were uniform in temperature. Obviously, this phenomenon is an indication of an insufficient understanding of the heat pipe and heat pipe cooled injection lance for that particular application. However, due to the time restriction the pilot plant trials got the go ahead without further investigation in the laboratory.

Pilot plant trials

During the second stage, 1991-1994, four pilot plant trials were conducted on the C-furnace of the Mitsubishi process at Kidd Metallurgical Division, Timmins, Ontario.

Peter Botos worked on the first two pilot plant trials. The procedures regarding the design and fabrication, as well as results from those two pilot plant trials and recommendations for further improvement were clearly documented in his thesis.

Two heat pipe cooled injection lances were designed, constructed and tested. Jon Kay worked on the fourth one. It was shown in Jon Kay's study[78] that the type of inert gas used in heat pipe cooled injection lances is an extremely important parameter for the operation of the heat pipe cooled injection lances. Laboratory scale experiments conducted in parallel with the fourth trial were done on a transparent low temperature heat pipe cooled injection lance which employed $C_{10}H_8$ (i.e. naphthalene) as the working fluid and SF_6 (i.e. sulfur hexafluoride) as the inert control gas.

It should be noted that all four heat pipe cooled injection lances used in the pilot plant trials at Kidd Creek were self-cooled, wickless, variable-conductance, annular, heat pipe cooled, injection lances. The working substance in all four cases was sodium.

The following are brief descriptions of the design and fabrication considerations for those pilot plant trial lances, as well as the results from the trials. Problems were identified for each of the lances, and improvements were made after each trial.

In the first trial, nitrogen was used as the inert gas. During the trial, the nozzle was blocked at the very beginning. Therefore, the lance was operated without blowing. To be precise, the first lance worked as an ordinary heat pipe for about 2 days and 7 hours before failing. The problems which were identified after the trial were bad welding quality and damage during shipping. Given the nature of the problems, the second lance was fabricated with professional welding and good packing and handling during shipping[5].

For the second lance, it was basically a copy of the first one but with professional welding and good packing and handling during shipping being emphasized. This time, the lance worked as a lance all the time and lasted for about 7 and one-half days. Based on the observation of a shadow on the condenser of the heat pipe, which was believed to be caused by the inner pipe contacting the outer pipe during the trial, and the observation of the appearance of cracks on the outer surface of the inner pipe after the trial, it was quite convincing that differing thermal stresses between the inner pipe and the outer pipe, as well as within the pipes were responsible for the failure. Given the improvement made on the life of the second lance from 55 hours to 180 hours, to reach the initial goal of 720 hours seemed to be only one more step away, and the only modification which was made to the next lance was to use a bellow to withstand differing expansion between the inner and outer pipes[77].

For the third lance, besides professional welding and good handling during shipping being emphasized, a bellow was applied on the outer pipe to withstand differing expansion between the inner and outer pipes. During the third trial, nothing seemed unusual. The lance worked with blowing, and lasted for about 4 days. During the post-mortem examination of the recovered lance, mainly the condenser part of the lance, it was found that most of the working fluid-sodium was trapped in the inert gas zone in the solid state, which led to a conclusion that the relatively short life of the third lance was caused by not enough working fluid circulating in the evaporator and condenser of the heat pipe. To everyone who was involved in this project, the discovery of most of the working fluid being held in the inert gas zone in solid state explained the early failure of the third lance. For a variable-conductance heat pipe with sodium as the working fluid, the phenomenon of the sodium vapor diffusing into the inert gas zone, and consequently condensing and even solidifying in it was well understood. The unusual aspect for this case was the rate of the diffusion and the fact that solidification happened in the inert gas zone. The phenomenon was studied by Jon Kay on a laboratory scale transparent heat pipe with

different combinations of working fluids and inert gases. The conclusion of that study was that the lighter is the inert gas, the slower the diffusion rate is. Therefore, for the next lance the lightest inert gas, helium, was used as inert gas[78].

In the last trial, professional welding and good handling during shipping were emphasized, a bellow was applied on the outer pipe to withstand differing expansion between the inner and outer pipes, and the lightest inert gas, helium, was employed. Unfortunately, this lance only lasted for about 2 days. This time, the crew was able to recover the entire lance. Prior to this test the evaporator portion had never been recovered. The failure was caused by an elongated hole about 300 mm above the lance nozzle.

2.4.5 Unsolved Problems

Given the modifications that were made on the last three lances, it is obvious that the mechanism behind the failures of all the lances had not been fully understood. Since the operation during those trials was relatively stable and the mechanism that causes the consumption of the consumable lance is understood well, the failures of those four lances were very likely due to the improper design of the heat pipes.

Because conventional heat pipes can usually last at least a few months under similar operating temperatures as the heat pipe cooled injection lances, the potential of this kind of heat pipe cooled injection lance still remains large. Therefore, it is necessary to pursue this project further by examining every aspect of the design. The underlying objective of this study is to enhance our understanding of heat pipes and, in particular, the heat pipe cooled injection lance in an effort to make it a viable metallurgical injection tool.

CHAPTER 3

HEAT PIPE DESIGN CRITERIA AND PRACTICAL CONSIDERATIONS

Heat pipe design criteria, design considerations, fabrication considerations, and operational considerations are presented in this chapter. The theory and techniques used in this project are described. Section 3.1 is devoted to heat pipe design criteria. Sections 3.2, 3.3 and 3.4 are devoted to design, fabrication, and operational considerations, respectively.

3.1 Heat Transport Limitations

The heat pipe is one of the most important heat transport devices that's been invented in the last few decades because of its very high thermal conductance and other unique properties. Since it is a convective heat transfer device, its overall performance is governed and limited by the principles of thermal fluid mechanics. Limitations to axial heat transport in heat pipes are dominated by limits that include the capillary limit, the viscous limit, the sonic limit, the entrainment limit, and the boiling limit. Heat pipes can only operate below all the heat transport limits. Thus, heat pipe technology is based on the full understanding of all these limits.

Figure 3.1 shows all the limitations to the heat transport in a vertical gravity-assisted heat pipe with sodium as the working fluid studied in this project. The heat pipe is

cylindrical in shape, 500 mm long, and 22.10 mm in inner diameter. Two layers of 100 mesh stainless steel screen are employed as wick structure. All the limitations were computed by using Eqs. 3.12, 3.13, 3.14, 3,15, and 3.18, respectively.

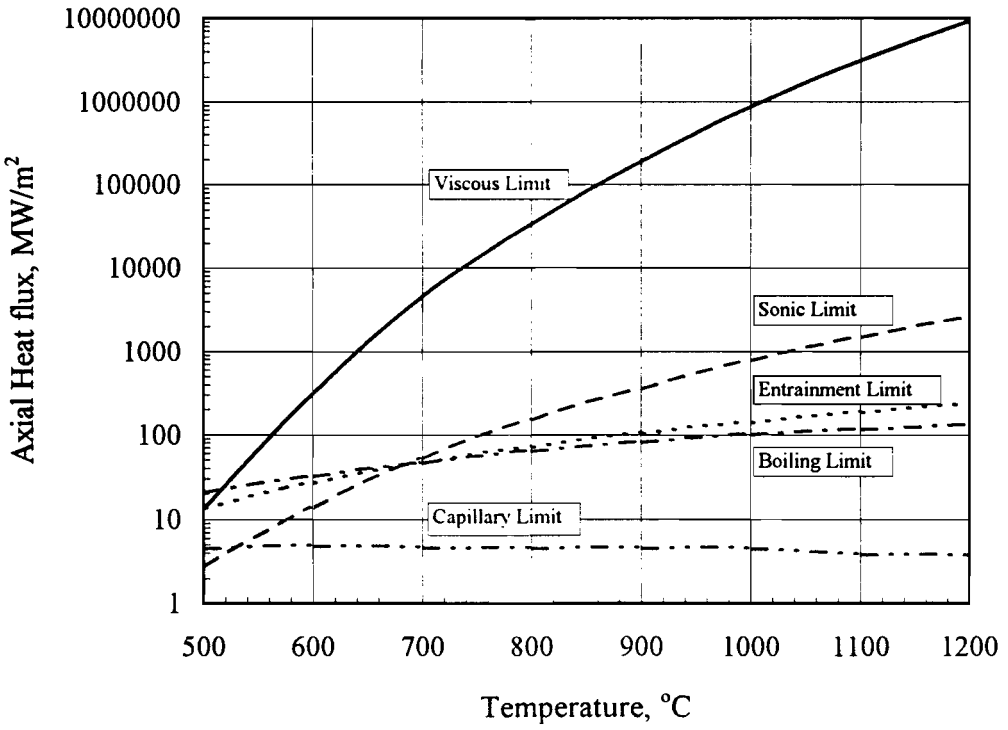

Figure 3.1 Limitations to heat transport in a sodium heat pipe

3.1.1 Capillary Limit[13]

The capillary limit is the highest heat transport rate that can be sustained by the capillary pressure in a heat pipe wick. It means that the maximum capillary pumping head $\Delta P_{cap\ max}$ must be greater than the total pressure drop in the pipe to ensure that the capillary structure can return enough working fluid back to the entire evaporator to keep the pipe operating autogenously.

Generally, the total pressure drop is made up of three components: ΔP_l (the pressure drop caused by the liquid in returning from the condenser to the evaporator), ΔP_v (the pressure drop caused by the vapor in flowing from the evaporator to the condenser), and ΔP_g (the pressure drop caused by gravity).

The capillary limit can be expressed in the following form:

$$\Delta P_{cap\ max} \geq \Delta P_l + \Delta P_g + \Delta P_v \tag{3.1}$$

All the pressure drop components are described in the following sections.

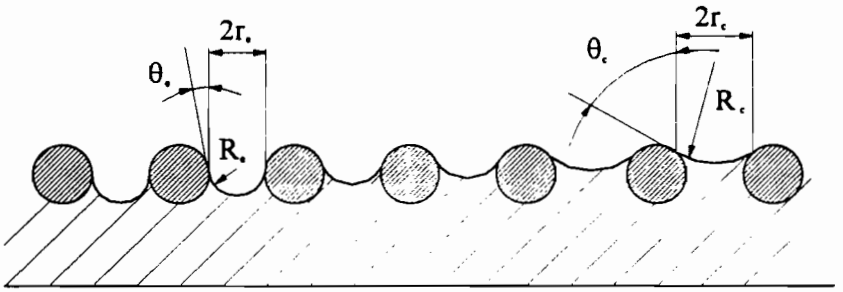

Figure 3.2 Wick and pore parameters in evaporator and condenser

Capillary pressure ΔP_{cap}

The capillary pressure drop across a curved liquid interface is:

$$\Delta P_{cap} = \frac{2\sigma_l}{R} \tag{3.2}$$

where ΔP_{cap} is the capillary pressure drop, σ_l the surface tension of the liquid, and R the radius of curvature of the liquid surface.

For a heat pipe with a screen type of wick as shown in Figure 3.2 the following equation can be derived:

$$R\cos\theta = r \tag{3.3}$$

where R is the radius of curvature of the liquid surface, θ the contact angle, and r the effective radius of the wick pores.

Therefore the capillary head at the evaporator and the condenser can be determined with Eqs. 3.4 and 3.5, respectively.

$$\Delta P_e = 2\sigma_l \frac{\cos\theta_e}{r_e} \tag{3.4}$$

and

$$\Delta P_c = 2\sigma_l \frac{\cos\theta_c}{r_c} \tag{3.5}$$

The resultant capillary head will be

$$\Delta P_{cap} = 2\sigma_l \left(\frac{\cos\theta_e}{r_e} - \frac{\cos\theta_c}{r_c} \right) \tag{3.6}$$

where σ_l is the surface tension of the liquid, θ_e and θ_c the contact angles on the evaporator section and condenser section, and r_e and r_c are the effective radii of the wick pores on the evaporator section and condenser section, respectively. ΔP_{cap} will have a maximum value when $\cos\theta_e$=1 and $\cos\theta_c$=0.

Pressure difference in the liquid phase ΔP_l

Darcy's 'Law' can be used to calculate the pressure difference in the liquid phase as expressed in the following way:

$$\Delta P_l = \frac{\mu_l \, l_{eff} \, \dot{m}}{\rho_l \, K A} \tag{3.7}$$

where μ_l is the dynamic viscosity of liquid, $\dot{m}$ the mass flow rate, ρ_l the density of the liquid, K the wick permeability, A the wick cross-sectional area, and l_{eff} the effective length of a heat pipe which can be described as follows.

$$l_{eff} = l_a + \frac{l_e + l_c}{2} \tag{3.8}$$

where l_a, l_e, and l_c are the lengths of the adiabatic section, the evaporator section, and the condenser section, respectively.

Gravitational head ΔP_g

The pressure difference caused by the gravitational head can be expressed in the following way:

$$\Delta P_g = -\rho_l \, g \, l \, \sin\phi \tag{3.9}$$

where ρ_l is the density of liquid, g the acceleration of gravity, l the length of the heat pipe, and ϕ the angle made by the heat pipe with the horizontal.

Pressure difference in the vapor phase ΔP_v

The total pressure difference in the vapor will be the sum of the pressure drops in the three regions, namely ΔP_{ve}, ΔP_{va}, and ΔP_{vc}. The total vapor pressure drop is given by:

$$\Delta P_v = \rho_v v^2 + \frac{8 \mu_v \dot{m} l_{eff}}{\rho_v \pi r_v^4} \tag{3.10}$$

for laminar flow and no pressure recovery, where v is the velocity of the vapor, and

$$\Delta P_v = \frac{8 \mu_v \dot{m} l_{eff}}{\rho_v \pi r_v^4} \tag{3.11}$$

for laminar flow and full pressure recovery.

Substituting Eqs. 3.6, 3.7, 3.9 and 3.11 into Eq. 3.1, the capillary limit is given for laminar flow and full pressure recovery, and steady state by Eq. 3.12a, and $\dot{Q}_{cap}$ will have a maximum value when $\cos\theta_e = 1$ and $\cos\theta_c = 0$.

$$\dot{Q}_{cap} = \left(2\sigma_l \frac{\cos\theta_e}{r_e} - 2\sigma_l \frac{\cos\theta_c}{r_c} + \rho_l g l \sin\phi \right) \frac{L}{\left(\frac{\mu_l}{\rho_l K A} + \frac{8 \mu_v}{\rho_v \pi r_v^4} \right) l_{eff}} \tag{3.12a}$$

The capillary limit can also be given in following way:

$$\dot{q}_{cap} = \frac{\dot{Q}_{cap}}{A} \tag{3.12b}$$

where $\dot{q}_{cap}$ is the capillary limit (i.e. W/m^2), and A the cross-sectional area of the vapor passage.

It should be noted that the liquid properties do not vary along the pipe and the wick is uniform along the length of the pipe as indicated by Eq. 3.12a.

3.1.2 Viscous Limit[23]

The viscous limit is the highest heat transport rate that can be sustained in a heat pipe for a specific vapor viscosity at the evaporator end of the heat pipe.

The viscous limit is given by Eq. 3.13.

$$\dot{q}_v = \frac{r_v^2 \, L \, \rho_v \, P_v}{16 \, \mu_v \, l_{eff}} \tag{3.13}$$

where $\dot{q}_v$ is the axial viscous limit in kW/m^2, r_v the vapor space radius in m, L the latent heat of vaporization in kJ/kg, ρ_v the density of vapor in kg/m^3, P_v the vapor pressure in N/m^2, μ_v the dynamic viscosity of vapor in kg/m-s, and l_{eff} the effective length of a heat pipe in m.

3.1.3 Sonic Limit[23]

The sonic limit is the highest possible heat transport rate that can be sustained in a heat pipe for a specific vapor temperature at the evaporator end of the heat pipe. It is temperature dependent.

The sonic limit is given by:

$$\dot{q}_s = 0.474 \, L \left(\rho_v P_v \right)^{\frac{1}{2}} \tag{3.14}$$

where $\dot{q}_s$ is the axial sonic limit in kW/m^2, L the latent heat of vaporization in kJ/kg, ρ_v the density of the vapor in kg/m^3, and P_v the axial pressure at the sonic limit in N/m^2.

3.1.4 Entrainment Limit[14]

The entrainment limit is the highest possible heat transport rate that the vapor flowing through a heat pipe at a sufficiently high velocity does not cause the entrainment of its counter-current flowing liquid. The entrainment limit is given by Eq. 3.15.

$$\dot{q}_e = \phi_e \sqrt{\frac{2\pi}{\Omega_e \lambda_w} (1 + z_e)} \tag{3.15}$$

where $\dot{q}_e$ the axial heat flux at the entrainment limit in W/m^2, ϕ_e in micron$^{1/2}$-W/m^2, Ω_e the momentum factor which depends on whether the vapor flow exiting the evaporator is laminar or turbulent (laminar: $\pi^2/8$, turbulent: 2.2), and λ_w is the characteristic dimension which can be identified for the capillary structure of heat pipe wick in microns (25.4×10^3/number of mesh). The parameters ϕ_e and z_e in Eq. 3.15 are given by:

$$\phi_e = 1.636 \times 10^6 \; A_e \left(\frac{P_v}{6895} \right)^{n_e} \tag{3.16}$$

where ϕ_e is in micron$^{1/2}$-W/m^2, and P_v in N/m^2, and

$$z_e = \frac{\lambda_w(n+\cos\theta)\rho_l g D_v}{2\pi\sigma} \tag{3.17}$$

where the values of the power law constants in Eq. 3.16 are given in Table 3.1 for some heat pipe working fluids.

In general, z_e may be considered as negligible unless the screen wick is very coarse.

Table 3.1 Power law constants for entrainment limit parameter ϕ_e

Fluid	Ammonia	Water	Sodium	Lithium
A_e	64.18	87.28	140.8	506.4
a_e	0.306	0.400	0.384	0.383

3.1.5 Boiling Limit[31]

The boiling limit is the highest possible heat transport rate that can be sustained in a heat pipe for a specific vapor temperature at the evaporator section of the heat pipe. It is limited by film boiling of working fluid.

The Boiling Limit is given by:

$$\dot{q}_b = 1.02\times10^{-6}\left[\frac{\rho_l-\rho_v}{\rho_v}\right]^{0.65}\frac{L^2\rho_v\,\mathrm{Pr}^{0.71}}{C_p\sigma} \tag{3.18}$$

where $\dot{q}_b$ is the surface heat flux at the boiling limit in kW/m^2, ρ_l the density of the liquid in kg/m^3, ρ_v the density of the vapor in kg/m^3, L the latent heat of vaporization in kJ/kg, k the liquid thermal conductivity in W/m-°C, Pr the Prandtl number of the liquid, C_p the heat capacity of the liquid in kJ/kg-°C, and σ the surface tension of the liquid in N/m.

3.2 Heat Pipe Design Considerations

The heat pipe design usually gives consideration to the following aspects: working fluid, container material, wick materials and structures, and heat transport limits. Each of these aspects is described in subsequent sections.

Table 3.2 Heat pipe working fluids

Medium	Melting point (°C)	Boiling point at atm pressure (°C)	Useful range (°C)
Helium	-271	-261	-271 to -269
Nitrogen	-210	-196	-203 to -160
Ammonia	-78	-33	-60 to 100
Pentane	-130	28	-20 to 120
Acetone	-95	57	0 to 120
Methanol	-98	64	10 to 130
Flutec PP2	-50	76	10 to 160
Ethanol	-112	78	0 to 130
Heptane	-90	98	0 to 150
Water	0	100	30 to 200
Toluene	-95	110	50 to 200
Flutec PP9	-70	160	0 to 220
Thermex	12	257	150 to 350
Mercury	-39	361	250 to 650
Cesium	29	670	450 to 900
Potassium	64	774	500 to 1000
Sodium	98	883	600 to 1200
Lithium	181	1347	1000 to 1800
Silver	960	2212	1800 to 2300

3.2.1 Working Fluid

The working fluid should satisfy as many of the following criteria as possible. The best suitable one may be chosen for a given system.

1. Chemical compatibility with wick and wall materials;
2. Good thermal stability;
3. Wettability of wick and wall materials;
4. Vapor pressures not too high or low over the operating temperature range;
5. High latent heat of vaporization;
6. High thermal conductivity;
7. Low liquid and vapor viscosities;
8. High surface tension;
9. Acceptable freezing or pour point.

Almost any fluid that satisfies the above criteria may be used as working fluid in a conventional heat pipe. The most useful working fluids are listed in Table 3.2. In this research, sodium, potassium, and water were chosen respectively as working fluids for a number of heat pipes and heat pipe injection lances.

Table 3.3 Recommended heat pipe wall and wick materials

Working fluids	Recommended Materials
Ammonia	Aluminum, Carbon, Nickel, Stainless Steel
Acetone	Copper
Methanol	Copper, Stainless steel
Water	Copper, Monel
Mercury	Stainless steel
Potassium	Nickel, Stainless steel, Inconel, Titanium,
Sodium	Stainless steel, Nickel, Inconel 800, Haynes
Lithium	Niobium-1% zirconium, Molybdenum, TZM
Silver	Tungsten-26% rhenium

3.2.2 Container Materials

Generally, the container materials should satisfy as many of the following criteria as possible. The best suitable one may be chosen for a given system.

1. Compatibility (with the working fluid);
2. Compatibility (with the reagent);
3. Compatibility (with the external environment);
4. High strength to weight ratio;
5. High thermal conductivity;
6. Ease of fabrication, including weldability, machinability, ductility;
7. Low porosity;
8. Wettability by the working fluid.

The container materials have to be compatible with the working fluid. The most useful container materials are listed in Table 3.3.

In this project, stainless steel SS-304, SS-316L, and Nickel-200 were chosen as the container materials.

Table 3.4 Wick structures

Wick Structure	Type of Wick
Single Wick	woven mesh screen, sintered metal powder, sintered metal fibers, groove
Combined Wick	two woven mesh screens, groove covered with one woven mesh screen
Artery Wick	one artery wick, two artery wick

3.2.3 Wick Materials and Structures

Generally, the wick materials and structures should satisfy as many of the following criteria as possible.

1. Compatibility with working fluid;
2. High thermal conductivity;
3. High porosity;
4. Wettability by the working fluid.

The wick can be made of the same material as that of the container. Some of them are given in Table 3.3.

Many wick structures have been suggested in the literature. The most available wick structures are listed in Table 3.4.

In this project, the wick structure is single wick, the type of wick is woven mesh screen, and the materials of the wick are SS-304 and SS-316.

3.2.4 Heat Transport Limits

All the heat transport limits have to be calculated once all the three components and dimensions of a heat pipe have been initially sized. This part of the design may need to be modified if the calculations show that the actual heat transport rate for the pipe will exceed one or more of the limits. In the end, the final design must ensure that the actual heat transport rate is less than all the limits. The equations which are used to evaluate the limits are denoted as Eqs. 3.12, 3.13, 3.14, 3.15, and 3.18.

3.2.5 Sample Design Procedure

An oxygen injection lance is required for laboratory steelmaking experiments, and the heat pipe is chosen as an external cooling method to protect the lance. The oxygen passage is a tube surrounded by the heat pipe with 6.35 mm O.D. × 0.889 mm wall thickness. The initial dimensions for the heat pipe container are 25.4 mm O.D. with 1.65 mm wall thickness and 500 mm long. The size of the evaporator is about 76.2 mm. About 1000 W needs to be dissipated by the heat pipe. The operating temperature of the heat pipe is 600°C. The following is a sample design procedure.

Selection of materials and working fluid

The criteria of selecting wick and container materials were already discussed in this chapter. Sodium is chosen as the working fluid. Stainless steel 316L is chosen for the container, and wick material.

The actual axial heat flux for the heat pipe at 600°C with the given dimensions is 2.842 MW/m^2. The limitations on heat transport are examined as follows.

Heat transport limits

The limits are given in Table 3.5 for 600°C operating temperature. The limits for the range 500°C-1200°C are given in Figure 3.1.

Because all the limits are above the actual axial heat flux, there is no need to make any modification to the original design.

There is no need to calculate the capillary limit, because it is a gravity-assisted heat pipe. The wick may still be useful for redistributing the working fluid driven down by gravity from the condenser section to evaporator section.

Table 3.5: Heat transport limits for the sample design at 600°C.

Names	Limits, MW/m^2	References
Capillary Limit	4.57	Eq. 3.12
Viscous Limit	319.00	Eq. 3.13
Sonic Limit	13.60	Eq. 3.14
Entrainment Limit	26.60	Eq. 3.15
Boiling Limit	31.80	Eq. 3.18

3.3 Heat Pipe Fabrication

The overall process of fabricating a heat pipe cooled injection lance includes preheating, cleaning, assembling, charging, conditioning, sealing, final testing, and coating for some cases. Given that this is a novel application, many of procedures had to be developed specifically for this project. Any mistake can lead to a failure of the heat pipe or a shortening of its life.

3.3.1 Preheating

Preheating is a procedure in which the materials of the container and wick are treated under a condition similar to that which the heat pipe will encounter in actual use. The purpose of this procedure is to reduce internal stresses and to increase wetting capability. This procedure is important when container and wick are make of metallic materials.

3.3.2 Cleaning

Cleaning is a procedure in which the materials of the container and wick are cleaned by following a sequence of steps in order to eliminate any foreign substance and to avoid contaminating the working fluid which may change the properties of the heat pipe shell, the wick, and the working fluid. It is a necessary procedure for all heat pipes.

For the heat pipes with stainless steel as container material and liquid metals as working fluids a procedure is described in reference 11. For the heat pipes with copper as container and wick material, and water as working fluid a procedure is described in reference 12.

3.3.3 Assembly

Assembly of the heat pipe is a procedure in which all parts are assembled into the final product. Usually, spot welding, arc welding and some other welding methods need to be used. Particular attention has to be paid to the different expansion and thermal stresses especially when stainless steel is chosen as the container material.

A most difficult and also most important stage in the assembly procedure is to insert and fix the wick in place. For a cylindrical system, the following procedures are very important:

1. maintain the integrity of the wick;
2. leave the gap between the inner surface and the wick and between different layers as small as possible;
3. use spot welding machine or spring to fix the wick.

3.3.4 Charging

Charging is a procedure in which the working fluid is put into the pipe by following safety procedures for the working fluid without contaminating it. The working fluid can be charged in solid or liquid states. Safety should be a great concern in this procedure when alkali metals are employed.

3.3.5 Conditioning

Conditioning is a procedure in which the heat pipe is operated under a condition similar to one it will ultimately encounter in actual trials. The purpose of conditioning is to allow any reactions between the working fluid and pipe to occur and to evacuate the heat pipe of any extraneous inert gases and gaseous reaction products. For high temperature heat pipes this procedure may take at least several hours. When this procedure is completed the connections between the pipe and the environment have to be cut off while maintaining an evacuated state.

3.3.6 Sealing

Sealing of the heat pipe is a procedure in which the pipe is sealed either permanently or temporarily. Obviously, for permanent sealing the quality of the seal is extremely important. Welding is typically employed for permanent sealing.

In this project, permanent sealing was applied to the liquid metal heat pipe and the heat pipe cooled injection lances, and temporary sealing was applied to the water heat pipe.

3.3.7 Final Testing

Final testing is a procedure in which the heat pipe is operated under a condition similar to that which the heat pipe is going to be exposed. Abnormal operation during the test is usually indicative of a problem in the sealing procedure or otherwise. It may require that one repeat the procedures from 3.3.5 to 3.3.7.

3.3.8 Coating

Coating is the final procedure on the list. It entails coating the evaporator of the pipe with materials which are compatible with the external environment by CVD, PVD or some other method. This is not essential but may be carried out to reduce wear of the pipe body.

3.4 Heat Pipe Operational Considerations

The operations of heat pipes can be classified into two categories: unsteady-state operation (start-up) and steady-state operation.

3.4.1 Unsteady-State Operation

Transient or start-up operation is an important stage. Any improper implementation can cause a problem or even destroy the pipe. The improper implementation refers to the following operation for those heat pipes when alkali metals are employed as working fluids: the pipe is heated up too slowly or too quickly. When the pipe is heated up too slowly, the working fluid will tend to freeze on the condenser instead of flowing back to the evaporator. When the pipe is heated up too quickly, the pipe will hit one or more heat transfer limits.

3.4.2 Steady-State Operation

Steady-state is the operating state in which the pipe spends the majority of its time. Most types of heat pipes are capable of running for quite a long period of time at the designed operating temperature.

CHAPTER 4

EXPERIMENTAL INVESTIGATION OF GRAVITY-ASSISTED HEAT PIPES

The investigation of the phenomena of hot-spot, and working fluid freeze up in the inert gas zone of the wickless, variable-conductance, gravity-assisted, heat pipe is presented in Sections 4.1 and 4.2, respectively. Operating temperature control of the vertical gravity-assisted heat pipes is presented in Section 4.3.

4.1 Wickless Heat Pipes (Thermosyphons)

Thermosyphons are often called wickless heat pipes. A thermosyphon can only operate for the positions that the evaporator section is below the condenser section. Theoretically, it is redundant to implement a wick structure in a vertical gravity-assisted heat pipe, on which the evaporator section is below the condenser section, because the gravitational force can play the role of moving the working fluid from the condenser section to the evaporator section as the capillary force does in basic heat pipes. However, this statement is valid if in the thermosyphon, the working fluid flows down uniformly along the inner wall of the pipe from the condenser section to the evaporator section.

Based on the assumption of the working fluid flowing down uniformly from the condenser section to the evaporator section, all the heat pipe cooled injection lances tested in the early stages prior to this study were really thermosyphon (wickless heat pipe) cooled

injection lances. As mentioned in Section 2.4, the failure of at least one of those heat pipe cooled injection lances did not occur at the hottest place - lance tip. This leads to a suspicion of the assumption.

In this study, the assumption of the working fluid flowing down on the inner wall of the pipe from the condenser section to the evaporator section as a uniform film was questioned first. The concept was re-examined

4.1.1 Phenomenon of Hot-Spots

To carry out the study a wickless, variable-conductance, gravity-assisted, heat pipe was designed, fabricated, and tested. 20 grams of sodium were used as the working fluid in the heat pipe. The heat pipe was cylindrical in shape. The pipe shell was a piece of 304 stainless steel tube 1000 mm long with 25.4 mm O.D. and 1.65 mm wall thickness. Both end caps were also made of 304 stainless steel. One thermocouple was positioned in contact with the inner surface of the end cap in the evaporator section of the heat pipe. A pressure transducer was connected to the heat pipe, and the initial pressure in the heat pipe was about 0.01 atm.

A series of tests were carried out in an electric resistance furnace to examine the performance of the heat pipe in the vertical position. The furnace temperature was fixed at about 850°C. The length of the evaporator section was 300 mm, the length of the condenser was about 400 mm, and the length of the adiabatic section was negligible. The temperature on the condenser section was around 600°C. The heat pipe was considered to be working well based on the information provided by the thermocouple and the pressure transducer, and the visual observation of the uniformity in temperature on the condenser section.

There was one specific test which made the tests change direction. It is the one when the heat pipe was taken out during its normal operation - a hot-spot on the evaporator section was clearly observed, as shown in Figure 4.1. Figure 4.1 is a snap shot taken a few seconds after the heat pipe was pulled out from the furnace and when the heat pipe was operating at steady-state. It shows the heat pipe and the furnace used as the heat source. The hot-spot was on the lower part of the heat pipe. It stretched out over most of the length of the evaporator section but did not appear on the lowest section of the evaporator, where the thermocouple was located. This explained why the hot-spot phenomenon was not picked up earlier. Since the heat pipe operated at about 600°C, the visible color associated with this temperature cannot be easily seen during daytime. However, the color associated with 850°C can, thus, the contrast between the hot-spot and the normal evaporator section is big enough to show the location and the shape of the

hot-spot on the evaporator section. Thus, the hot-spots on the wickless heat pipes were first identified experimentally.

Obviously, hot-spots on any heat pipe are not acceptable whatsoever, especially on high temperature heat pipes. The next step was to determine what caused the hot-spots to form.

Figure 4.1 Hot-spot on the wall of a thermosyphon

4.1.2 Mechanism of Formation of Hot-Spots

Hot-spot is not a new terminology in the heat pipe field. The hot-spot is a well known problem during the starting up from a frozen-state for basic heat pipes with liquid metals as the working fluids. Lack of working fluid to cover the entire evaporator section is the reason for the generation of hot-spots. However, during steady-state a basic heat pipe usually does not encounter the hot-spot problem.

As mentioned above, the hot-spots were observed during steady-state on a

wickless gravity-assisted heat pipe. Based on the definitions of the basic heat pipe and the wickless gravity-assisted heat pipe, the differences between the two is the wick structure. The fundamental difference is that the basic heat pipe relies on the capillary force to recycle the working fluid, but the wickless, gravity-assisted, heat pipe relies on the gravitational force to recycle the working fluid. Obviously, somehow the gravitational force is not enough for the wickless unit. In this case it is not the lack of the working fluid on the evaporator section because it is at steady-state. The question is about how to evenly redistribute the working fluid over the entire evaporator section. It is in this framework that the gravitational force does not have the same capacity of redistributing the working fluid uniformly as the wick structure does.

Given the analysis provided above, it is clear that the assumption of the working fluid flowing down uniformly from the condenser section to the evaporator section under gravity in a wickless heat pipe is not valid. In reality, the working fluid tends to flow down from the condenser to the evaporator unevenly. In the extreme, some places on the evaporator section are not covered by any working fluid at all during normal operation. Sections not covered by working fluid will forego the cooling which should be provided by the heat pipe and they will be heated up to the hot furnace environment temperature, as indicated in Figure 4.1.

Moreover, the temperature of a hot spot on a heat pipe cooled injection lance may be even higher than that of a non-cooled lance. This is because the non-cooled lance is cooled directly by the reagent flowing through it, but a hot-spot on a heat pipe cooled injection lance has basically nothing to cool it. Therefore, the hot spot phenomenon can be one of the issues which were responsible for the failures of those early stage heat pipe cooled injection lances.

The reason why the hot-spot was not stretched all the way down to the lowest section of the evaporator was that there was a pool of working fluid at the bottom of the evaporator section. Thus, the hot-spot could not be generated in the liquid pool.

4.1.3 Solution for Eliminating Hot-Spots

Generally, there are two possible solutions available for resolving the problem of hot-spot formation on the evaporator section. They are outlined as follows.

The first possible solution for the hot-spot problem is to fill the entire evaporator section with working fluid. This solution can be implemented very easily. However, it raises another concern that too much working fluid will reduce the efficiency of the heat pipe. This is the downside of this solution. Explanations as to why this is will be detailed in subsequent sections.

The other possible solution for the hot-spot problem is to employ a wick structure in the heat pipe. The working fluid in the wick can be redistributed evenly on the inner wall of the evaporator section by capillary forces. Although this solution cannot be implemented as easily as the first solution, it has no side-effect on the performance of the heat pipe.

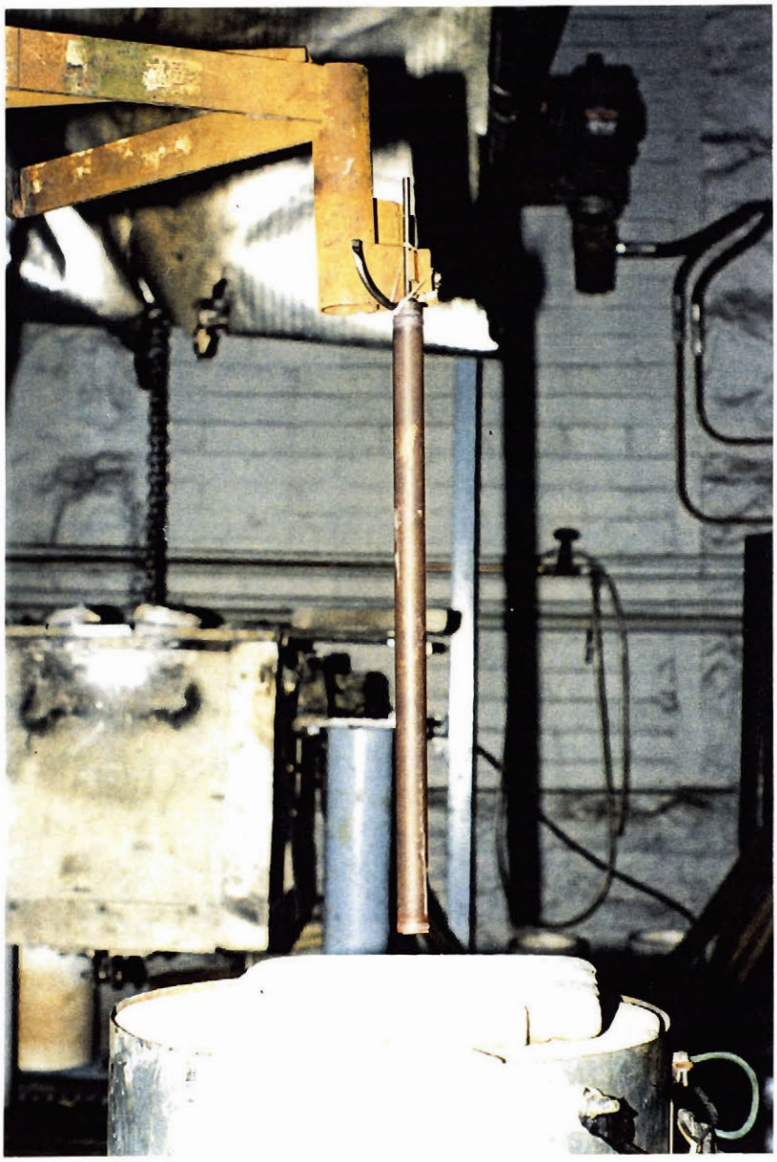

Figure 4.2 Temperature profile on a heat pipe

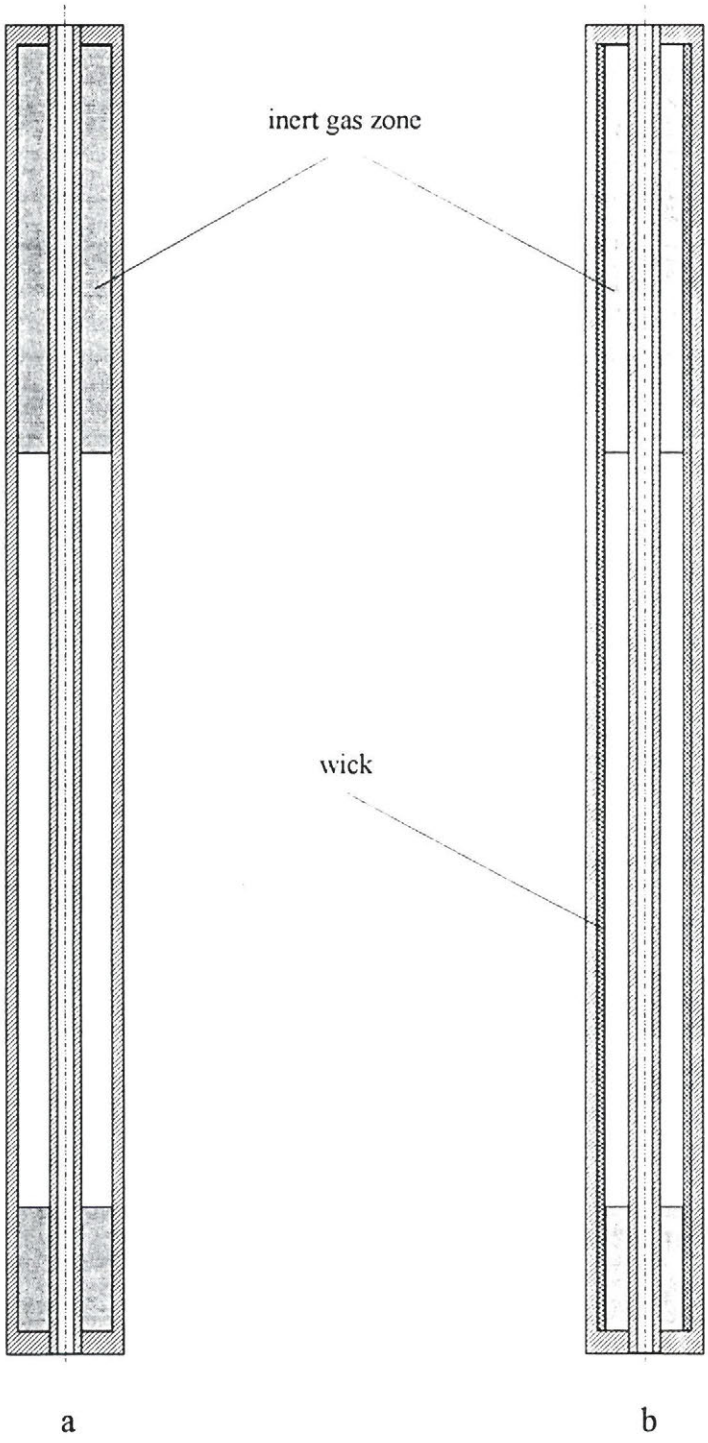

Figure 4.3 Schematic diagrams of heat pipes before (a) and after (b) the modification of eliminating hot-spots

In this study a number of the gravity-assisted heat pipes with screen wick were designed, fabricated, and tested. To get both the capillary force big enough to redistribute the working fluid evenly and to get the passage big enough for the working fluid to go through it, a wrap comprising two or three layers of 100 mesh of stainless steel screen was chosen as the wick for each of the heat pipes.

To test the viability of the second solution a gravity-assisted heat pipe was fabricated and tested in this investigation with 20 grams of sodium as the working fluid. The heat pipe was cylindrical in shape. The tube used for the container was 600 mm long and 25.4 mm O.D. with 1.65 mm wall thickness, the pipe and both end caps were made of 304 stainless steel. A wrap of two layers of stainless steel screen was used as the wick. The heat source for the test was provided by an electric resistance furnace. The furnace temperature was fixed at about 850°C. The length of the evaporator was 300 mm.

Figure 4.2 is another snap shot taken a few seconds after the gravity-assisted heat pipe was pulled out from the furnace. It visually shows that there were no hot-spots on the evaporator.

Figure 4.3 shows the modification of the original design. Figure 4.3a shows the original design of a wickless heat pipe cooled injection lance. Figure 4.3b shows the improved design of a heat pipe cooled injection lance. The difference between the original one and modified one is the wick structure.

In this study it was proven experimentally that the assumption of the working fluid flowing down from the condenser section to the evaporator section uniformly in a wickless heat pipe is not necessarily valid. Hot-spots were observed on the evaporator section. These were formed when the inner surfaces were not wetted by the working fluid and thus were not cooled by evaporation. A simple solution for solving this problem was implemented throughout this study - the screen wick was used in all the heat pipes and the heat pipe cooled injection lances. After the modification the hot-spot was no longer an issue.

4.2 Variable-Conductance Heat Pipes

After the first improvement was made to both the heat pipes and heat pipe cooled injection lances, the performance of the variable-conductance heat pipes was re-examined, because it had caused the problem in previous pilot plant trials of heat pipe cooled injection lances.

Variable-conductance heat pipes (VCHP) are often referred to as gas-loaded heat pipes, into which a certain amount of inert gases are loaded. Because basic heat pipes with

liquid metals as the working fluids have exhibited difficulties when starting up from frozen-states, inert gas loading is a possible solution for the frozen-state startup problem. Basically, this is the reason why the idea of the variable-conductance heat pipes was promoted in the US patent 5,310,166 - self cooling lances and tuyeres. However, the variable-conductance heat pipes may cause the problem of the working fluid freeze up in the inert gas zone. Not much attention had been paid to this problem.

4.2.1 Identification of Working Fluid Freeze Up

The problem of working fluid freeze up in the inert gas zone of the variable-conductance heat pipe was identified during the plant trial of the third heat pipe cooled injection lance at Kidd Metallurgical Division in 1993. After the third trial the phenomenon of working fluid freeze up was studied for that project[78]. Based on the study it was concluded that 'The choice of inert gas is an extremely important parameter in gas-loaded thermosyphon operation. In order to produce a stable interface with minimal penetration of migrating vapor, the lightest possible inert gas should be selected. Helium, a gas which is non-reactive, extremely light and commercially available is the suggested choice for all applications.' One thing that should be noted is that this conclusion was drawn based on the study of low temperature heat pipes. Obviously, the solution at that stage was to replace argon with the lightest inert gas, helium. The fourth heat pipe cooled injection lance was fabricated and carried out in 1994 with helium as its inert gas. But, the life of the fourth lance was not improved compared to the third one.

As mentioned in Section 4.1 the failure of the fourth heat pipe cooled injection lance was caused by hot-spots on the evaporator. However, this does not mean that the working fluid freeze up in the inert gas zone of the variable-conductance heat pipe is not a problem. It only means that in some cases the hot-spot is a more serious problem than the working fluid freeze up in the inert gas zone, or the hot-spot problem occurs earlier than that of the working fluid freeze up in the inert gas zone. It was shown clearly that the failure of the third heat pipe cooled injection lance may have been caused by the working fluid freeze up in the inert gas zone of the variable-conductance heat pipe. As a result no working fluid was left at the bottom of the heat pipe. This implies that the working fluid freeze up is indeed an important issue on implementation of the patented heat pipe cooled injection lances. Since only low temperature heat pipes were used to study the working fluid freeze up in the inert gas section prior to this study, how the results fit in with the high temperature heat pipes with liquid metals as the working fluids is unknown. Therefore, a high temperature heat pipe with sodium as working fluid was designed, fabricated, and studied to identify the working fluid freeze up problem.

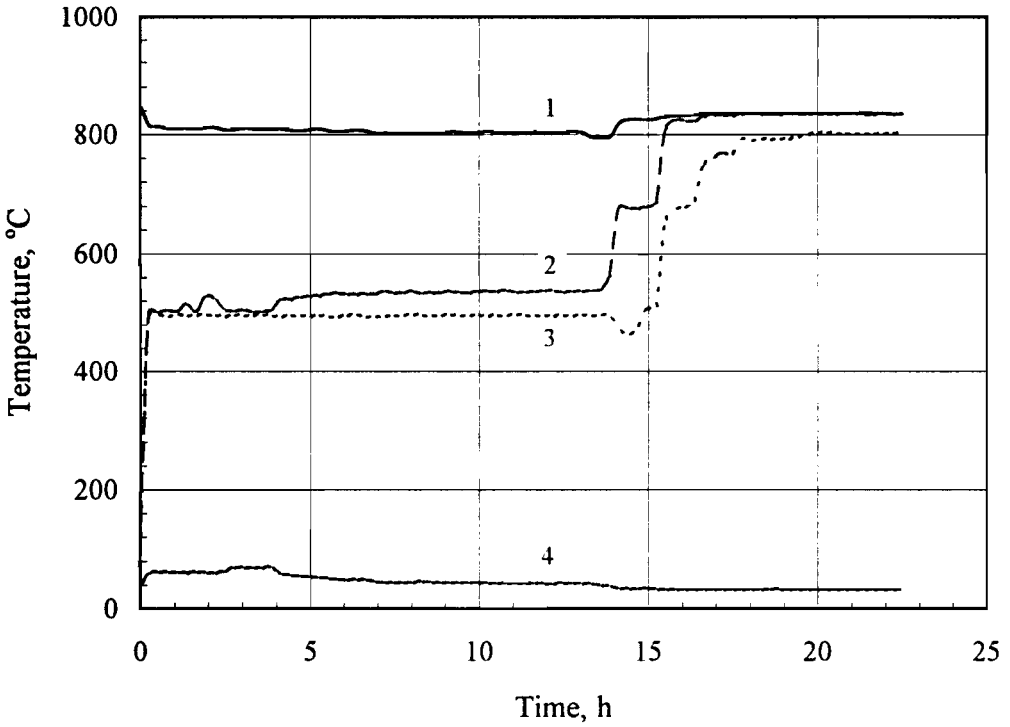

Figure 4.4 Temperature profile of a variable-conductance heat pipe

For this study, the heat pipe was 600 mm long, and the pipe shell was 28.58 mm in outside diameter with 1.65 mm wall thickness. A small tube, 6.35 mm in outside diameter with 0.89 mm wall thickness, goes through the heat pipe in its axial direction for the temperature measurements. This tube, in effect, constitutes a thermocouple well. The tests were carried out in an electric resistance furnace. Approximately 200 mm of the heat pipe was positioned in the furnace as the evaporator section. The heat pipe was in the vertical position. Figure 4.4 shows what happened in the heat pipe after 18 hours of operation. Three thermocouples were positioned at different locations in the thermocouple well to monitor the performance of the heat pipe. Thermocouple #2 was positioned right at the bottom of the heat pipe, thermocouple #3 was 100 mm up from the bottom, and thermocouple # 4 was 500 mm up from the bottom (i.e. 100 mm from the top). Thermocouple #1 was used to monitor the temperature of the heat source. During the experiment, the condenser was cooled continuously with a blast of air to a temperature below the melting point of the working fluid. As shown in Figure 4.4 after running for about 12 hours, the heat pipe encountered some problem. At this time, the bottom of the heat pipe started to dry out, as shown on the curve #2. Two hours later, the dry region

moved past thermocouple #3, located 100 mm up from the bottom, and the temperature started to shot up. Eventually, both thermocouples reached close to the furnace temperature. During the whole operation, thermocouple #4 was well below the melting point of the working fluid (sodium, 97.8°C), and thermocouple #1 stayed at a relatively constant level.

The results of this experiment clearly show that the freeze up of the working fluid could dry out the evaporator section from the lowest point to some distance up, or even all the way to the interface between the evaporator section and the adiabatic section. For high temperature applications such as those in the pyrometallurgical industry, heat pipes may be destroyed soon after the dry out region is created with most of the working fluid freeze up in the inert gas zone.

Comparing with the hot-spot problem the freeze up of the working fluid is a similar type of problem. In some cases, it may even be a more serious problem because for a vertical gravity-assisted heat pipe cooled injection lance a dry spot caused by the working fluid freeze up will occur first at the bottom of the evaporator section, which usually has to handle the highest heat flux.

4.2.2 Mechanism of Working Fluid Freeze Up

The reason for the working fluid freeze up in the inert gas zone is that the vapor of the working fluid diffuses through the inert gas zone and solidifies in it[78]. Apparently, it is a very simple process. For a variable-conductance heat pipe all the working fluid may freeze up in the inert gas zone in some period of time, because the melting points of sodium and some other alkali metals used as working fluids for the heat pipes are higher than average room temperature. As the vapor of the working fluid diffuses into the inert gas zone it will not only condense in it but it may also freeze in the inert gas section if the temperature is low enough. This is a problem for heat pipes with potassium, sodium, lithium, and some other liquid metals as the working fluid. The melting points of three of the most useful alkali metals, potassium, sodium, and lithium are listed in Table 4.1.

Table 4.1 Some physical properties of three alkali metals

Name of alkali metals	Melting point, °C	Boiling point, °C
Potassium	63.65	774
Sodium	97.81	883
Lithium	180.54	1347

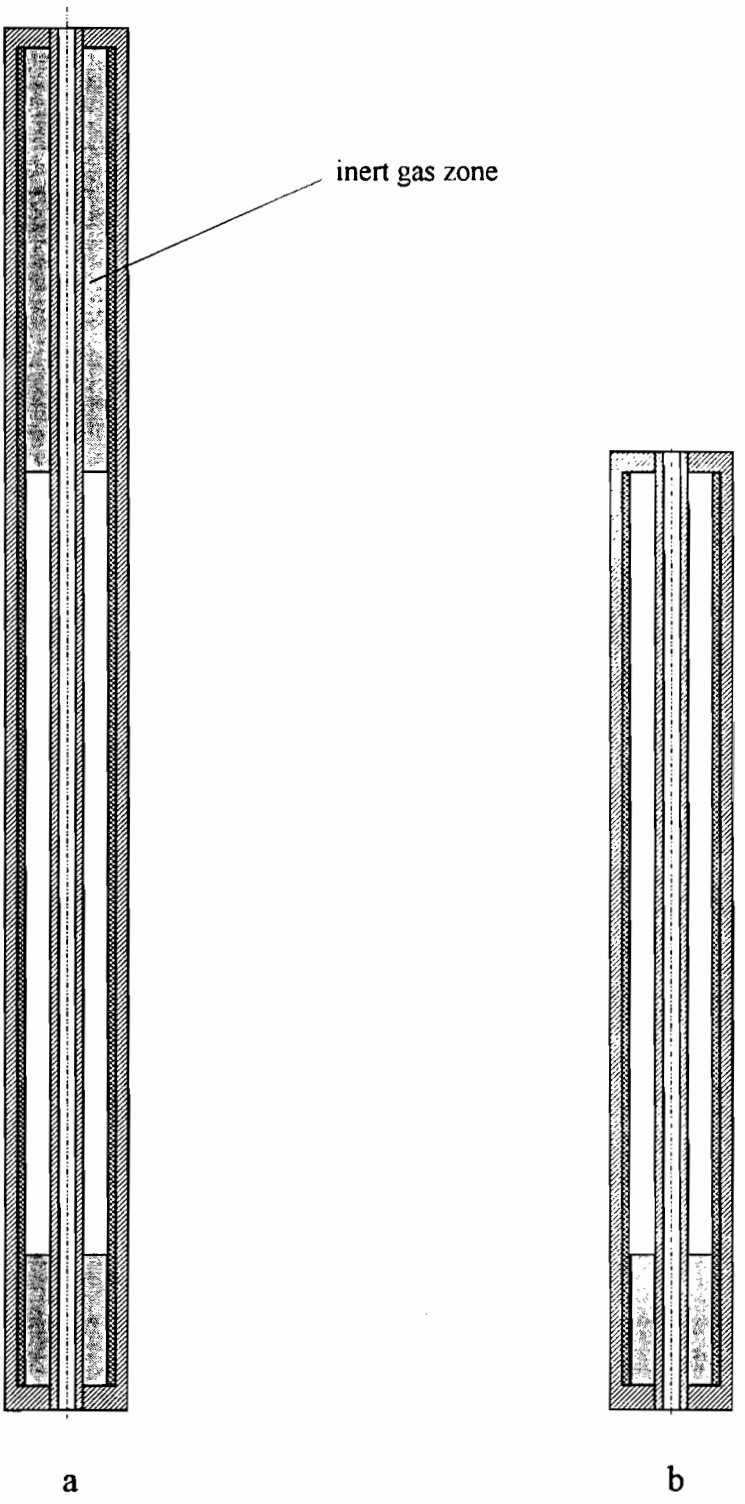

Figure 4.5 ***Schematic diagrams of heat pipes before (a) and after (b) the modification of eliminating the freeze up of working fluid***

Although the rate of working fluid vapor diffusing through the inert gas zone is relatively small, the process is indeed an irreversible one. Eventually, there will be no working fluid at the bottom of the heat pipe, and most of the working fluid may be frozen up in the inert gas zone, as long as the temperature in the inert gas zone is colder than the melting point of the working fluid.

4.2.3 Solutions

Basically, for the patented heat pipe cooled injection lances with potassium, sodium, or lithium as working fluid, the freeze up of the working fluid is caused by the coexistence of three things: the inert gas, the melting point of the working fluid being higher than the pipe shell temperature in the inert gas zone, and diffusion between the vapor of the working fluid and the inert gas. Obviously, there are three means to solve the working fluid freeze up problem corresponding to each factor mentioned above.

The first solution is to eliminate the inert gas zone, which means that basic heat pipes are used to protect lances instead of the variable-conductance heat pipes. The problem of frozen state startup for the basic heat pipes with alkali metals as the working fluids can be handled by the manner of operation. The second solution is to keep the temperature of the pipe wall in the inert gas zone well above the melting point of the working fluid. And the third solution is to have the diffusion coefficient as small as possible. This is the solution which had been proposed, studied, and used on the pilot plant trials prior to this study. Apparently, the solution does not solve the problem completely.

Comparing the three solutions, the first one, replacing the variable-conductance heat pipes with basic heat pipes, is considered to be the most promising solution. It should be noted that the process of eliminating the inert gas zone is very time consuming. For example, for getting all the non-condensable gases out of a heat pipe with sodium as the working fluid, the whole process could last as long as 24 hours. Fortunately, the whole process can be stopped and resumed at any time until the procedure is completed.

In this study not only do all the heat pipes and heat pipe cooled injection lances have wick structures in them, but they are also basic heat pipes or basic heat pipe cooled injection lances with no inert gas zone in them.

4.3 Forced Cooling of the Condenser

Based on the study presented in the last section, the idea of using variable-conductance heat pipes to control the operating temperatures of the heat pipe cooled injection lances was abandoned, which means that the function of using an inert gas zone as a buffer to control the operating temperature is no long available. In this section, a better method for controlling the heat pipe operating temperature is adopted. The method is based on forced convection cooling of the condenser.

4.3.1 Concentric Pipe Heat Exchangers

Convection is the term applied to the energy transfer process which is observed to occur in fluids mainly because of the transport of energy by means of the motion of the fluid itself. When the fluid motion is caused by the imposition of external forces in the form of pressure differences, this mechanism is called forced convection. The pumping of a fluid over a solid surface which is functioning with a temperature difference is an example of forced convection. For a given solid surface, the cooling rate of forced convection is a function of a group of parameters which include the bulk velocity of the moving fluid - a parameter which is not explicit in free convection correlations.

The process of exchanging heat between two different fluid streams is one of the most important and frequently encountered processes found in engineering practice. The modern petrochemical industry, energy generating plants, etc., are based on innumerable processes involving the use of devices to exchange heat between two fluid streams without physically mixing them. Such devices are generally termed heat exchangers. Apparently, with cooling provided by forced convection on the condenser section, the heat pipe may be considered as a typical heat exchanger for exchanging heat from the working fluid of the heat pipe to the cooling media.

Because the heat pipe used for cooling an injection lance usually is cylindrical in shape, it is natural to form a concentric system with a cooling jacket surrounding the heat pipe. This kind of system is termed a concentric pipe exchanger (or double-tube exchanger), of which one of the most frequently encountered is the shell-and tube heat exchanger.

Given the isothermal feature of the heat pipe, the system with cooling applied on the condenser of the heat pipe is a simple heat exchanger - flow past an isothermal surface. Thus, it is necessary to have a good understanding of the performance of the concentric pipe heat exchanger. The analysis of this type of heat exchanger is relatively straight forward.

4.3.2 Performance of Concentric Pipe Heat Exchangers

Consider the flow of a fluid over an isothermal surface of known temperature and surface area, t_s and A. Figure 4.6 depicts such a case in which a fluid of known inlet temperature, t_{fi}, flows at a known mass flow rate, $\dot{m}$, in an annular passage of known circumference, C, of the outer surface of the inner tube of length, L. Heat exchange is ignored through the outer tube. The specific heat of the fluid, c_p, is known, as is the temperature of the outer surface of the inner tube, t_s, and the heat transfer coefficient at that surface, h. For this case, the desire is to find the cooling effect of the cooling medium on the heat pipe - the outlet temperature of the fluid, t_{fo}, and the total heat transferred to it, q. The fluid temperature increases with distance along the tube, x, and at $x=L$, the exit fluid temperature is t_{fo}. In any incremental portion of the tube the heat transfer to the fluid is expressed in two ways, in terms of a heat balance on the fluid and in terms of the exchange between the fluid and the surface as denoted by Eqs. 4.1 and 4.2, respectively.

$$dq = \dot{m} c_p dt_f \tag{4.1}$$

$$dq = hC\, dx (t_s - t_f) \tag{4.2}$$

For the entire tube length where $A=LC$ is the total surface area, integrated forms of the above equations are:

$$q = \dot{m} c_p (t_{f_o} - t_{f_i}) \tag{4.3}$$

$$q = hA\, (t_s - t_f)_m \tag{4.4}$$

The term $(t_s - t_f)_m$ represents some suitable mean value of the surface-to-fluid temperature difference which varies from $t_s - t_{fi}$ at the tube entrance to $t_s - t_{fo}$ at the exit. It is t_{fo} and q which are sought, given t_{fi}, $\dot{m}$, c_p, h, A, and t_s. Thus, equating Eqs. 4.1 and 4.2 yields:

$$dq = hC\, dx (t_s - t_f) = \dot{m} c_p dt_f \tag{4.5}$$

The above may be rewritten in the following form since t_s is assumed as constant:

$$\frac{d(t_f - t_s)}{t_f - t_s} = -\frac{hC}{\dot{m} c_p} dx \tag{4.6}$$

When integrated from $x=0$, $t_f = t_{fi}$, to $x=x$, $t_f = t_f$, Eq. 4.6 gives, when h is taken as constant,

$$\ln\left(\frac{t_f - t_s}{t_{fi} - t_s}\right) = -\frac{hC}{\dot{m} c_p} x \tag{4.7}$$

or

$$\frac{t_f - t_s}{t_{fi} - t_s} = \exp\left(-\frac{hC}{\dot{m}c_p}x\right) \tag{4.8}$$

Eq. 4.8 shows that the bulk temperature of the cooling media varies exponentially with distance along the pipe.

To find the total heat transferred over a pipe length L, Eq. 4.5 may be integrated to yield

$$q = hCL(t_s - t_f)_m = \dot{m}c_p(t_{fo} - t_{fi}) \tag{4.9}$$

where $(t_s - t_f)_m$ is the mean of the temperature difference $(t_s - t_f)$ over the length L. Furthermore, when x=L, $t_f = t_{fo}$,, Eq. 4.8 becomes

$$\frac{t_{fo} - t_s}{t_{fi} - t_s} = \exp\left(-\frac{hCL}{\dot{m}c_p}\right) \tag{4.10}$$

By combining Eqs. 4.9 and 4.10, the mean temperature difference can be expressed as the following:

$$(t_s - t_f)_m = \frac{(t_s - t_{fi}) - (t_s - t_{fo})}{\ln\left(\frac{t_s - t_{fi}}{t_s - t_{fo}}\right)} \tag{4.11}$$

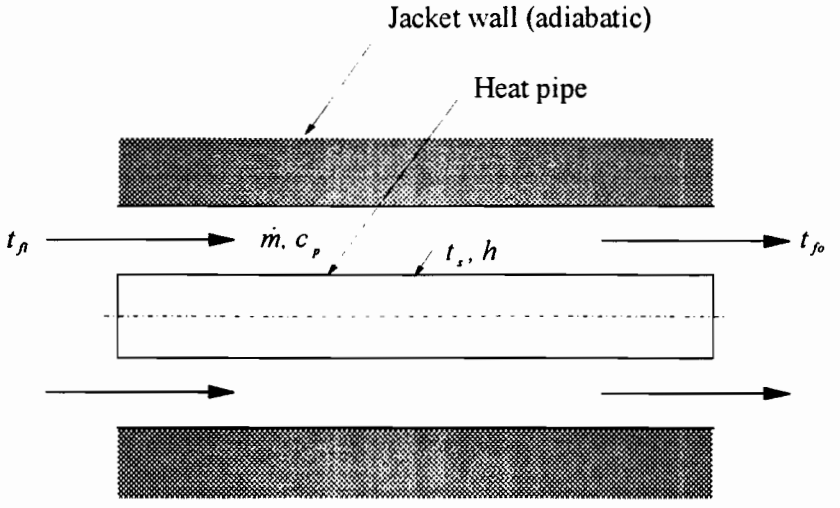

Figure 4.6 Schematic diagram of fluid flow past an isothermal surface

Given t_{fi}, $\dot{m}$, c_p, h, A, and t_s, the mean-temperature-difference method determines the performance parameters as follows:

1. Find t_{fo} from Eq. 4.10;
2. Find the mean temperature difference from Eq. 4.11;
3. Find q from Eq. 4.9.

For a real system, all the parameters can be measured except the heat transfer coefficient, h. Given t_{fi}, t_s, $\dot{m}$, c_p, and A, the heat transfer coefficient can be found from Eq. 4.10. In this study, this technique was used to determine the heat transfer coefficient for the design of a heat pipe cooled injection lance.

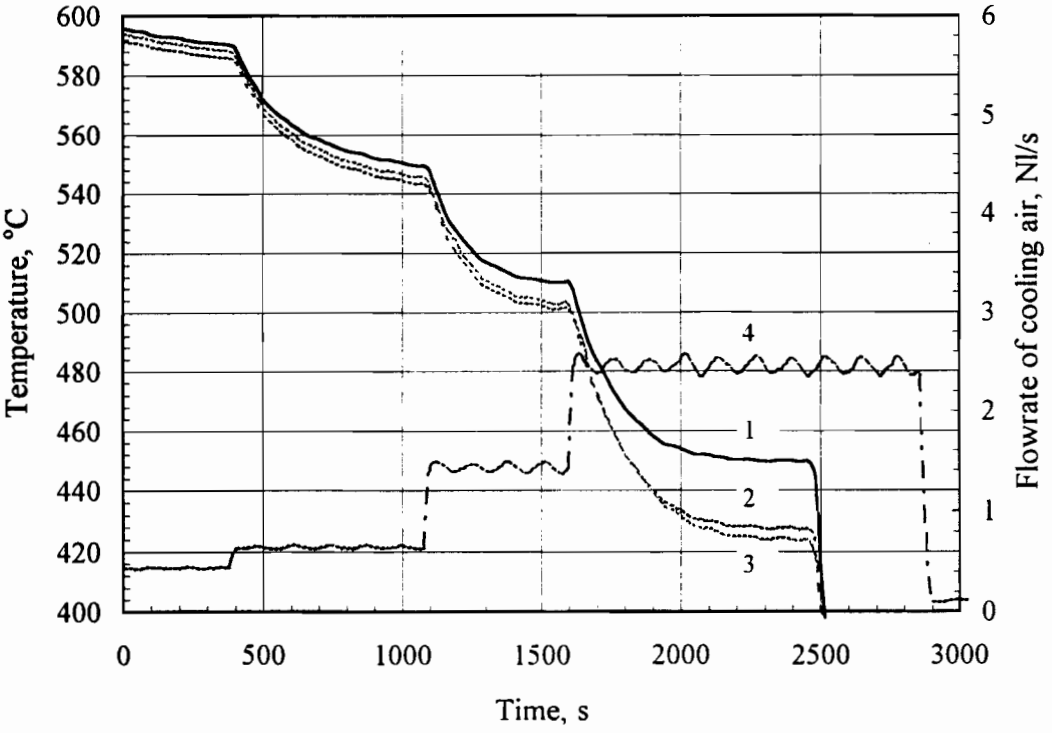

Figure 4.7 Temperature profiles at different steady-states

Figure 4.7 shows the results obtained from an air-cooled heat pipe. In Figure 4.7 three sets of steady-state results can be obtained, as shown in Table 4.2. Since the size of the air-cooled condenser is 25.4 mm in diameter by 220 mm long, the total area of the air-cooled condenser is 0.017555 m^2. Then, the mean temperature difference of the cooling-air can be calculated by Eq. 4.11 when the inlet temperature of the cooling-air is 15°C, as shown in Table 4.2, and the heat transfer coefficient between the surface of the condenser

and the cooling air can be calculated by Eq. 4.9, as also shown in Table 4.2.

The analysis presented above is important in determining the heat transfer coefficient between the surface of the condenser and the cooling-air. In Chapter 7 this method will be used to determine the heat transfer coefficient based on the information gathered during tests. In Chapter 8 the determined heat transfer coefficient will be used as input for mathematical modeling.

Table 4.2 Calculated mean temperature difference and heat transfer coefficient

Operating temperature, °C	Outlet temperature of cooling air, °C	Flowrate of cooling air, l/s (STP)	Mean temperature difference, °C	Heat transfer coefficient, W/m^2-°C
546.3	363.4	0.657	326.7	51.5
502.9	300.3	1.413	324.6	91.3
423.7	233.1	2.367	285.9	132.7

4.3.3 Cooling Media of Concentric Pipe Heat Exchangers

The two most common cooling media used in engineering are water and air. In this study, the cooling medium chosen for force convection is air. There are a number of reasons to choose air as the cooling medium. Firstly, given the redistribution of heat fluxes by heat pipes, air is a viable coolant, especially when several hundred degrees Celsius of driving force are available. Secondly, it does not require transportation because of its availability, and is free of charge for this type of cooling purpose as long as it is not contaminated. Lastly, it is much safer than water if it comes in contact with liquid metal which may happen if a heat pipe cooled injection lance fails.

There are number of reasons for not choosing water as the cooling medium. Firstly, water is not compatible with alkali metals. Although alkali metals as working fluids are separated from the cooling medium by the heat pipe shell, the possibility for the cooling medium to leak into the heat pipe and contact the working fluid still exists. The consequence of water contacting alkali metals is a vigorous explosion. Secondly, water is also not compatible with the liquid metal bath. A similar explosion can happen if water is released in a liquid metal bath. Thirdly, compared to air, the use of water is expensive.

For the heat pipe, because of its isothermal feature, an easy and efficient way for

cooling the condenser is to build an annular system. Air goes through the annular gap formed by the outer surface of the heat pipe and the inner surface of the air jacket.

In order to avoid any possible freeze up of the working fluid, air should be introduced upwards for the vertical gravity-assisted heat pipe. By doing this the entire condenser can be heated up to a temperature which is above the melting point of the working fluid regardless of the amount of inert gas remaining in the heat pipe.

4.3.4 Advantages of Forced-Cooling over Self-Cooling on Condenser

Self-cooling has advantages in the design of a heat pipe cooled injection lance as claimed in U.S. patent 5,310166. However, forced-convection provides the possibility of running the heat pipe cooled injection lance at a lower temperature. If operating temperature is an issue, then the decision of choosing between a cooling method that includes forced convection and one of free convection (self-cooling) is simple. Forced convection cooling is the obvious choice.

For a given heat pipe, its normal operating temperature range is defined by its working fluid. The normal operating temperature ranges of some working fluids are shown in Table 3.3. Below the low end of the range, the pressures corresponding to the saturation temperatures are too low to allow the heat pipes to maintain their properties. Above the high end of the range, the pressures corresponding to the saturation temperatures are too high to allow the working fluids to be confined in the heat pipe shell safely. By controlling the flow rate of cooling air, the heat pipe cooled injection lance can operate at any temperature within the operating temperature range. Generally, a lance should operate at a temperature which is as low as possible, because the lower is the operating temperature, the longer the life of the heat pipe will be. For some cases, the lowest possible temperature may be too low to keep the nozzles free. Forced convection on the condenser provides a possibility of optimizing the operating temperature for the heat pipe cooled lancing system.

Figure 4.8 shows one set of the results relating to forced air cooling of a heat pipe. The heat pipe used for this study was a gravity-assisted heat pipe. It was about 500 mm long. The length of the evaporator section was about 200 mm. The rest of the length worked as the condenser section, and was enclosed by a jacket. Four thermocouples and one flowmeter were used to monitor the performance of the heat pipe. Thermocouples #1 to #3 were positioned at different locations to measure the heat pipe temperature, while thermocouple #4 was used to measure the outlet temperature of the cooling air. Curve #5 is the flow rate of the cooling air. It shows how effective air cooling can be.

Furthermore, forced air cooling can reduce the size of condensers significantly. For

example, for a condenser of 500°C in an environment of 20°C, the equivalent heat transfer coefficient by radiation and free convection is about 33 W/(m^2-°C), but for an air-cooled condenser it is not difficult to get a heat transfer coefficient an order of magnitude larger. Thus the condenser can be as small as 10% of the natural cooled condenser.

The advantages of forced cooling of a condenser over self-cooling are as follows:

1. Full control of the operating temperature of the heat pipe;
2. Much shorter condenser is needed in comparison to a natural cooled condenser.

Figure 4.9 shows two schematic diagrams of heat pipe cooled injection lances. Figure 4.9a is the one before the modification, Figure 4.9b is the other one after the modification at this stage.

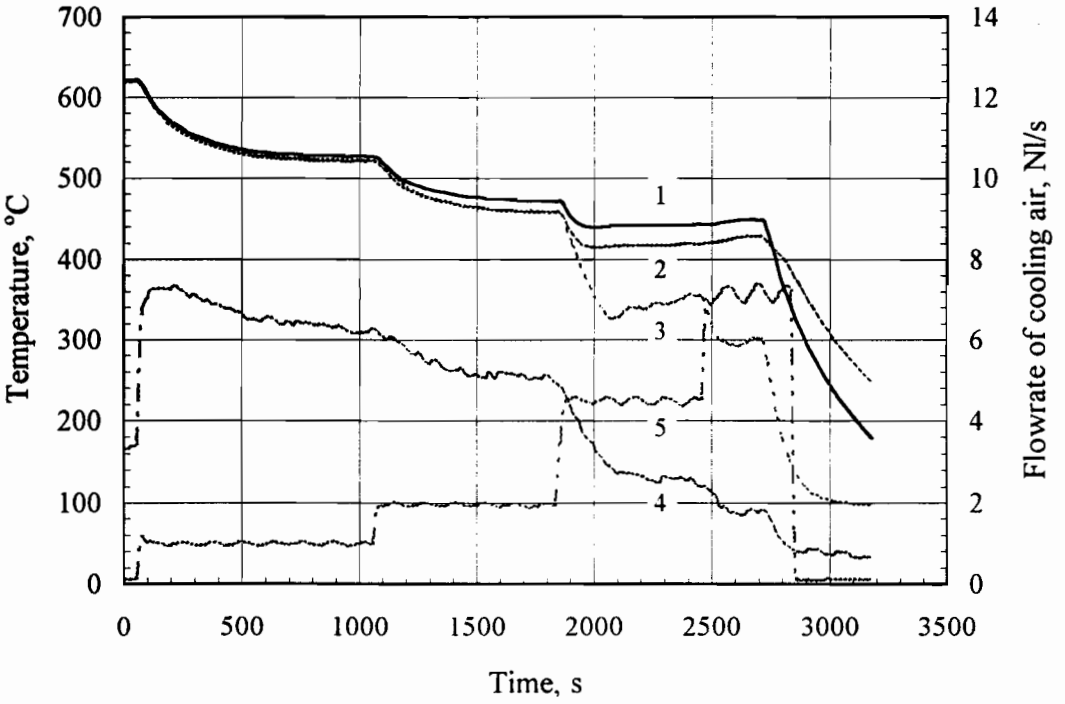

Figure 4.8 Temperature profiles under different cooling rates

4.3.5 Design Consideration - Differing Thermal Expansion

Most bodies expand as their temperatures increase. This phenomenon plays an important role in numerous engineering applications. For example, thermal expansion joints must be included in buildings, railways, concrete highways, and bridges to compensate for changes

in dimensions with temperature variations.

Compared with buildings, railways and other objects, heat pipe cooled injection lances are small in size. However, considering the environment they are going to be in and the different cooling rates of different pipes, thermal expansion may be an important issue. Therefore, differential thermal expansion should be considered in the design.

Suppose the linear dimension of a pipe along the longitudinal axis is l at some temperature. The length increases by an amount Δl for a change in temperature ΔT. Based on the basic equation for the expansion of a solid the Δl can be expressed as following:

$$\Delta l = \alpha \, l \, \Delta T$$

where the proportionality constant α is called the average coefficient of linear expansion for a given material. Table 4.3 gives the expansion coefficients for some materials near room temperature.

Differing thermal expansion between heat pipe and cooling jacket

Basically, during operation the condenser of a heat pipe with a cooling jacket around it is a typical concentric heat exchanger. Differing thermal expansion can be a very big problem for this kind of system. For example, suppose there is an air cooled heat pipe operating at 600°C with a one meter long condenser covered by a bigger, concentric pipe as cooling jacket, and the mean temperature of the cooling jacket is 300°C. If the heat pipe and the jacket are all made of mild steel, the difference of thermal expansion is about 3.3 millimeters. This case indicates that the jacket cannot be simply fixed at the two ends, some precaution needs to be taken.

Table 4.3 Expansion coefficients for some materials near room temperature

Material	Linear expansion coefficient, α $(°C)^{-1}$
Lead	29×10^{-6}
Aluminum	24×10^{-6}
Copper	17×10^{-6}
Steel	11×10^{-6}
Stainless steel (304)	17×10^{-6}

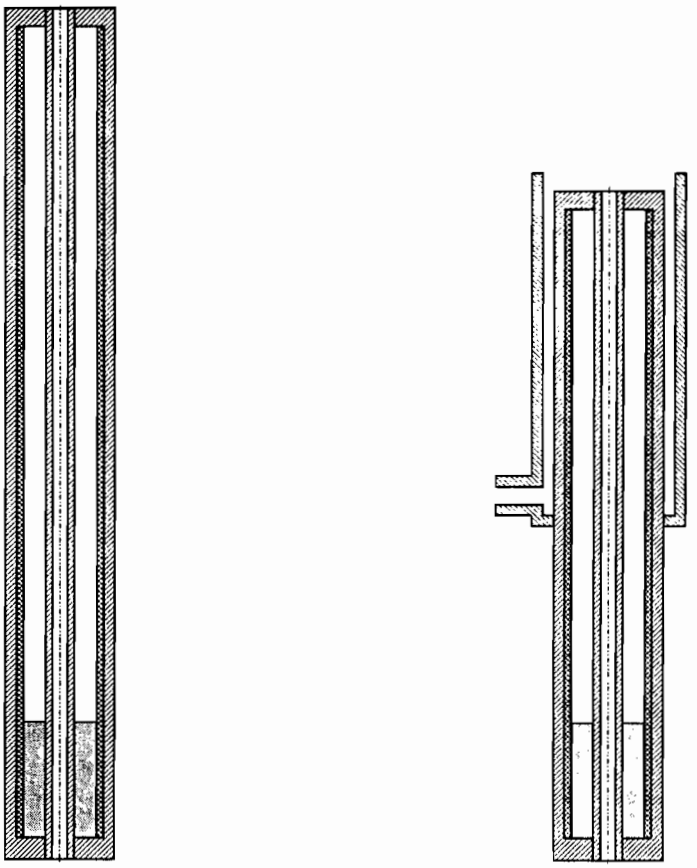

Figure 4.9 ***Schematic diagrams of heat pipes before (a) and after (b) the modification of applying cooling jacket***

Differing Thermal Expansion Between the Heat Pipe and the Reagent Conduit

In the patented annular heat pipe cooled injection lances, a part of the heat pipe shell works as the evaporator and the rest works as an adiabatic section and a condenser. Meanwhile, the entire length of the reagent conduit pipe is encased in the heat pipe and acts as a condensing surface for the vaporized working fluid. Because the heat extraction rate on the reagent conduit pipe is bigger than that of the heat pipe shell, the average temperature of the reagent conduit pipe is lower than that of the heat pipe shell. If the same material is chosen for both the reagent conduit pipe and the heat pipe shell, there is

different thermal expansion between the reagent conduit and the heat pipe shell.

Because of the restriction on the ends of both the inner and outer pipes, the differential thermal expansion is translated into compression and tensile stresses on the outer pipe and the inner pipe, respectively. For a given amount of deformation, the tensile stress is more critical than the compressive stress. Meanwhile, the cross-sectional area of the heat pipe shell is much bigger than that of the reagent conduit. Therefore, the tensile stress on the inner pipe may pose some serious problems.

While the heat pipe can maintain a constant temperature on the outer surface of the inner pipe, reagent flowing downwards through the conduit is heated up continuously and thus the temperature difference between the reagent and the inner wall of the inner pipe gets progressively smaller. This then translates to the fact that the temperature on the inner wall of the inner pipe gets hotter and hotter. The hottest place on the inner wall of the inner pipe is right at the connection between the reagent conduit pipe and the bottom plate. Thus, the weakest area of the inner pipe is this connection.

CHAPTER 5

SUPERHEAT IN LIQUID POOL OF WORKING FLUID

In this chapter, the superheat requirement for nucleate boiling in the liquid pool of the working fluid in the vertical, gravity-assisted, heat pipe is investigated. A unique method which can minimize the superheat requirement for nucleate boiling in the liquid pool is proposed and tested.

5.1 Introduction

Usually, for a vertical gravity-assisted heat pipe, there is a liquid pool of working fluid at the bottom of the heat pipe. It is well documented that the liquid pool may cause two problems on the heat pipe. One is the significant superheat which may appear in the liquid pool. The superheat in the liquid pool creates a controversy as to the isothermal feature of the heat pipe. The other is the slugging of the working fluid which may occur during the startup of the heat pipe. The slugging in this case refers to a non-stationary state of the working fluid where slugs of liquid, with a characteristic dimension equal to the heat pipe diameter, are periodically ejected from the pool, traverse some distance toward the condenser, and disappear into the liquid film along the heat pipe wall. The slugging is usually caused by the flash vaporization of the working fluid within the pool[34]. These two issues are unsolved problems for gravity-assisted heat pipes. The pool of working fluid has

been causing problems for the application of heat pipes in the nuclear industry[34] and in some other industries.

For a heat pipe, a relatively large superheat in the liquid pool obviously reduces the heat transport capacity through the liquid pool. For a heat pipe cooled top-blowing injection lance, the nozzle is covered by the liquid pool. This region typically withstands the biggest heat fluxes and is exposed to the highest oxidation rates. It is thus the place which requires the most cooling. It is an area where every additional degree of temperature can be of concern. Therefore, the big superheat in the liquid pool may be too costly for the life of the heat pipe cooled injection lance.

This section is about finding some method to reduce the superheat requirement for nucleate boiling in the liquid pool. In this section the phenomenon of pool boiling is reviewed. The superheat requirement for nucleate boiling in the liquid pool is examined. A possible solution is presented, the validity of the proposed method is proven experimentally, and the mechanism of operation behind this new method is discussed.

5.2 Liquid Pool in Gravity-Assisted Heat Pipes

Figure 5.1 shows the schematic diagram of a vertical gravity-assisted heat pipe with a liquid pool at the bottom end of its evaporator section. Apparently, the working fluid is one of three essential components which make up the heat pipe. Because of this, the difficulty of calculating the right amount of working fluid for the heat pipe, and the dynamic features of the heat pipe lead to an over charging of a heat pipe. Since all gravity-assisted heat pipes have to be charged with some amount of excessive working fluid to insure that they can operate under various operating conditions, the presence of a liquid pool is inevitable. In addition to that, working fluid over and above that required to simply maintain a vertical gravity-assisted heat pipe functional is needed to insure that the heat pipe does not encounter any difficulty at startup from a frozen state. Usually, the amount of working fluid in the liquid pool is decided by the heat extraction rate, the heating speed at the startup stage, the wick structure in the heat pipe, and the thermal mass of the heat pipe. However, excessive working fluid may cause the heat transport capacity of the heat pipe to decrease. This decrease in heat transport capacity relates to the heat transfer mode in the liquid pool.

In the heat transfer literature, when a heating surface is submerged in an otherwise quiescent pool of liquid, and heat is transferred to the liquid by free convection and bubble agitation, the process is termed pool boiling. The liquid pool formed by the working fluid

in a vertical gravity-assisted heat pipe undergoes the process of pool boiling.

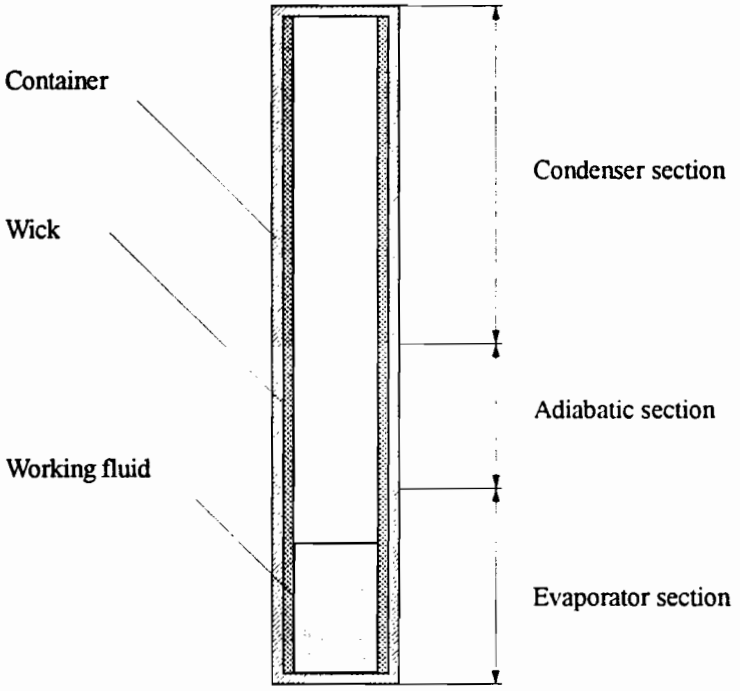

Figure 5.1 Schematic diagram of a heat pipe with a pool of working fluid

5.2.1 Pool Boiling Phenomenon

For pool boiling, there are several stages: free convection boiling, nucleate boiling, partial film boiling, and film boiling. Figure 5.2 is a typical boiling curve for water, which displays several regimes of pool boiling.

In the range of low Δt, region *A-B* in Figure 5.2, no bubbles are generated even though the liquid is slightly superheated. Heat is transported from the heating surface to the bulk of the liquid mainly by free convection effects. All vapor produced at this stage is by evaporation of the liquid at the free surface. This region is called free convection boiling.

Continued increase in Δt causes the process to enter the regime of nucleate boiling, denoted by *B-C* in Figure 5.2. In this region bubbles are formed on the heating surface. The bubbles first appear at certain favorable sites or nuclei. As Δt increases, more and more sites are activated. In the lower end of the region *B-C*, the bubbles leave the surface

and may recondense in the bulk of the liquid. As Δt is increased more, the bubbles rise all the way to the liquid surface to release vapor. This bubble activity causes the liquid near the heating surface to become highly agitated and a marked increase in the heat flux occurs. The upper limit of the nucleate boiling regime, point C, is referred to as the peak heat flux.

Additional increase of Δt beyond that of the peak heat flux causes the process to enter the regime of transition boiling, or partial film boiling, denoted by C-D in Figure 5.2. At any location on the surface, an unstable condition exists in which the process oscillates between nucleate boiling and film boiling in which the surface is blanketed with a film of vapor. Eventually, the regime of stable film boiling, D-E-F in Figure 5.2, is reached in which the surface is completely covered with a blanket of vapor.

Generally, region A-B, free convection boiling, and region B-C, nucleate boiling, are the most important regions for transferring heat by boiling. In most of the cases, the pool of working fluid in a heat pipe operates in the regime of nucleate boiling.

In the regime of nucleate boiling, when a liquid boils on a heated surface the temperature of that surface is always greater than the bulk temperature of the boiling liquid. It can be seen from the simple force-balance bubble-equilibrium equation based on the assumption of spherical bubbles constituting the vapor phase that:

$$p_v = p_l + \frac{2\sigma}{r} \tag{5. 1}$$

where p_v is vapor pressure corresponding to the temperature of the adjacent liquid t_l ($\approx t_w$, t_w is the wall temperature of the hot plate), p_l the liquid pressure for which t_{sat} is the corresponding saturation temperature, σ the surface tension of the liquid, and r the radius of the spherical bubbles.

Because there is a correlation between pressure and corresponding temperature, $t = f(p)$, the superheat requirement for nucleate boiling in the liquid pool can also be expressed in the following form:

$$t_l - t_{sat} = f(p_v) - f(p_l) \tag{5. 2}$$

Substitution of Eq. 5.1 into Eq. 5.2 gives:

$$t_l - t_{sat} = f(p_l + \frac{2\sigma}{r}) - f(p_l) \tag{5. 3}$$

Basically, the superheat requirement for nucleate boiling in the liquid pool is a function of the system pressure p_l, the surface tension of the liquid, and the radius of the spherical bubbles. Eq. 5.3 can be simplified to the following:

$$t_l - t_{sat} = F\,(p_l, \sigma, r) \tag{5.4}$$

In order to achieve high heat transfer efficiency, the heat transfer mode in a liquid pool should be controlled within the free convection boiling region and the nucleate boiling region only.

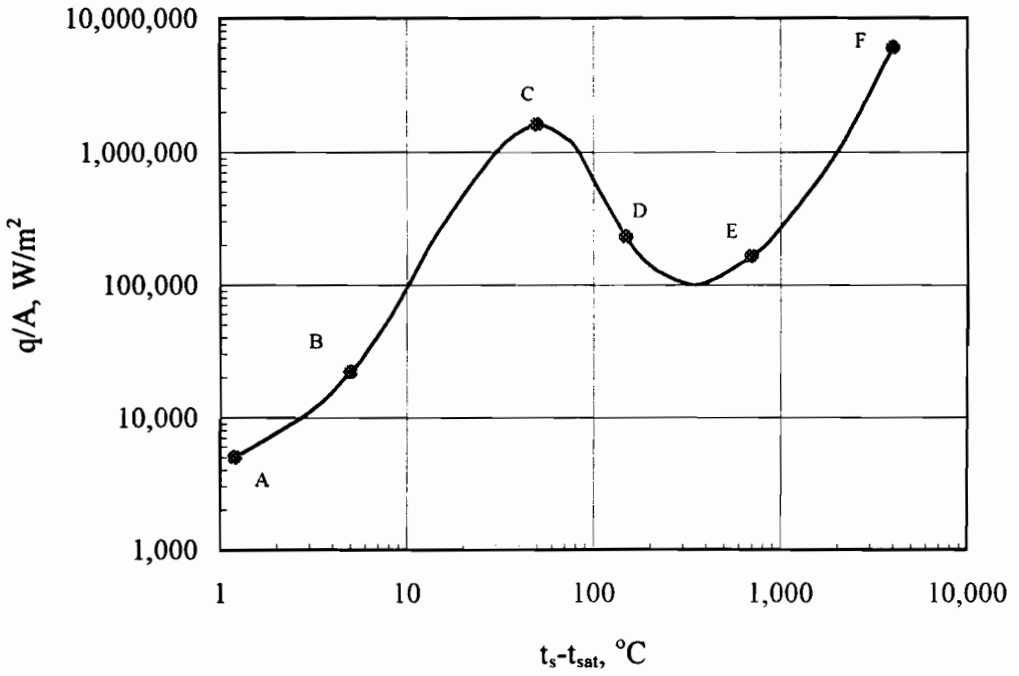

Figure 5.2 A typical pool boiling curve for water

5.2.2 Nucleate Boiling of Alkali Metals

Alkali metals have similar boiling characteristics as water, although it should be noted that the heat fluxes on a heating surface in the free convection boiling region and the nucleate boiling region for alkali metals are substantially bigger than that for water. These two regions play very important roles in alkali metal heat pipes. For high heat transport rates, nucleate boiling usually dominates.

Alkali metals, owing to their chemical reduction power, generally wet their containers very well. They also wet the larger cavities and render them inactive. This tends to make the nucleate-boiling superheats for alkali metals higher than those of ordinary liquids. There are two other reasons why alkali metals tend to give higher nucleate-boiling wall superheats than those of ordinary liquids: (a) they have less steep vapor pressure

curves in the practical temperature range, and (b) their capacity to dissolve inert gases increases, rather than decreases, with increase in temperature. The latter characteristic causes alkali metals to absorb inert gases from potential nucleating cavities[80].

During the extensive study on the nucleate boiling of alkali metals for the nuclear industry a theoretical analysis was established[80]. When t_l represents the temperature of liquid and t_{sat} represents the saturation temperature corresponding to the system pressure, the difference between the liquid temperature and the saturation temperature, $t_l - t_{sat}$, is known as the superheat requirement for nucleate boiling in the liquid pool. The corresponding pressure difference, $p_v - p_l$, is given by Eq. 5.5:

$$p_v - p_l = \frac{2\sigma}{r} - \frac{\beta}{(r')^3} t_l \qquad (5.5)$$

where p_v is vapor pressure inside bubbles, p_l the liquid or system pressure, σ the surface tension of the liquid, r the radius of nucleation sites, r' the radius of unwetted nucleation sites, β the system parameter, and t_l the liquid temperature.

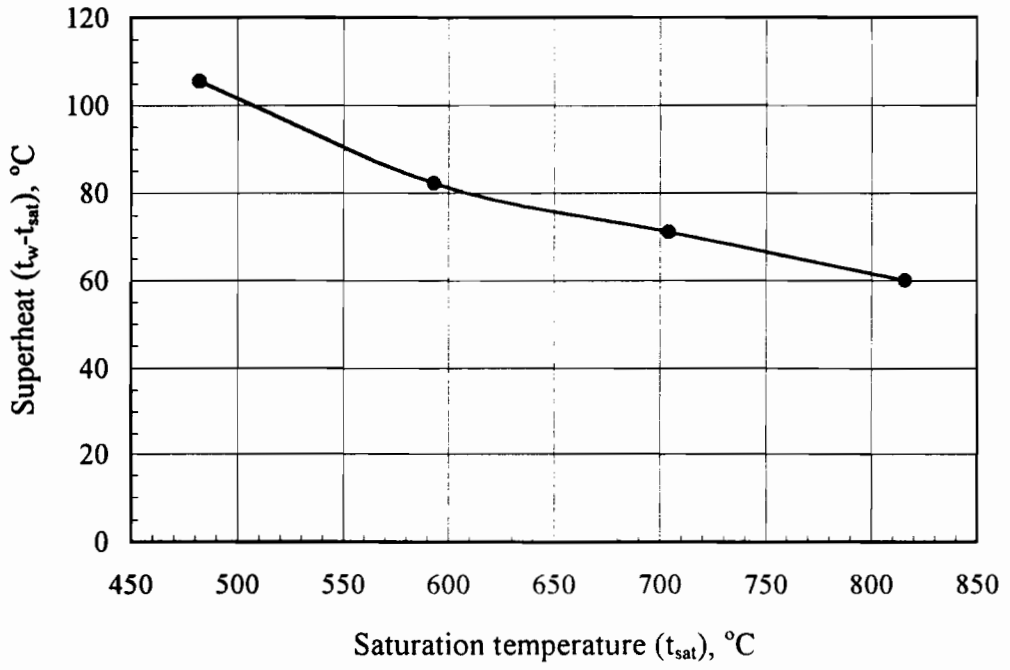

Figure 5.3 Superheat for nucleate pool boiling of sodium

The nucleate boiling superheats in the liquid pools of alkali metals were studied by Chen[81] on potassium and by Holtz and Signer[82] on sodium. Another study was carried out by Dwyer[80] to show the good agreement between predicted and measured nucleate

boiling superheats. Some superheat models were recommended to predict nucleate boiling superheats.

As an example, Figure 5.3 shows the superheat requirement for nucleate boiling in the liquid pool of sodium, which was obtained by Holtz and Singer[82]. It indicates that for nucleate boiling in the liquid pool of sodium the superheat requirement is a function of the saturation temperature.

5.2.3 Nucleate Boiling in Vertical Gravity-Assisted Heat Pipes

The pool of working fluid in a vertical gravity-assisted heat pipe can undergo a typical pool boiling process. To achieve a high heat transport rate through the heating surface and the liquid pool in a heat pipe, nucleate boiling is the stage for the liquid pool of the working fluid to operate at. The superheat requirements for nucleate boiling in the liquid pools were reported when potassium and sodium were chosen as the liquids[81, 82]. These were also confirmed in this study.

Figure 5.4 shows the superheat requirement for nucleate boiling in the liquid pool in a vertical gravity-assisted heat pipe with sodium as the working fluid. In Figure 5.4, as determined in the present study, curve #1 is the pool temperature, while curve #2 is the saturation temperature. The superheat requirement for nucleate boiling in the liquid pool varies between 60°C and 80°C for a saturation temperature ranging between 540°C and 570°C.

In addition to the measurements on the sodium system, the potassium and water systems were also studied. Figure 5.5 shows the superheat requirement for nucleate boiling in the liquid pool in a vertical gravity-assisted heat pipe with potassium as the working fluid. In Figure 5.5, curve #1 is the pool temperature, while curve #2 is the saturation temperature. The superheat requirement for nucleate boiling in the liquid pool varies between 60°C and 80°C for a saturation temperature between 330°C and 360°C. Figure 5.6 shows the superheat requirement for nucleate boiling in the liquid pool in a vertical gravity-assisted heat pipe with water as the working fluid. In Figure 5.6, curve #1 is the pool temperature, while curve #2 is the saturation temperature. The superheat requirement for nucleate boiling in the liquid pool varies between 5°C and 20°C.

The significant superheat in the liquid pool of the working fluid is a distinct feature which the vertical gravity-assisted heat pipe has.

Basically, there are two parts which contribute to the temperature difference between the heating surface of the bottom cap and the free surface of the liquid pool. One is the temperature difference between the heating surface of the container and the adjacent liquid. The other is the superheat in the liquid pool.

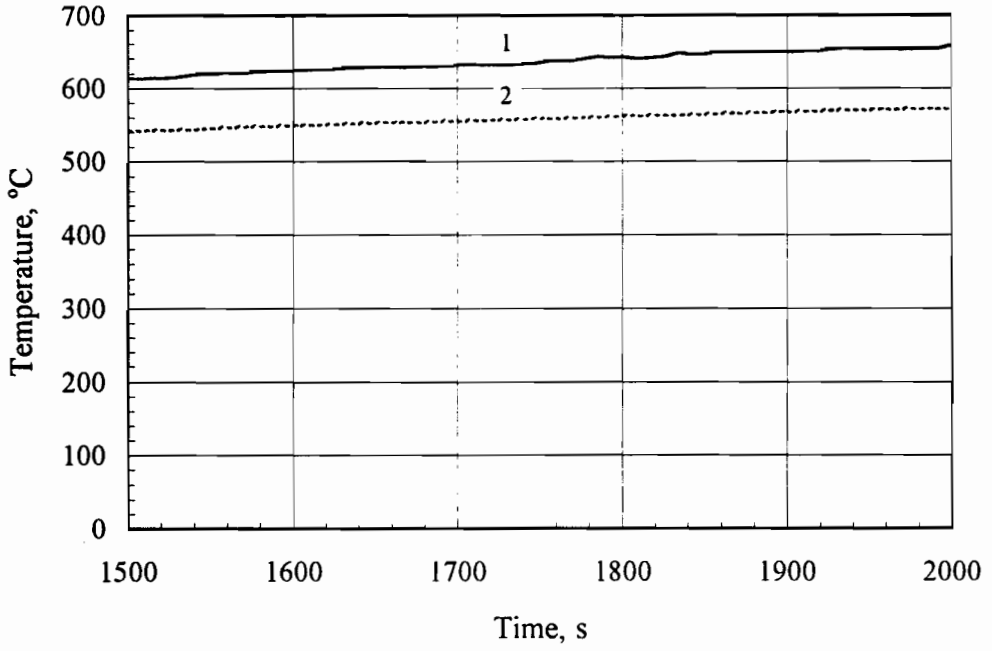

Figure 5.4 Temperature profile of a sodium heat pipe

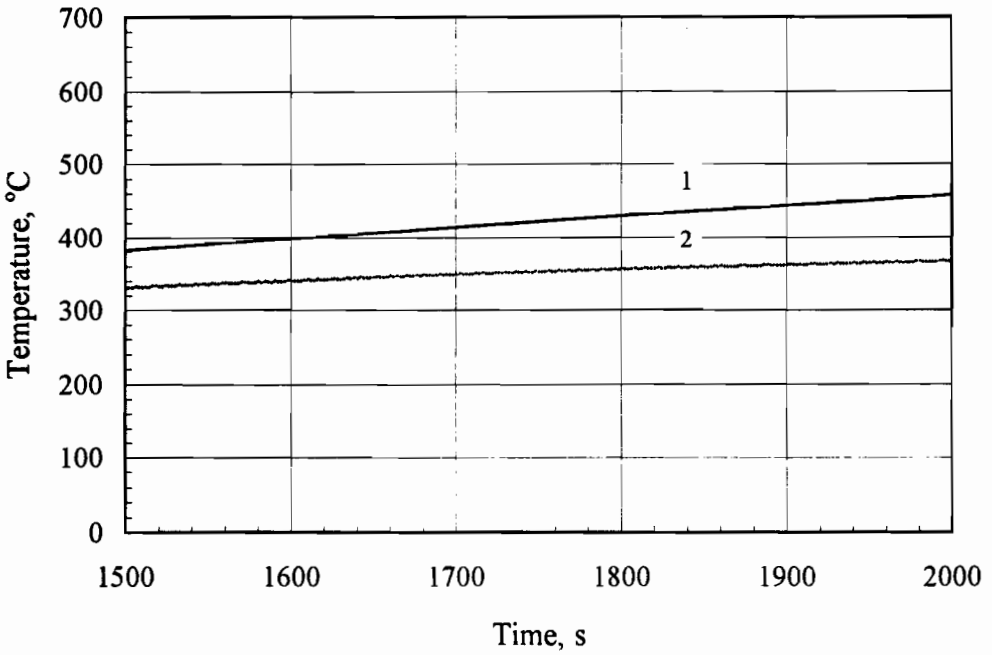

Figure 5.5 Temperature profile of a potassium heat pipe

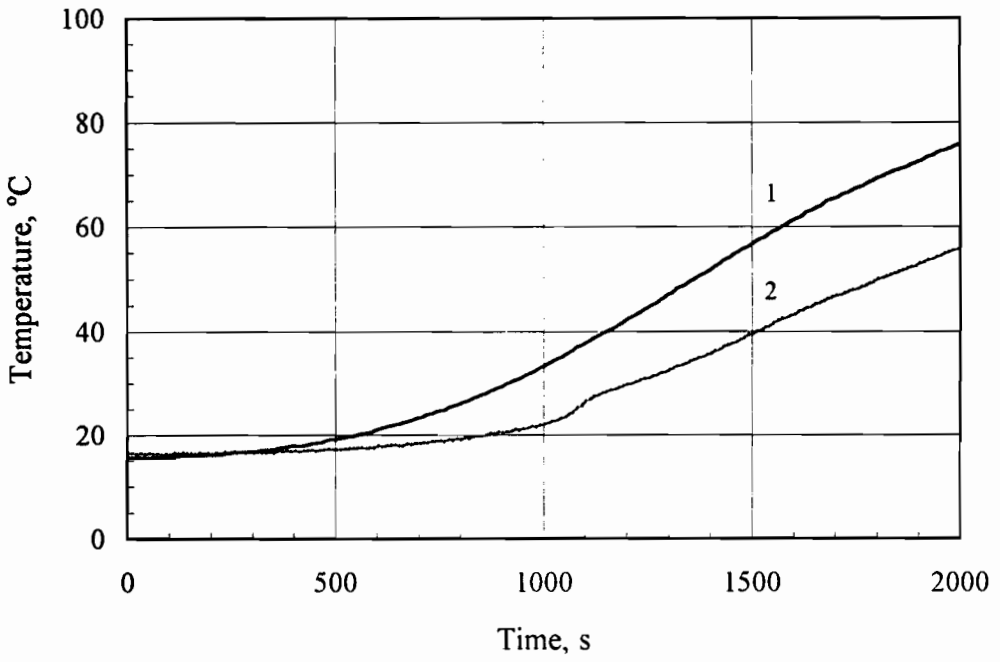

Figure 5.6 Temperature profile of a water heat pipe

It has been well documented that partial film boiling and film boiling have to be prevented because of a huge temperature difference between the heating surface and the bulk of the liquid. On the other hand, free convection boiling cannot be maintained for high heat transport rates. Therefore, to achieve the best heat transport results from pool boiling, the most useful regime is nucleate boiling.

5.2.4 Temperature Profile of Nucleate Boiling

As described in the last section, the most important regions for achieving high heat transfer coefficients are the free convection boiling region and nucleate boiling region. Based on Figure 5.2, as heat flux increases, the heat transport mode in the liquid pool switches from free convection boiling to nucleate boiling. However, one parameter that should be noticed is the depth of the pool. It is another parameter, which also determines when the heat transfer mode changes from the free convection boiling to the nucleate boiling as heat flux increases.

Suppose a pool of sodium undergoes free convection boiling. If heat is applied to the bottom and the side-wall of the container, and the heat fluxes on the bottom and on

the side-wall are the same, then, the temperature difference through the pool is a function of the heat flux applied on the container-wall and the depth of the pool. If the pool is stationary (i.e. motion is negligible), the relationship between the temperature difference, the heat flux, and the depth can be determined by the basic law governing heat conduction:

$$\dot{q}'' = k\frac{\Delta T}{\Delta x} \tag{5. 6}$$

For example, the evaporator of a 600 mm long heat pipe with 25.4 mm O.D. and 1.65 mm wall thickness is exposed to 875°C hot furnace environment and the heat pipe operates at 600°C. If the emissivity of the evaporator is 0.8 and ambient temperature is 27°C, then, the heat flux on the free surface of the liquid pool is given in Table 5.1. Assuming the heat flux applied to the evaporator is the same, the smaller the depth of the liquid pool is, the smaller the total surface area of the evaporator immersed in the liquid pool is. Therefore, the heat flux on the top free surface of the liquid pool is proportional to the depth of the liquid pool. According to Figure 5.3, 81°C of superheat in the liquid pool is required to have the heat transfer mode change from free convection boiling to nucleate boiling while the saturation temperature is 600°C. Then, the thickness of the free convection boiling layer can be calculated by Eq. 5.6 , and is shown in Table 5.4, assuming the thermal conductivity of sodium at 600°C is 64.6 W/m-°C. Therefore, for the conditions given in the above example, nucleate boiling will not occur when the depth of the liquid pool is less than 20 mm, because the thickness of the free convection boiling layer is bigger than the actual depth of the liquid pool. The temperature difference through the layer of free convection boiling decreases as the depth of the liquid pool decreases from 20 mm. The temperature difference through the layer of free convection boiling can be significantly smaller than the superheat required by nucleate boiling when the depth of the liquid pool is small enough. For instance, the temperature difference for nucleate boiling is 81°C for this case, but the temperature difference through the liquid pool is only 7.7°C when the depth of the liquid pool is 5 mm, and 22.8°C for 10 mm. However, nucleate boiling will occur when the depth of the liquid pool is slightly bigger than 20 mm.

Based on the analytical results presented above, 5 to 10 mm depth of liquid pool is ideal for the heat pipe, because the temperature differences are much smaller than the superheat required for nucleate boiling. Unfortunately, 5 mm depth of liquid pool with 22.098 mm internal diameter translates to 1.5 grams in weight for sodium at 600°C. Thus, in practice, it is not practical to fix the depth of liquid pool to 5 or 10 mm because of the dynamic features of the heat pipe and because of the amount of the working fluid required at the startup stage. This leaves a big question mark on how to find a practical way to control the temperature difference through the liquid pool to within a much smaller range

(say 10 to 15°C) than the superheat required by nucleate boiling, when the liquid in the pool has to transfer heat by the nucleate boiling mode.

Table 5.1 The heat flux on the evaporator

Depth of the liquid pool (mm)	Heat flux on top free surface of the liquid pool (W/m^2)	Thickness of free convection boiling layer (mm)
10	0.147×10^6	35.6
20	0.242×10^6	21.6
30	0.337×10^6	15.5
40	0.432×10^6	12.1
50	0.527×10^6	9.9

5.3 Possible Solution for Reducing Superheat in Nucleate Boiling

As mentioned in the last section, for a vertical gravity-assisted heat pipe with an alkali metal as working fluid, the depth of liquid working fluid pool is usually more than 20 mm depending on the size of the evaporator and total length of the heat pipe. For most of the high temperature applications of heat pipes, the heat transfer mode in liquid pools is nucleate boiling.

As mentioned in Section 5.2, the superheat required for nucleate boiling is a function of the radius of bubbles in the liquid pool, and the radius of the bubbles is decided by the size of nucleation sites. The smaller the size of the nucleation site is, the higher the superheat in the liquid pool that is required. To achieve smaller superheat, the size of the nucleation sites should be increased. However, the size of nucleation sites is a function of the quality of the internal surface of container wall, and not much difference can be made to physically increase the size of nucleation sites on the internal surface of the container wall. Typically, the radii of the bubbles are between 1 to 10 micrometers.

It has been shown that a way for reducing the superheat in nucleate boiling is to increase the radius of bubbles, and it needs to be done by some method other than physically increasing the size of the nucleation sites on the internal surface of the container wall.

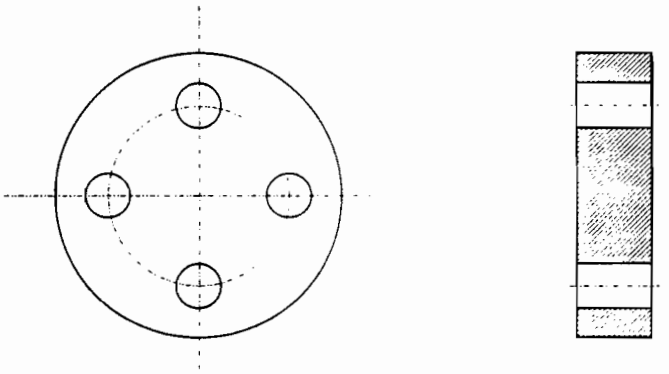

Figure 5.7 Schematic diagram of a temperature stabilizer

5.3.1 Proposal

Much attention was paid to this aspect in this study. Six vertical gravity-assisted heat pipes were made to investigate the superheat phenomenon of nucleate boiling in the liquid pool. One possible solution which was found during this study is to separate the liquid pool into two parts at the place of 5 to 10 mm above the bottom by using a plate with a few holes on it. In the pool below the plate, the heat will be transported by free convection boiling. In the pool above the plate, the heat will be transported by nucleate boiling. Using this method, the superheat requirement for the nucleate boiling in the liquid pool above the plate may be controlled to within 15°C, because it is no longer the function of the amount of the liquid in the pool. Figure 5.7 shows a drawing of a piece of plate which needs to be embedded in the liquid pool to initiate the much bigger bubbles than normal bubbles with the radius between 1 and 10 micrometers. Practically, it is an easy solution. For implementation of the new method, the plate made from the same material as that of the container is fixed in the liquid pool parallel to the upper surface of the bottom cap with a 5~10 millimeter gap in between. There are a number of holes, usually 3 to 5 holes, normal to the surface of the plate. The holes are usually about 3 mm in diameter through the plate. This plate is referred to as a temperature stabilizer in this study. The purpose of the temperature stabilizer is to reduce the difference between the liquid temperature and the saturation temperature to the minimum. Figure 5.8 shows two diagrams of before and after the modification at this stage. The following is an explanation of how the temperature stabilizer works to reduce the superheat in the liquid pool.

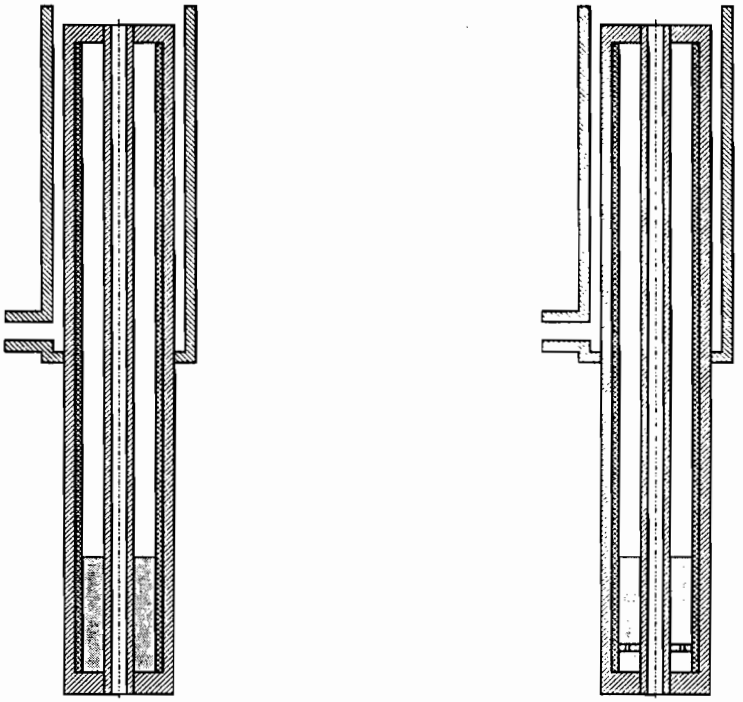

Figure 5.8 Schematic diagrams of heat pipe before (a) and after (b) the modification of reducing the superheat in its liquid pool

5.3.2 Mechanism

In a vertical gravity-assisted heat pipe with the proposed temperature stabilizer in the liquid pool, the liquid pool is separated by the temperature stabilizer into two sections. The heat transfer modes are different in these two sections.

In the bottom section, it usually undergoes free convection boiling. Because the depth of the bottom section is only about 5 mm, the superheat can only be 7.7°C if the operating temperature of the heat pipe is 600°C and the heat source is about 875°C. From the example given in Section 5.2, it has been shown clearly that under the same heat fluxes in a liquid pool of about 5 mm depth the temperature difference can be an order of magnitude less than the superheat required for nucleate boiling in a pool of several times

the depth of 5 mm. Based on the observation in this study, there is no perfect contact between the liquid and the bottom surface of the temperature stabilizer, which means there is a free liquid surface in the bottom section. Vapor generated on the free liquid surface is forced to go through those holes on the temperature stabilizer. Generally, at relatively low heat load, the bottom section works as a heat pipe while the bottom surface of the temperature stabilizer works as the condenser. As heat load increases, at some point the evaporation will exceed the condensation in the bottom section, which leads to some vapor generated in the bottom section to go into the top section through the holes on the temperature stabilizer.

In the top section, when there is no vapor getting into it from the bottom section, it performs as a regular liquid pool, low superheat for free convection boiling and high superheat for nucleate boiling. When there is vapor getting into it from the bottom section, the size of the bubbles is no longer 1 to 10 micrometer as generated by the nucleation sites. If it is assumed that vapor forms spherical bubbles when it gets into the top section and the radius of the spherical bubbles equals the radius of those holes on the temperature stabilizer, it is clear that the radii of the new bubbles are orders of magnitude bigger than that of the initial bubbles generated in the nucleation sites on the heating wall. According to Eq. 5.4, the pressure difference will decrease as the radius of the bubbles increases. Therefore, the superheat in the top section will be significantly reduced as the bubble size increases from 1 to 10 micrometers to more than 1000 micrometers.

5.3.3 Experimental Results

Based on the better understanding of the boiling process in liquid pool, and the development of the temperature stabilizer, a number of heat pipes and heat pipe cooled injection lances which incorporated the temperature stabilizer were designed, fabricated and tested. As to be shown, they all worked as expected and reduced the superheats substantially.

Figure 5.9 shows the experimental result of a vertical gravity-assisted heat pipe with sodium as working fluid. In Figure 5.9, curve 1 represents the temperature in liquid pool, and curve 2 represents the saturation temperature in the evaporator. The difference between curve 1 and curve 2 represents the superheat of the liquid sodium. In this sodium heat pipe, thermocouple #1 was positioned in the bottom section of the liquid pool. In Figure 5.9, temperature curves can be divided into three regions on time axis. The first region is the one from 0 to 180 seconds, the second region is the one from 180 to 2400 seconds, and the third region is the one after 2400 seconds. In the first region, the temperature in the liquid pool was lower than the temperature in the rest of the evaporator

because of different thermal mass in these two sections. After the heat pipe was heated for 180 seconds, the temperature of the liquid sodium caught up, and then passed over the saturation temperature in the rest of the evaporator. In the second region, the superheat of the liquid increased to as big as 100°C as if the temperature stabilizer was not in the liquid pool because the temperature stabilizer was not functioning. At 2400 seconds, the temperature stabilizer started to function as shown on curve 1 and curve 2. When the temperature stabilizer started to work, the temperature of the liquid decreased as much bigger bubbles passed through the liquid pool, and the saturation temperature in the rest of the evaporator increased slightly at the same time, which indicates the heat pipe worked more efficiently. The superheat of the liquid sodium was reduced to about 25°C, which is substantially smaller than the superheats on those heat pipes and heat pipe cooled injection lances prior to the modification.

Figure 5.10 shows the experimental result of a vertical gravity-assisted heat pipe cooled injection lance with potassium as working fluid. In Figure 5.10, curve 1 represents the liquid temperature, and curve 2 represents the saturation temperature. In this potassium heat pipe cooled injection lance, thermocouple #1 was positioned right above the temperature stabilizer in the top section of the liquid pool. In Figure 5.10, there are two peaks on curve 1. At time 300 seconds, curve 1 peaked out. It indicates that the temperature stabilizer started to work. Between 350 and 950 seconds, the temperature stabilizer was working, and the superheat of the liquid was a function of the saturation temperature of the heat pipe. It is shown in Figure 5.10 that the superheat decreased as the saturation temperature increased. Between 950 and 1050 seconds, the curve 1 peaked out again. This peak indicates how big the superheat of the liquid can be if the temperature stabilizer was not working. After the second peak, the superheat of the liquid was about 5°C, which is substantially smaller than the superheats on those heat pipes and heat pipe cooled injection lances prior to the modification.

Figure 5.11 shows the experimental result of a vertical gravity-assisted heat pipe cooled injection lance with water as working fluid. In Figure 5.11, curve 1 represents the temperature of water, and curve 2 represents the temperature of steam above the liquid pool. As in the potassium heat pipe cooled injection lance, thermocouple #1 was positioned right above the temperature stabilizer in the top section of the liquid pool. In Figure 5.11, both curve 1 and curve 2 indicated that the temperature stabilizer made three attempts to become functional, and finally, it stayed functional. During the period of the temperature stabilizer staying functional, the superheat of the liquid was within 2°C, which is substantially smaller than the superheats on those heat pipes and heat pipe cooled injection lances prior to the modification also.

5.3.4 Boiling Signal from Modified Heat Pipes

The working mode of the temperature stabilizer not only can be identified from the temperature difference but also can be identified by the sound caused by big bubbles breaking the surface of the pool. Our tests with sodium, potassium, and water were consistent and in all cases a pinging sound was initiated as the temperature stabilizer began to function. The sound persisted as long as the stabilizer functioned. If the stabilizer stopped working, the sound ceased.

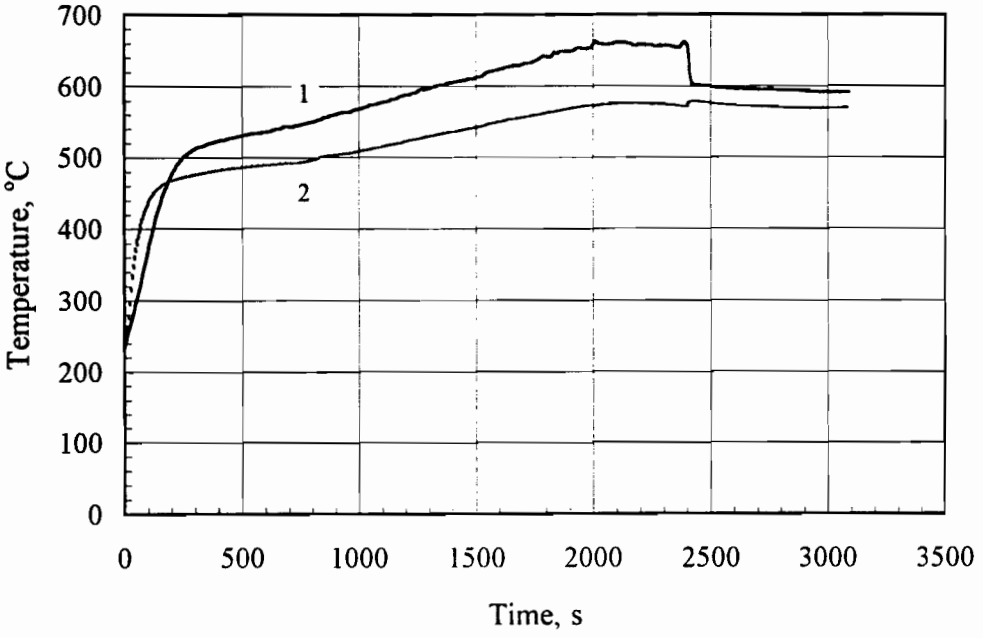

Figure 5.9 Temperature profile of a sodium heat pipe with temperature stabilizer

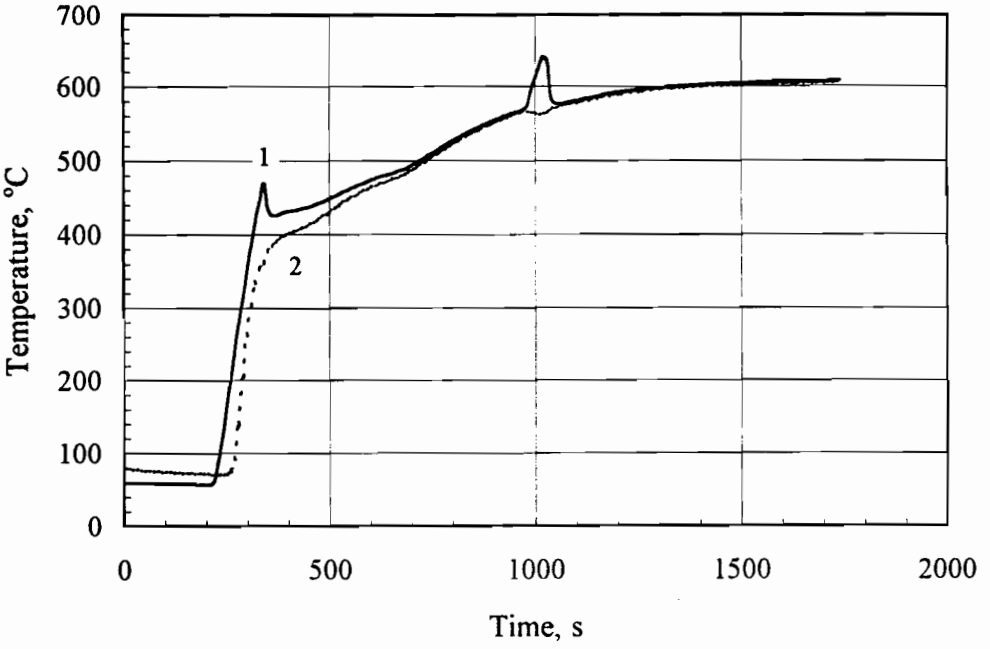

Figure 5.10 Temperature profile of a potassium heat pipe with temperature stabilizer

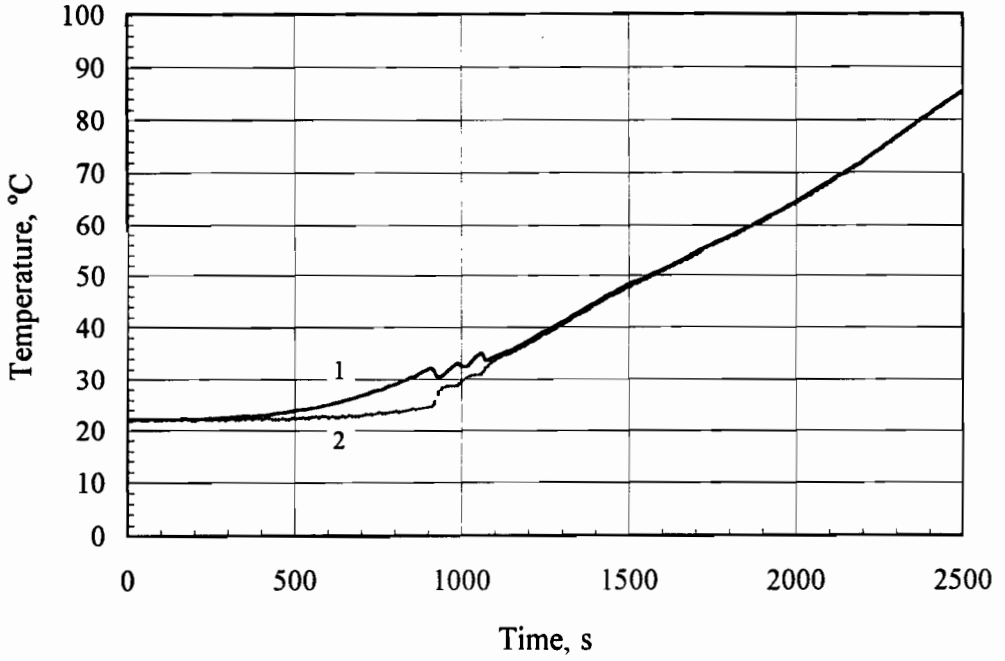

Figure 5.11 Temperature profile of a water heat pipe with temperature stabilizer

CHAPTER 6

MASS BALANCE OF WORKING FLUID IN HEAT PIPE COOLED INJECTION LANCES

In this chapter, the study is extended to heat pipe cooled injection lances. The mass balance of working fluids in heat pipe cooled injection lances is studied.

6.1 Introduction

The mass balance of working fluid is not a new concept in heat pipe technology. In steady-state a liquid working fluid has to cover the entire evaporator, and the quantity of the working fluid that is evaporated has to equal the quantity of the working fluid that is recycled by capillary forces from the condenser to the evaporator. Basically, this is the concept of the mass balance of working fluid in heat pipes.

Typically, the mass balance of working fluid in heat pipes is not of concern. In a basic heat pipe the condensed working fluid will only be removed to the evaporator along the inner surface of the pipe shell by capillary forces. In a gravity-assisted heat pipe working fluid will be recycled from the condenser to the evaporator on the inner surface of the pipe shell by both capillary forces and the gravitational force. Nothing is changed for calculating the mass balance of working fluid for an annular heat pipe[76] because the inner pipe is not used specifically for heating or cooling purpose. Usually, the mass balance of working fluid in these heat pipes is controlled by the capillary limit. These heat pipes can

operate without getting into the problem of the mass imbalance as long as the heat transport rates are lower than the capillary limit. Because the mass balance is measured by the capillary limit for these heat pipes, it was taken for granted that the same rule applies to the patented annular heat pipe cooled injection lances. Unfortunately, it is not the case for an annular heat pipe cooled injection lance as the results from this study will show.

With respect to physical configurations there is no difference between an annular heat pipe and an annular heat pipe cooled injection lance. The only difference between these two is the boundary condition applied to the inner pipe. Generally speaking, there is no gas (or coolant) that goes through the inner pipe during the normal operation of an annular heat pipe, however, there is always a reagent that goes through the inner pipe during the normal operation of an annular heat pipe cooled injection lance because that is what the inner pipe is for. It was found out in this study that the reagent gas may cause mass imbalances in some cases when the reagent gas goes through the inner pipe of a vertical gravity-assisted heat pipe cooled injection lance. In other words, the different boundary conditions applied on the inner surface of the inner pipe may lead to discrepancies when calculating the mass balance of working fluid. For the patented annular heat pipe cooled injection lance the capillary limit that is used for a typical heat pipe is not enough to represent the mass balance of the working fluid. Therefore, the mass balance of the working fluid for an annular heat pipe has to be reconsidered, and a new methodology developed.

In the patented annular heat pipe cooled injection lance, the entire length of the reagent conduit pipe acts as a condensing surface for the vaporized working fluid. This is so because in the vast majority of cases the reagent is introduced into the lancing system at a temperature that is relatively low in comparison to the operating temperature of the lance. The working fluid condensed on the outer surface of the inner pipe flows down toward the lance nozzle and into the liquid pool of the working fluid accumulated at the nozzle region. This liquid returning via the central conduit is effective in cooling the nozzle and the immediate evaporator region. If the non-evaporator section of the heat pipe shell is configured in such a way that it can dissipate heat, it will condense working fluid. The quantity that it condenses together with that condensed on the inner conduit comprises the total condensed and must at steady state equal the total quantity of working fluid that is evaporated from the entire evaporator section. With the annular arrangement stipulated in the patented heat pipe cooled injection lances, the upper section of the evaporator is fed liquid working fluid only originating from condensation on the outer pipe while the lower section of the evaporator is fed liquid originating from condensation on the inner conduit. The nozzle and leading end section of the lance will accumulate a

quantity of working liquid because of the initial imbalance between the rate at which the working liquid flows down the central conduit and the rate at which the working fluid is vaporized from the leading section of the lance. A portion of the evaporator located between the upper and lower sections will under conditions of high heat transfer become deficient in working fluid with the result that this intermediate region straddling the upper and lower regions operates in 'dry-out' mode. In effect, there is at steady state an excess of liquid in the lower section and deficiency of liquid working fluid in the intermediate section of the evaporator. The result is that this intermediate section of the pipe is not cooled by evaporating working fluid and hence heats up to a temperature approaching that of the hot furnace environment. Since cooling of the entire evaporator is a necessity to avoid failure by chemical attack, or by high temperature corrosion or simply by fusion (i.e. 'burn-out'), then, it stands to reason that non-cooled portions of the evaporator ultimately will fail.

To clarify this issue, assume that the wick in a patented annular heat pipe cooled injection lance has no ability of pumping working fluid up from liquid pool and that the lance is in the vertical position; then there is no possibility for the liquid working fluid to move upwards against gravity. To achieve the mass balance of working fluid at steady-state in this pipe, the quantity of the working fluid condensed on the outer surface of the inner pipe must be less than or equal to the quantity of working fluid evaporated from the liquid pool of the working fluid. Thus, if any quantity of the working fluid evaporated from the liquid pool condenses on the inner surface of the outer pipe, the condensed working fluid will be recycled from the condenser to the liquid pool via the evaporator by gravitational and capillary forces. Otherwise, if the quantity of the working fluid condensed on the outer surface of the inner pipe is more than the quantity of the working fluid evaporated from the liquid pool of the working fluid, some quantity of the working fluid evaporated from the inner surface of the outer pipe will have to be condensed on the outer surface of the inner pipe. Obviously, this quantity of the liquid working fluid can flow down to the liquid pool, however, based on the assumption made earlier it has no chance to go upwards to the place where it is evaporated to complete the cycle. Therefore, steady-state will no longer exist, with the result that the evaporator will not be covered completely, and thus dry-out regions will develop on the part of the evaporator which has no liquid working fluid on it. Overall, if the quantity of the working fluid condensed on the outer surface of the inner pipe is more than the quantity of the working fluid evaporated from the liquid pool of the working fluid, the evaporator region right above the liquid pool of the working fluid will have no liquid working fluid to be evaporated and will be heated up and approach the hot furnace temperature. This hot

region is expected to appear as a ring because of the wick structure on the inner surface of the evaporator. This occurrence has been termed the 'hot-ring' in this study. The phenomenon of the 'hot-ring' will be demonstrated in the example to follow.

As mentioned in Section 4.1, a hot-spot on a wickless heat pipe was identified by simply pulling the pipe out from a hot environment during normal steady-state operation. It can also be identified by monitoring temperatures on the evaporator along the axis of the heat pipe. Since then, all the heat pipes and heat pipe cooled injection lances, including patented heat pipe cooled injection lances used in this research, were examined in the same way in this study. However, no hot-ring was observed. The question which needs to be answered is why the hot-ring was not observed on all the laboratory scale patented heat pipe cooled injection lances. To answer this question, the role of the wick in heat pipes needs to be examined further.

It was assumed in the previous analysis that the wick structure cannot pump liquid from the liquid pool of working fluid. In reality capillary forces can indeed pump liquid working fluid up from liquid pool, and the ability of capillary forces can be determined easily. Based on the analysis presented in Section 3.1.1, the capillary limit for a heat pipe can be calculated by Eq. 3.12b. However, compared to the gravitational force, the capillary force is much weaker. That is why it was almost to everyone's surprise that the capillary force can be used successfully to recycle liquid working fluid from the condenser to the evaporator in two phase heat transport devices (i.e. heat pipes) when they were invented in 1964. Nonetheless, the capillary force can indeed remove the liquid working fluid from the condenser to the evaporator when the heat pipe is in the vertical position.

Table 6.1 Capillary limit for different orientations

Orientation	Capillary limits (W/m^2)
Vertical (evaporator below condenser)	4.57×10^6
45° inclined (evaporator below condenser)	3.52×10^6
Horizontal	1.00×10^6
45° inclined (evaporator above condenser)	-1.52×10^6
Vertical (evaporator above condenser)	-2.57×10^6

Generally, the capillary force can circulate working fluid between two points within a wick structure if the cavities of the working fluid on the wick are different at

these two points. Table 6.1 shows capillary limits for five different orientations of the heat pipe which was designed for this part of the study. In Table 6.1, the results show that the capillary force can circulate the working fluid with different rates for the first three positions, but it can not circulate the working fluid for the last two positions. Apparently, the capillary force does not have the ability to pump the working fluid all the way up (i.e. 500 mm) against the gravitational force if the heat pipe is positioned vertically, and the evaporator is on top of the condenser.

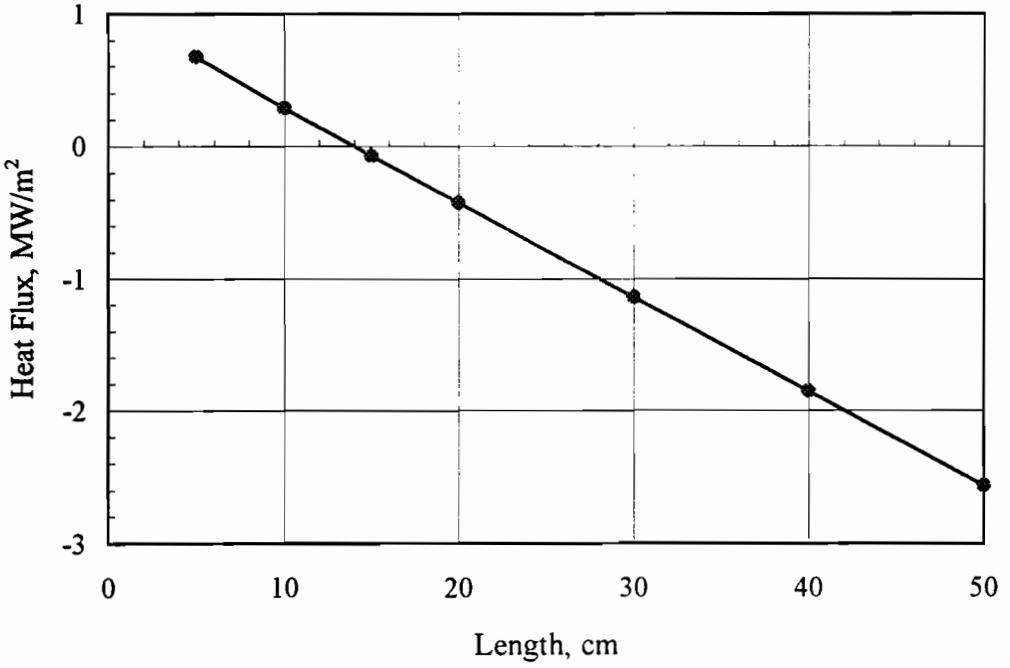

Figure 6.1 Capillary pumping ability for a sodium heat pipe with two-wraps of 100 mesh stainless steel screen as wick

Typically, the capillary force is used for removing working liquid from the condenser to the evaporator in a basic heat pipe. But for the situation being discussed here, the question is not whether the capillary force can remove the working fluid from the condenser to the evaporator. It has been shown in Table 6.1 that for a vertical gravity-assisted heat pipe the capillary limit may be as big as 4.57×10^6 W/m^2. Obviously, it is big enough for most of applications. The question however is how much the capillary force

can do to move working liquid from the liquid pool up to the evaporator when there is not enough working fluid returning from the condenser to cover the entire evaporator.

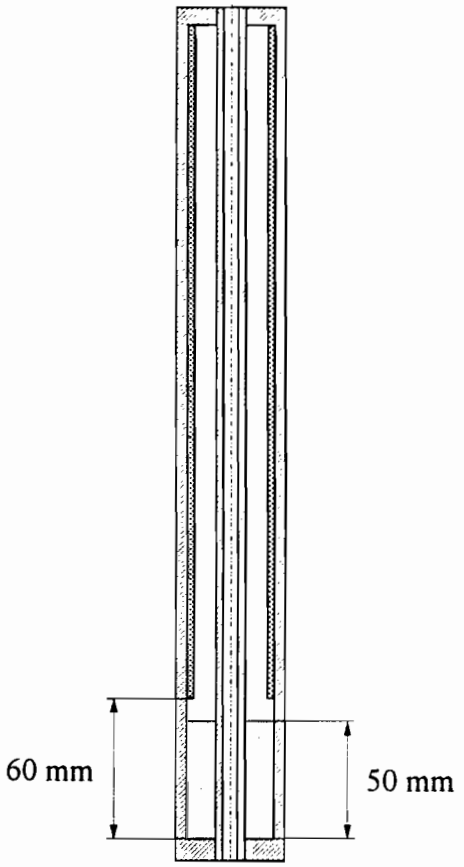

Figure 6.2 Schematic diagram of a heat pipe cooled injection lance employed to investigate the mass balance of working fluid

For a vertical gravity-assisted heat pipe, Figure 6.1 shows the capillary limit for a wick structure of two layers of 100 mesh stainless steel to pump liquid sodium straight up at 600°C. The result shows that the capillary force can indeed pump the working fluid up for about 140 mm against the gravitational force, as shown in Figure 6.1. Since for all the laboratory scale patented heat pipe cooled injection lances the depth of the liquid pool of working fluid was about 50 mm, the working fluid from the liquid pool pumped by

capillary force may cover up to 190 mm of evaporator from the bottom cap. Since the sizes of the evaporators of all the laboratory scale patented heat pipe cooled injection lances never exceeded 200 mm, it stands to reason that as long as the working fluid coming from the condenser covers at least 10 mm of the evaporator, the entire evaporator is covered. This explains why the hot-ring was not observed on the patented heat pipe cooled injection lances developed for laboratory testing.

However, the laboratory scale heat pipe cooled injection lance is not a final product. To commercialize heat pipe cooled lancing technology, heat pipe cooled injection lances need to be scaled up. Since the capillary force is not a function of the size of a heat pipe, it cannot be scaled up along with the heat pipe. Therefore, just because no hot-ring appeared on the laboratory scale annular heat pipe cooled injection lance does not mean that there will be no hot-ring for the bigger scale annular heat pipe cooled injection lances. For commercializing heat pipe cooled lancing technology in the future, the mass balance of working fluid on the evaporator needs to be investigated.

For large scale heat pipe cooled injection lances, the problem associated with the patented heat pipe cooled injection lances is likely the mass imbalance of working fluid. The mass imbalance may result in a dry section on the evaporator. It is termed as a 'hot-ring', similar to the hot-spot phenomenon that was seen on the wickless heat pipe, and the hot-bottom phenomenon that appeared on the variable-conductance alkali heat pipe when most of working fluid was frozen in the inert gas section.

6.2 Identification of Mass Imbalance

The phenomenon of the mass imbalance in a sizable annular heat pipe cooled injection lance was predicted based on theoretical analysis in this study. To validity the conclusion of the analysis, an annular heat pipe with sodium as working substance was designed, fabricated, and tested. The pipe was about 500 mm long. The inner tube was 6.35 mm in outside diameter with 0.89 mm wall thickness, and the outer tube was 25.4 mm in outside diameter with 1.65 mm wall thickness. Two layers of 100 mesh stainless steel screen were used as wick for the pipe. It should be noted that a modification to the wick structure was made only to this annular heat pipe cooled injection lance. Details of the modification and the ensuring results follow.

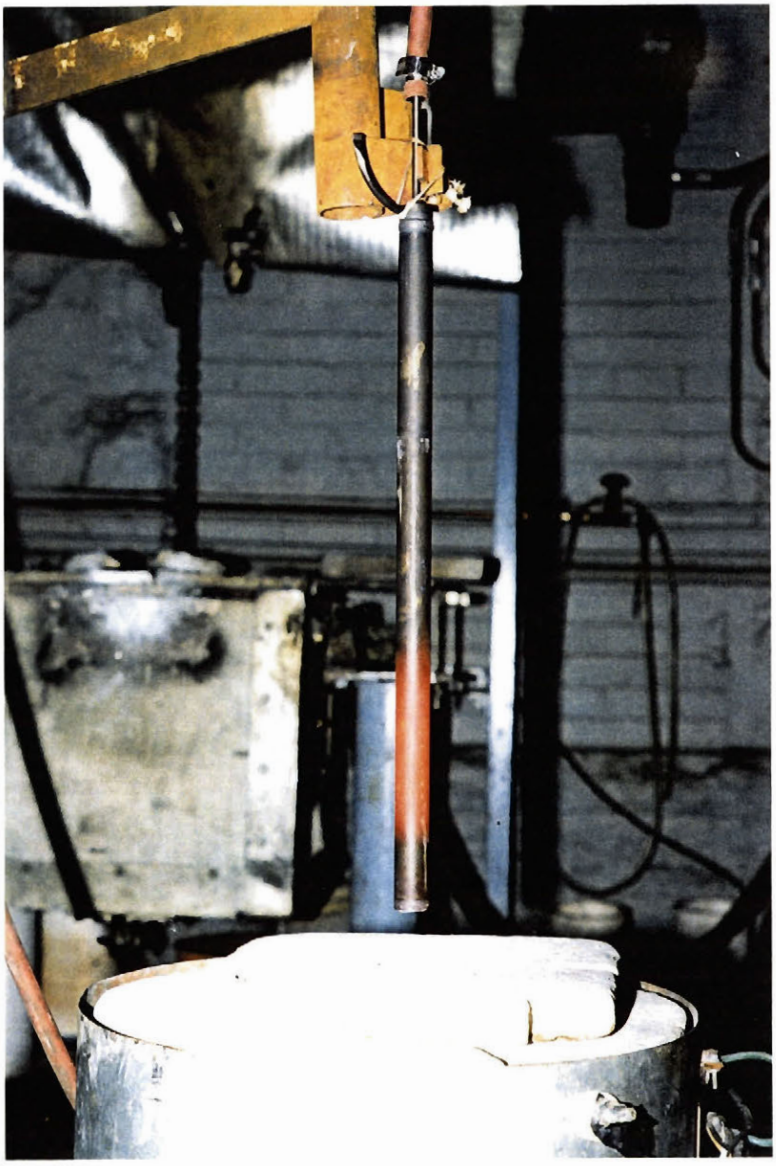

Figure 6.3 Photograph of a hot-ring with the cooling rate of reagent at 0.15 Nl/s

Because of the restriction of this study, the hot-ring phenomenon could only be studied in the laboratory. However, based on the analysis conducted in the last section and the observation in this study, the hot-ring phenomenon would not appear on small scale annular heat pipe cooled injection lances. In order to study the mass imbalance of working fluid in the laboratory, it was necessary to disable the function of wick structure from moving liquid working fluid from the liquid pool to the rest of the evaporator by the capillary force.

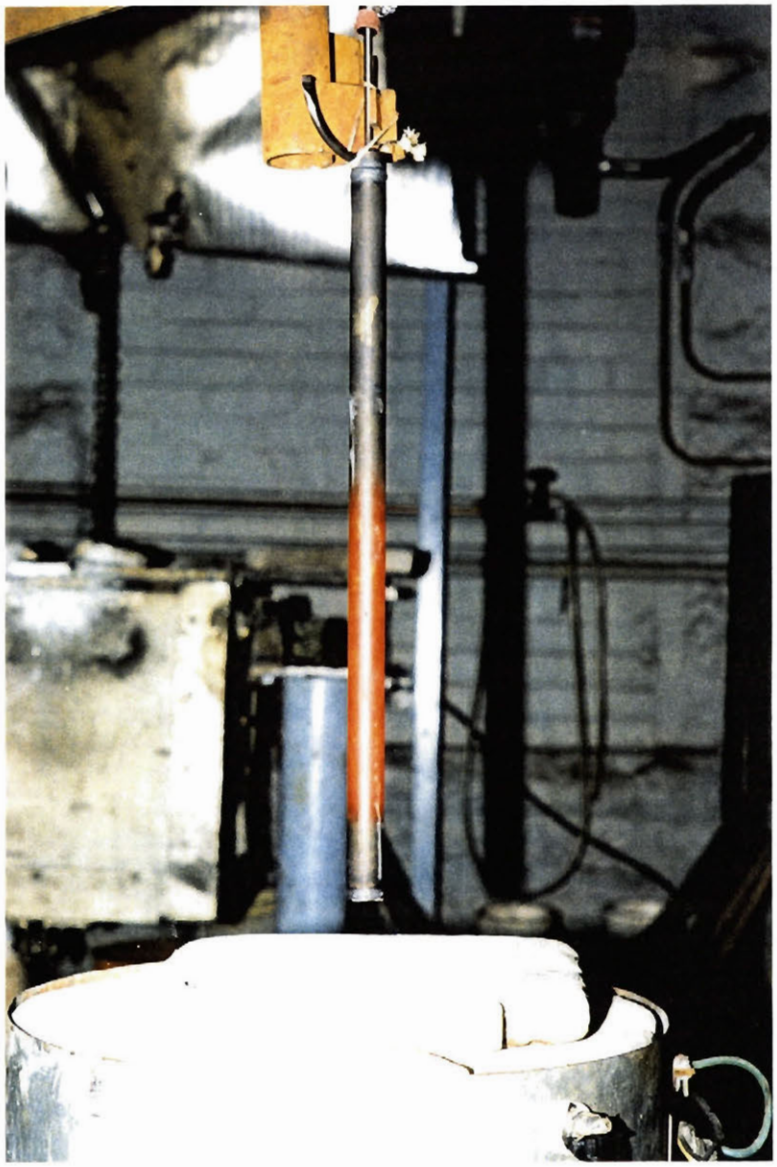

Figure 6.4 Photograph of a hot-ring with the cooling rate of reagent at 0.40 Nl/s

Given the constraints in the laboratory, one can make sure that working fluid has no way to be pumped up by positioning the wick in the sodium heat pipe to cover the entire inner surface of the heat pipe shell except for the lowest 60 mm of the evaporator, in which the pool of working fluid occupied the lowest 50 mm of the evaporator. Basically, between the surface of the liquid pool and the lowest point of the wick on the inner wall of the heat pipe shell there was a 10 mm gap with no wick to cover the inner surface of that portion, as shown in Figure 6.2. The heat pipe operated vertically as a

gravity-assessed heat pipe. When there was no reagent going through the inner tube, the pipe worked as an ordinary heat pipe, which means there were no hot-spots, no working fluid freeze up, and no hot-bottom occurred on and in the pipe. The mass imbalance of the working fluid did not occur. However, as it was predicted theoretically, the heat pipe lost its isothermal characteristics when there was reagent going through the inner tube and flowrate was big enough. Under this circumstance the heat pipe can be visually divided into three sections from the bottom to the top - cold, hot, and cold sections. This phenomenon is shown in Figure 6.3. In Figure 6.3, the picture was taken right after the pipe was pulled out from an electric resistance furnace with 0.15 Nl/s of air passing through the inner pipe.

As expected, the size of the hot-ring was proportional to the flowrate of reagent. Figure 6.4 shows another picture under the same operating conditions as Figure 6.3 except for the flow rate. The flow rate of the reagent for this case was 0.40 Nl/s. One can clearly see that the size of the hot ring was increased when the flow rate of air was increased. As detailed above, the enhanced cooling with the higher air flowrate resulted in more condensation on the inner pipe (and less on the outer pipe) with the net effect of a drier evaporator.

6.3 Possible Solutions to the Mass Imbalance

There are a number of solutions that have been identified which follow two avenues of thinking. One is to physically move the liquid working fluid condensed on the outer surface of the inner pipe to the inner surface of the outer pipe shell at the condenser-evaporator interface. It can be done by gathering the liquid working fluid condensed on the outer surface of the inner pipe at the interface of the condenser and evaporator, and redirecting it to the inner surface of the outer pipe. The other direction is to reduce the quantity of the liquid working fluid condensed on the outer surface of the inner pipe, and to make it less than that of the working fluid evaporated from the liquid pool of working fluid. This can be done either by insulating the inner pipe, or by preheating the reagent gas before it enters the central conduit. In this study the method of preheating the reagent gas was adopted. In reality, there are two ways to preheat the reagent gas. It can be heated up either before entering the lancing system or after entering the lancing system. In this study the second option was chosen.

The patented annular heat pipe cooled injection lance called for the conveying of reagent through the central conduit spanning the entire length of the lance, the present

new generation of heat pipe cooled injection lances calls for conveying the reagent through a jacket which is applied on the outer surface of a portion of the condenser wall. The jacket ideally is located directly above the evaporator. The lowermost segment of the jacket is connected to an opening in the outer wall of the heat pipe. The hole in the outer wall of the heat pipe is fitted with a conduit which carries the reagent to the tip of the lance. Thus, the reagent enters the jacket, is preheated and subsequently leaves the jacket and continues into the evaporator traveling through a central conduit to the nozzle. The jacket is configured and sized so that most of the preheating of the reagent occurs in the jacket. In this way the reagent is preheated by the energy extracted from the condensation of working fluid on the inner wall of the outer pipe with only limited condensation on the outer surface of the new inner conduit.

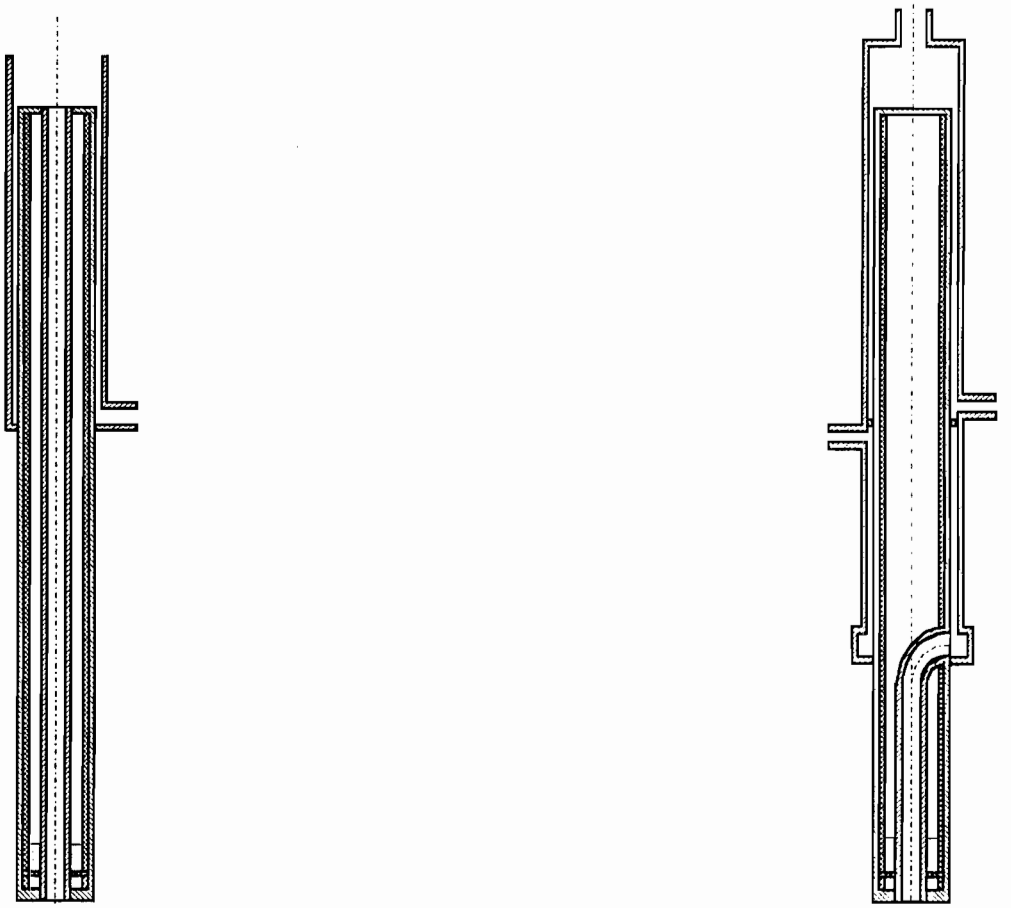

Figure 6.5 Schematic diagrams of heat pipe cooled injection lances before (a) and after (b) the modification of ensuring the mass balance of working fluid

While the importance of preheating has not been discussed, it must be noted that preheating of the reagent is, in many metallurgical applications, a desirable feature which can have substantial financial benefits. Moreover, it promotes greater energy utilization efficiencies and lower entropy generation. Thus, the degree of preheating should, under normal circumstances, be optimized. As the incentives for preheating are great, the existing heat pipe technology utilizing an annular configuration (U.S. Patent 5,310,166) capitalizes on the preheating of reagent but in so doing subjects portions of the lance to insufficient cooling and the resultant creation of a hot-ring.

The preheating jacket is an essential feature of the findings of the present study which overcomes the limitation of hot-ring formation in high temperature metallurgical applications by removing the central conduit from the condenser section and instead having the reagent flow through an outer jacket. In this way, working fluid is forced to condense on the inner surface of the outer wall of the condenser and to flow down this wall and cool the evaporator surface. In the patented annular heat pipe cooled injection lance, working fluid condensed on the central conduit and flowed down the conduit to the nozzle. While this arrangement cooled the nozzle effectively, it did not cool the evaporator wall sufficiently.

In addition to the preheating jacket, one may incorporate another jacket which resides directly above the preheating jacket. This jacket, to be termed the cooling jacket as shown in Chapter 6, can be used to pass a fluid (e.g. air, water etc.) from the uppermost region to the lowermost region where the cooling fluid is exhausted. To avoid solidification of the working fluid in the uppermost section of the chamber, the flow of coolant can be reversed such that it enters via the lowermost section and exits the uppermost section. Regardless of the direction of the flow, one can control the degree of cooling of the upper portion of the condenser by controlling the mass flow rate of cooling fluid; thus, this new heat pipe lance features user-controllable rates of heat extraction.

Each of the jackets contains enlarged inlet and outlet headers. These allow the reagent and coolant to be homogenized and uniformly distributed. The relative length of each jacket depends on the application the lance is to be subjected to. While the desired degree of preheat for the reagent is one parameter that influences the length of the jacket to be used, other factors such as reagent flow rate must also be considered in determining the size. In the limit the lance may contain no preheating jacket with a long cooling jacket or it may contain a long preheating jacket with no cooling jacket, with a compromise between these two extremes normally prevailing.

As the jackets will typically reside outside the furnace environment, even though it is equally viable to have the jackets in whole or in part residing within the furnace, they

can be produced as half sections which snap together over the outer section of the lance and presealed by high temperature gaskets. Moreover, the jackets need not be circular in cross-section, they can be of any shape deemed appropriate for the prevailing heat transfer conditions. In the event of failure of the lance, the jackets can be removed and reapplied onto a new lance with relative ease. For applications in which lance life can be considerable, it may be more practical to weld circular jackets onto the outer body of the lance thereby avoiding the use of sealing gaskets.

The operating orientation of the lance is by no means limited to the vertical. With the proper use of a wick in the working fluid chamber and the judicious selection of jacket cross-section so as to promote greater heat extraction on the upper axial positions along the pipe as opposed to the lower axial positions, the lance can be operated at any inclination from the vertical down to the horizontal. Near-horizontal operation can be used to describe the working orientation of a submerged tuyere. All aspects of the present ideas as described for lances are equally applicable to submerged heat pipe tuyeres extending into a melt. Thus, one should construe the present ideas to encompass both lances and tuyeres equally.

The schematic diagrams of the heat pipe cooled injection lance before and after the modification at this stage are shown in Figure 6.5

6.4 Description of Design

The new generation of heat pipe cooled injection lances will now be described with reference to the accompanying drawings in which: Figure 6.6 is a diagram depicting the longitudinal cross-section of the heat pipe lance. Figure 6.7 is a view of the radial cross-section of the heat pipe lance at section F. Figure 6.8 is a view of the radial cross-section of the heat pipe lance at section G. Figure 6.9 shows the longitudinal cross-section of the annular heat pipe lance as described in U.S. Patent 5,310,166.

The longitudinal cross-section of the heat pipe cooled injection lance shown in Figure 6.6 comprises a lance body, 7 on whose inner surface is applied a wick, 8. The working fluid, predominantly in the vapor state, fills the heat pipe chamber, 15, which is defined by the lance body, 7, reagent conduit, 9, bottom cap, 23, and top cap, 21. At the leading end of the heat pipe one may find a small pool of liquid working fluid, 16. In the liquid pool, a plate, the temperature stabilizer, 18, is placed parallel to the bottom cap, 23. On the temperature stabilizer, 18, there are several holes, 17, normal to the surface of the temperature stabilizer. The holes, 17, work as bubble initiators. The upper section of the

lance is fitted with a cooling jacket, 1, into which coolant is pumped through inlet, 10, via feed pipe, 4. The coolant then travels through the annular heat transfer gap, 5, to the outlet distribution header, 20, and out through the exhaust port, 12.

Below the cooling jacket, 1, is the reagent preheating jacket, 2, into which reagent is introduced via inlet, 11, through reagent feed pipe, 3. The reagent flows through the annular preheating gap, 6 to the outlet distribution header, 19. The reagent then enters through conduit inlet, 13, which penetrates through the wick, 8, and the wall of the heat pipe, 7. The reagent is forced through the central conduit, 9, to the lance nozzle, 14.

The coolant and reagent jackets depicted in Figure 6.6 are separated by a ring, 25. Both the coolant and reagent may need to be equipped with dual intake pipes and inlets, 4 and 10 for the coolant circuit and 3 and 11 for the reagent circuit to provide better homogenization. Also shown in Figure 6.6 is nipple, 22, which is used to permanently seal the working fluid chamber 15, prior to the application of the coolant jacket, 1.

Figure 6.7 shows a view of the radial cross-section of the heat pipe lance at location, F. Reagent is contained by the outlet distribution header, 19, and the lance wall, 7. As it flows through the preheating gap, 6, reagent enters the central conduit inlet, 13, and travels through conduit, 9, on its way to the nozzle. The working fluid chamber, 15, is bounded by the wick, 8.

Figure 6.8 shows a view of the radial cross-section of the heat pipe lance at location, G. Coolant is contained by the coolant jacket, 1, and the lance wall, 8, as it flows through the annular heat transfer gap, 5. The working fluid chamber, 15, is bounded radially by the wick, 8.

Figure 6.9 shows a longitudinal cross-section of a typical, annular heat pipe lance as detailed in U.S. Patent 5,310,166. The working fluid chamber, 15, is bounded by the inner surface of the outer heat pipe wall, 7, and the outer wall of the inner conduit, 22. A wick, 8, is applied on the inner surface of the heat pipe wall. Reagent enters the inner pipe, 22, via the inlet, 24, flows through the passage, 6, and is discharged into the melt by the nozzle, 14. A pool of working fluid, 16, resides on the base of the lance.

Also indicated in Figure 6.9 are six surface areas as denoted by the labeling *a* through *f*. Surface area, *a* refers to the evaporator surface area formed by the base of the leading end of the heat pipe. Surface area, *b* indicates the vertical surface area of the outer pipe in direct contact with the pool of working fluid. Surface area, *d*, refers to the intermediate vertical surface area of the evaporator while surface area, *e*, refers to the top vertical surface area of the evaporator. The two remaining surfaces, *c* and *f*, represent surface areas available for condensation. Surface area, *c*, is delineated by the outer surface of the central conduit spanning the entire length of the conduit. Surface area, *f*, represents

the inner vertical surface of the outer pipe extending from the top of the evaporator to the top of the heat pipe.

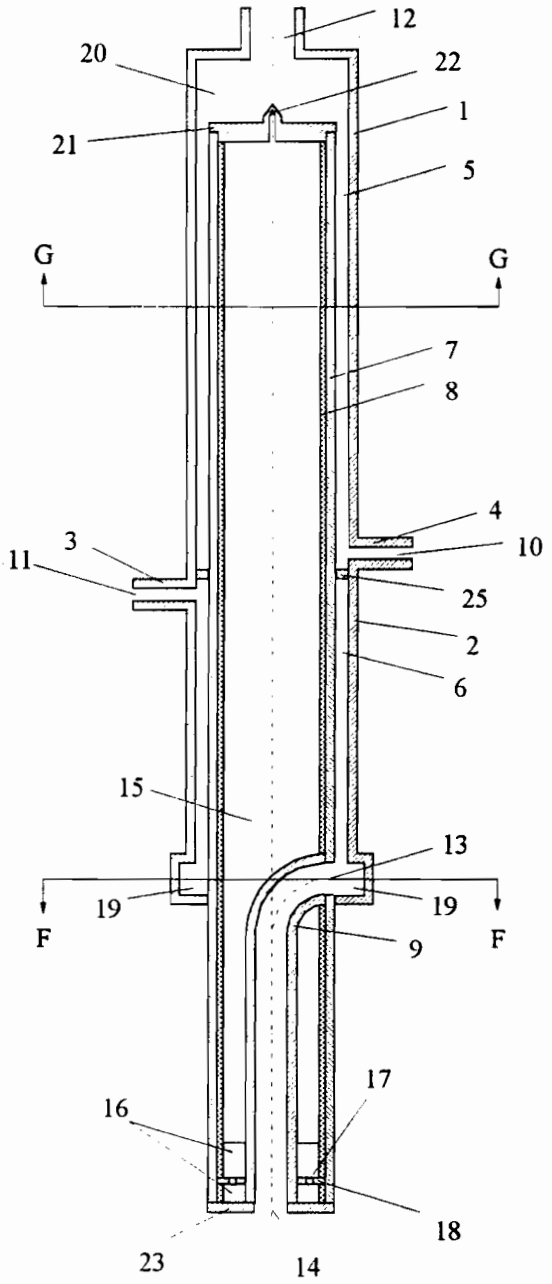

Figure 6.6 Schematic diagram depicting the longitudinal cross-section of a heat pipe cooled injection lance

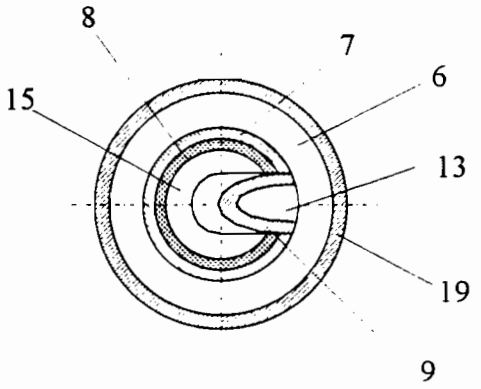

Figure 6.7 ***View of the radial cross-section of the heat pipe cooled injection lance at section F-F of Figure 6.6***

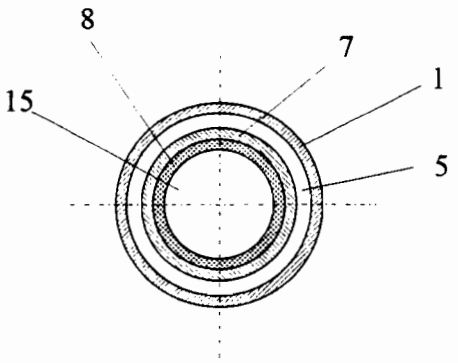

Figure 6.8 ***View of the radial cross-section of the heat pipe cooled injection lance at section G-G of Figure 6.6***

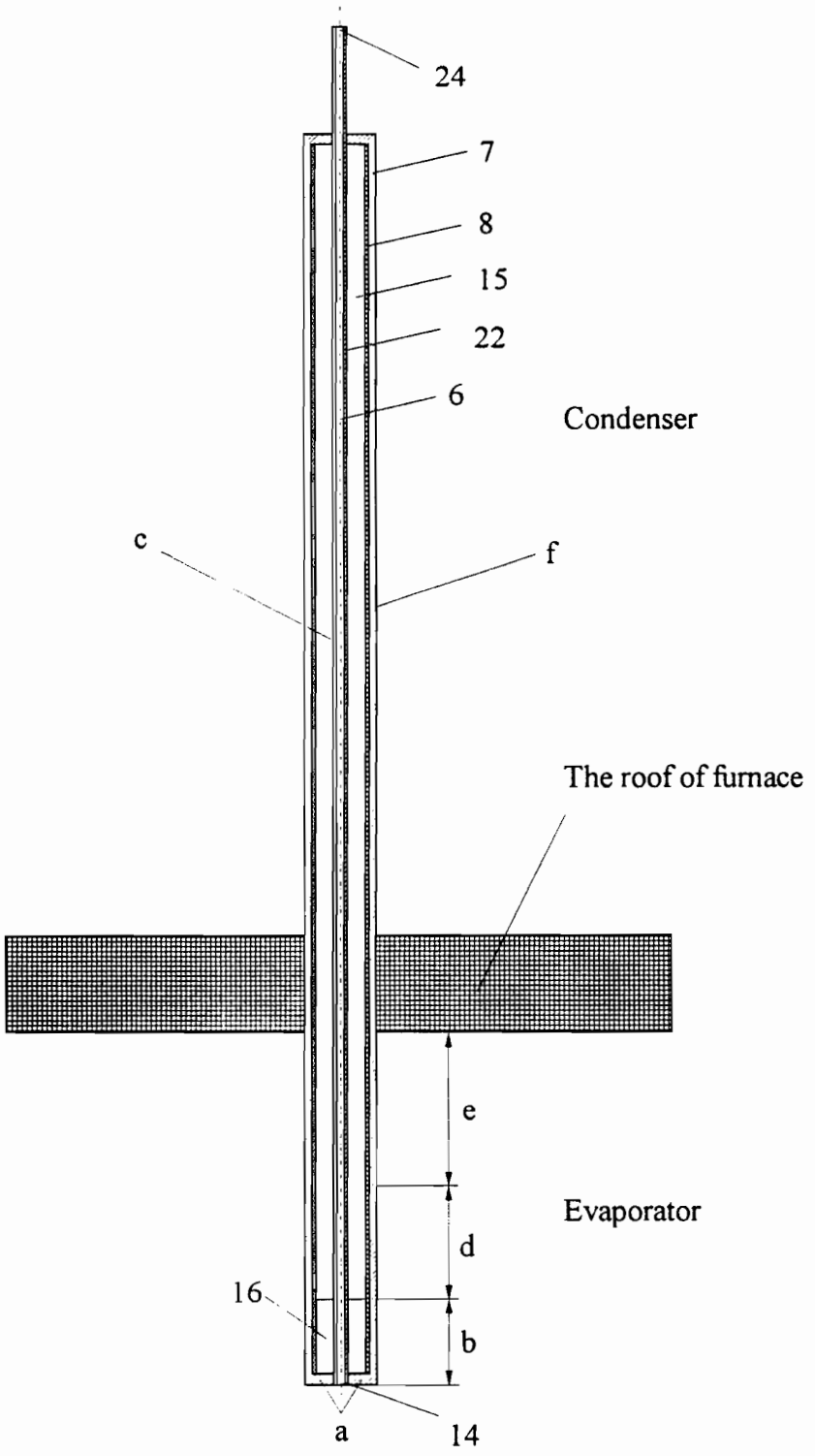

Figure 6.9 Longitudinal cross-section of the annular heat pipe lance as described in the prior art (U.S. Patent 5,310,166)

Removal of a large part, if not all, of the inner conduit that constitutes a major feature of the annular heat pipe lance as proposed in U.S. Patent 5,310,166 is a prerequisite to the execution of the present heat pipe cooled injection lance. Since the inner conduit carrying the reagent to the melt acts as a condenser for the working fluid, it stands to reason that whatever is condensed on the inner conduit flows down the walls of the conduit to the nozzle region. Thus, this condensate bypasses the evaporator walls. Under high heat flux and hard blowing conditions, a peculiar set of circumstances may culminate in the drying up of the evaporator walls starting from somewhere above the liquid pool and extending upwards, until in the limit, the vast majority of the evaporator may be dry.

The drying up of the evaporator occurs when the rate of condensation of working fluid on the inner conduit exceeds the rate of evaporation from the liquid pool. With reference to Figure 6.9 depicting the annular heat pipe lance detailed in U.S. Patent 5,310,166, it can be shown that when the rate of condensation on surface *c* exceeds the combined rates of evaporation from surfaces *a* and *b*, then some working fluid vaporized on the top and intermediate evaporator surface is diverted and condensed on the inner conduit. The continuance of this situation can lead to a virtual drying up of the intermediate evaporator. Moreover, as the intermediate and then the top evaporator area is dried up, the outer condenser is also dried up, with the result that the bulk of the evaporator walls become excessively hot and subject to the usual failures encountered in such processes. However, it will be noted that such failures typically will occur at locations above the liquid pool that collects in the nozzle region.

Thus, the rate of condensation on surface c must be less than the combined rates of evaporation from surfaces *a* and *b*. Transforming this statement into one of mass flows, it is clear to someone knowledgeable in the art that the mass flow of condensate (i.e. C) produced on surface *c* must be less than the combined mass flows of evaporation from surfaces *a* (i.e. A) and *b* (i.e. B). Thus,

$$C < A + B$$

where the units of C, A and B are in mass of working fluid per unit of time. As the rate of condensation on surface *c* is directly linked to the heat extraction capability of the reagent, it is obvious, for example, that for a given reagent, heat extraction increases with increasing reagent velocity. Since the rate of heat extraction is directly linked to the rate of condensation by the thermodynamic property called the heat of vaporization, it then stands to reason that C will increase with increasing reagent flow velocity. If conditions are such

that C exceeds the sum of A and B, the creation of a hot-ring on the evaporator wall will be the outcome. Given adequate wicking of the evaporator walls, the hot spot will manifest itself in the shape of a ring that envelopes the entire circumference and covers the intermediate vertical surface area of the evaporator. The width of the hot ring is dictated by the degree of imbalance between mass flow C and the sum of mass flows A and B. Once equality is established between these streams, the width of the hot ring stabilizes and steady state is said to be attained. To force the elimination of the hot ring (i.e. intermediate surface area, d) requires that C be maintained at a level which is less than the sum of A and B. Under this operating constraint, the hot ring (i.e. intermediate surface area, d) will disappear and isothermal processing will be restored.

By virtue of the present elaboration, one can surmise that C (the mass flow of condensate on the inner conduit) can be reduced by decreasing *c* (the surface area of the inner conduit active in the condensation of working fluid), or alternatively by insulating area *c* thus reducing its effectiveness in condensing working fluid. The use of insulation, however, entails limited heat extraction by the reagent with the result that preheating of the reagent and energy recycling are both reduced. An energy efficient solution as detailed in the present study calls for the preheating of the reagent in an outer jacket. In this way, energy is recycled to the reagent and condensation is forced to the inner surface of the outer wall of the heat pipe lance.

As has already been stated, the heat pipe lance can be operated in positions other than the vertical. In such cases, it is necessary to ensure the proper refluxing of the entire evaporator walls with liquid working fluid. To achieve this, it may be necessary, in addition to the use of a wick, to compartmentalize the coolant and reagent jackets to ensure that sufficient condensation occurs on the upper sections of the jackets. To illustrate this feature of multiple (i.e. split) jackets, one can consider a heat pipe tuyere configuration for which a portion of the tuyere extends through the vessel lining and into the melt. The tuyere is angled such that it is near horizontal although a slight inclination towards the melt is preferable (i.e. angle of inclination from the vertical $< 90^0$).

Example

A heat pipe lance as described in U.S. Patent 5,310,166 was tested in a radiation furnace. The lance measured 500 mm in length and 25.4 mm in outer diameter with a wall thickness of 1.65 mm. A central conduit spanning the entire length of the heat pipe measured 6.35 mm in outer diameter with a wall thickness of 1 mm. The lance nozzle was 2 mm in internal diameter. Two wraps of 100 mesh screen were embedded on the inner surface of the outer wall of the pipe. All construction materials were 304 stainless steel. The pipe was charged with 17 g of sodium, evacuated and sealed.

A test was run to determine the effect of injecting reagent through the central conduit on a number of outer wall operating temperatures of the heat pipe. The furnace was set at 843°C for the entire test. Four distinct blowing conditions wherein air was used as the reagent were studied. In the first trial, no reagent was blown through the lance of which 300 mm were positioned within the hot furnace environment. Eleven thermocouples were strapped onto the outer surface of the pipe at various vertical positions. Once steady state was attained, the readings from the thermocouples were noted and the flow rate changed to the next level of 0.15 Nl/s. Once again, the new temperature readings were recorded after steady state was attained. Two other reagent gas flow rates of 0.30 and 0.40 Nl/s were also tested. The results from all four tests are shown in Figure 6.10. It will be noted that with no flow through the central conduit, the evaporator section which spans the first 30 cm was very uniform in temperature (approx. 735°C). Beyond the evaporator and extending to the top of the pipe, the temperature dropped to 630°C in an ambient environment of 20°C.

With a reagent flow rate of 0.15 Nl/s, the temperature of the evaporator at the bottom decreased to about 721°C at steady state. A hotter intermediate zone measuring about 70 mm in height was detected as can be determined from the data presented in Figure 6.10. At this flow rate, the condition of C being initially greater than the sum of A and B must have existed. In other words, the rate of condensation of working fluid on the central conduit exceeded the rate of evaporation from the base and lower area of the evaporator. This then led to the formation of the intermediate area, D on the evaporator from which vaporization of working fluid was impeded with the consequence that surface area, b, of the liquid pool increased and the equality of C with the sum of A and B was established. At this point in time, steady state was said to be achieved and stable operation of the heat pipe lance could be maintained.

When the flow rate was increased to 0.30 Nl/s, The temperature of the evaporator at the bottom decreased to 712°C at steady state. The hot intermediate zone in this case increased to about 210 mm in length. While the condenser temperature dropped to about 517°C, the evaporator surface temperature peaked at about 824°C - only 19°C below the furnace temperature.

An increase in the flow rate to 0.40 Nl/s showed a similar trend, the bottom evaporator temperature decreased to about 678°C while the condenser temperature dropped to 411°C. However, the intermediate hot zone grew in length to about 270 mm and attained a peak temperature of about 817°C. This clearly illustrates that by forcing condensation of working fluid on the inner conduit, one can greatly distort the operating characteristics of the heat pipe lance. A lance operated in this fashion can readily fail in

high temperature applications. As a final point, it is to be noted that the hot ring was clearly visible during those tests with a reagent flow rate of 0.15 Nl/s or greater thus confirming the temperature data. No hot ring was present with zero flow as expected.

A similar test to the above was carried out with a lance designed with the embodiments of the present study. The reagent air entered a preheating jacket which was 200 mm in length, was preheated and then allowed to flow into a central conduit leading to the nozzle. As before, flow rates of 0, 0.15, 0.30, and 0.40 Nl/s were tested. In all four cases, the temperature of the outer heat pipe evaporator surface was maintained at a relatively uniform level. There was no evidence of the onset of a hot spot. While the steady state temperature of the evaporator decreased with increasing flow rate, as was expected, the temperature of the entire length of evaporator was uniform for each flow rate.

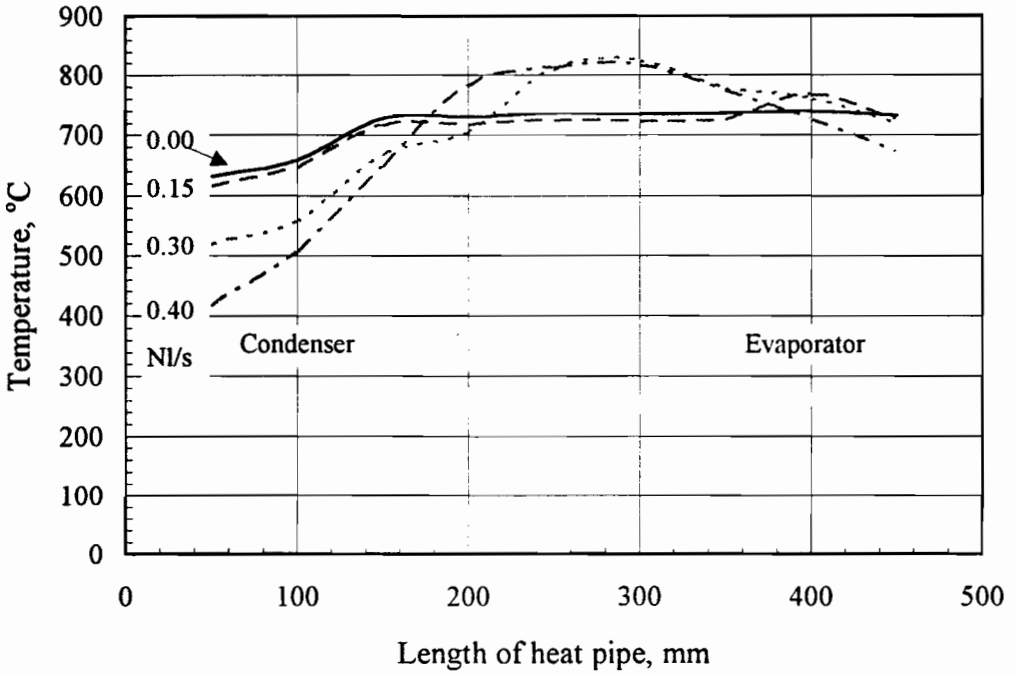

Figure 6.10 Temperature profiles of hot-rings for different flowrates of reagent

CHAPTER 7

LABORATORY TESTS OF HEAT PIPE COOLED INJECTION LANCES

A new generation of heat pipe cooled injection lances featuring all the improvements made in this study and as outlined in previous chapters was tested in the laboratory in hot furnace environments and in three distinct pyrometallurgical processes. The results are presented in this chapter.

7.1 New Generation of Heat Pipe Cooled Injection Lances

After all the improvements made in this study, as presented in Chapter 4, 5, and 6, a new generation of heat pipe cooled injection lances has emerged, as shown in Figure 6.5b, and described in Section 6.4. This new generation of heat pipe cooled injection lances has worked as well as expected in laboratory conditions. Although it will take a substantial investment to commercialize the heat pipe cooled injection lancing system, the possibilities are tremendous.

7.1.1 The Characteristics of the New Heat Pipe Cooled Injection Lance

All the improvements made in this study were implemented in a laboratory scale heat pipe cooled injection lance. A wick was employed in the heat pipe to prevent the formation of

hot-spots. All non-condensable gases were taken out from the heat pipe chamber to eliminate both the possibility of the formation of an inert gas zone and the possibility of freeze up of working fluid in the inert gas zone. An air-cooling jacket was built on the condenser section to achieve better control over operating temperature than a self-cooling heat pipe can offer. With the air-cooling jacket in place, the heat pipe cooled injection lance can be operated at relatively low temperatures under different operating conditions. A temperature stabilizer was incorporated in the liquid pool to reduce superheat in the pool and to consequently reduce the temperature at the lance nozzle and prolong the life of the lance. In order to maintain the mass balance of working fluid, an oxygen-preheating jacket was built around the condenser to preheat oxygen before being introduced into the central reagent conduit. The details about the final heat pipe cooled injection lance follow.

All components of the entire heat pipe cooled injection lance were made of stainless steel 316L except for the tip of the lance. The lance tip was made of nickel 200 for better heat transport. The heat pipe shell was a piece of 25.4 mm O.D. tubing, 500 mm long, and 1.65 mm wall thickness. Two wraps of 100 mesh screen were chosen as wick structure for the heat pipe. The wick covered the entire inner surface of the heat pipe shell. A piece of 31.8 mm O.D. tubing 260 mm long by 1.65 mm wall thickness was used as the air-cooling jacket. The jacket was concentric with the heat pipe shell. It covered 220 mm of condenser starting from the top cap, and the other 40 mm of the jacket stuck out from the top of the condenser to protect the sealing tube, as shown in Figure 6.5b. 80 mm of the same type of tubing as used for the air-cooling jacket was employed as the oxygen-preheating jacket and was positioned right below the air-cooling jacket in a concentric position with the heat pipe shell, as shown in Figure 6.5b. A piece of 6.35 mm O.D. tubing 200 mm long by 0.89 mm wall thickness was used as the central reagent conduit. It passed through the heat pipe to connect the oxygen-preheating jacket and the nozzle while the nozzle was of the straight bore variety with a 2 mm opening. The bottom 200 mm of the heat pipe shell was left free, which is then the maximum size that the evaporator can be. A temperature stabilizer plate was positioned in the evaporator 8 mm above the bottom cap of the heat pipe with a thickness of 4 mm. Three holes of 3.18 mm diameter were spaced evenly and transversed through the plate in the normal direction. A piece of 6.35 mm O.D. tubing 500 mm long by 0.89 mm wall thickness was positioned axially in the heat pipe. It served as a thermocouple well with the leading end closed and in contact with the temperature stabilizer. The other end was welded on the top cap and left open.

The heat pipe cooled injection lance was conditioned in a hot furnace environment ranging between 750°C and 900°C. Not only was no inert gas charged into the heat pipe, but also all the non-condensable gases generated during the conditioning procedure were

taken out of the heat pipe with a vacuum pump.

7.1.2 Amount of Working Fluid in the Heat Pipe

For heat pipes and heat pipe cooled injection lances a big unknown is the depth of the liquid pool. To have a better understanding of a heat pipe and in particular the heat pipe cooled injection lance, the depth of liquid pool should be quantified. It can be determined analytically and/or measured experimentally.

In this final version of the heat pipe cooled injection lance, 20 grams of potassium were charged as working fluid. Based on the size of the heat pipe shell and a liquid density of potassium of 725.4 kg/m^3 at 500°C, the depth of the liquid pool can be calculated to be about 78.3 mm. However, this calculated depth of the liquid pool is only a maximum depth in the heat pipe. The actual depth of the liquid pool is always less than the maximum depth in the heat pipe because a portion of the working fluid will be taken out along with all the non-condensable gases during the conditioning procedure. To have an idea about how much of the working fluid actually remains in the heat pipe after it is sealed, it has to be measured experimentally. This was done to the new laboratory scale heat pipe cooled injection lance developed in this study.

To measure the depth of the liquid pool the entire available evaporator was positioned in an elevated temperature environment, 150°C for this case. The temperatures at different locations along the axis of the heat pipe shell were recorded. Temperatures were recorded during transient state (i.e. heat up) in order to pick up the different boundary conditions around the 6.35 mm diameter thermocouple well used for temperature measurement. To make it easier to understand the principal of this measurement, the following example may be considered.

When the entire evaporator, which is partially filled with some quantity of potassium, is heated up in a 150°C hot furnace environment, the temperature in the liquid pool tends to be uniform because of 1) the relatively high thermal conductivity of liquid potassium, 2) the relatively low thermal resistance between the hot furnace environment and the liquid potassium, and 3) the relatively low heat load on the liquid pool. Since the small tubing for measuring temperature runs through the entire evaporator, the portion which is in the liquid pool faces much less thermal resistance than the rest of it which is not in the liquid pool. In a transient state, it will take a shorter time for the portion which is in the liquid pool to reach a steady-state than the rest of the tube which is not in the liquid pool. Therefore, during the transient state, the portion of the thermocouple well which is out of the liquid pool is cooler than the portion in the liquid pool. Meanwhile, the portion in the liquid pool tends to be uniform in temperature even during the transient

state. By using this principal, the depth of the liquid pool can be measured based on the temperature profile obtained in the thermocouple well.

Figure 7.1 shows one set of results from this kind of measurement. Based on the principal presented above, the depth of the liquid pool was determined to be slightly above 40 mm when the heat pipe was held vertically as concluded from the data shown in Figure 7.1. This result indicates that the amount of working fluid was within the desirable range, 40~60 mm in depth, and that the temperature stabilizer was well below the free surface of the liquid pool to allow it to function.

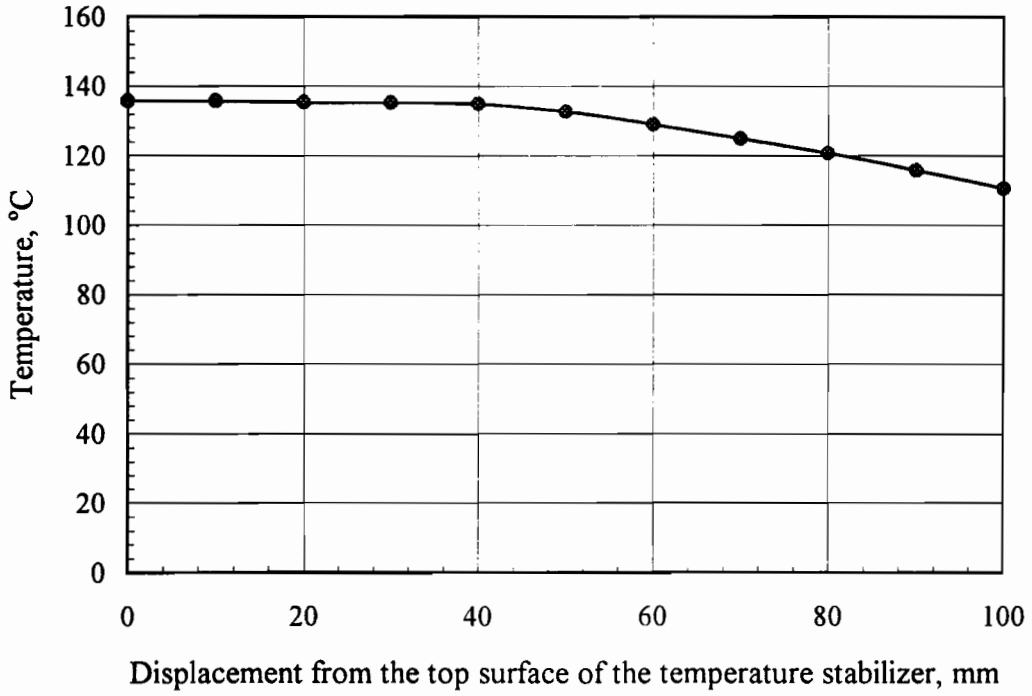

Figure 7.1 Temperature profile on the evaporator of the final version heat pipe cooled injection lance

7.2 Laboratory Tests with no Blowing of Reagent

At this stage, the heat pipe cooled injection lance was tested as a regular heat pipe in a hot environment with no reagent flowing through the reagent-preheating jacket and the central reagent conduit. Both transient and steady-state behaviors were determined as follows.

Figure 7.2 illustrates a schematic diagram of the setup for this portion of this

study. The heat source was provided by an electric resistance furnace. The heat pipe was suspended above the furnace. The evaporator was enclosed in the hot furnace environment. The active size of the evaporator was about 170 mm.

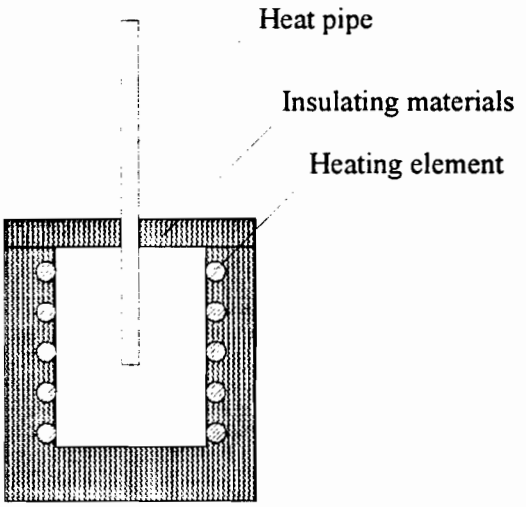

Figure 7.2 Schematic diagram of experimental setup in an electric resistance furnace

7.2.1 Performance of the Heat Pipe under Transient Conditions

The performance of the new heat pipe cooled injection lance under transient heating conditions was studied with two heating rates, a low and high heating rate.

The low heating rate was achieved by positioning the heat pipe cooled injection lance in the electric resistant furnace when both the pipe and furnace were at room temperature and then by turning the furnace on. Figure 7.3 shows the temperature profiles (i.e. heating curves) for the low heating rate. In Figure 7.3 curve 1 represents the temperature right above the temperature stabilizer plate, and curves 2 and 3 represent the temperatures 100 mm up from bottom cap in the evaporator and 100 mm down from top cap in the condenser, respectively. The gap between curve 1 and 2 represents the superheat of the liquid pool. It shows clearly that in the time range 2000 and 2500 seconds the temperature stabilizer attempted to homogenize the liquid pool a couple of times and then started to work continuously after 2400 seconds at 430°C. The heat pipe worked well as expected. Figure 7.4 is a magnified view of Figure 7.3. The plateau on curve 1 (between 300 and 400 seconds) shows the melting point of the working fluid, potassium.

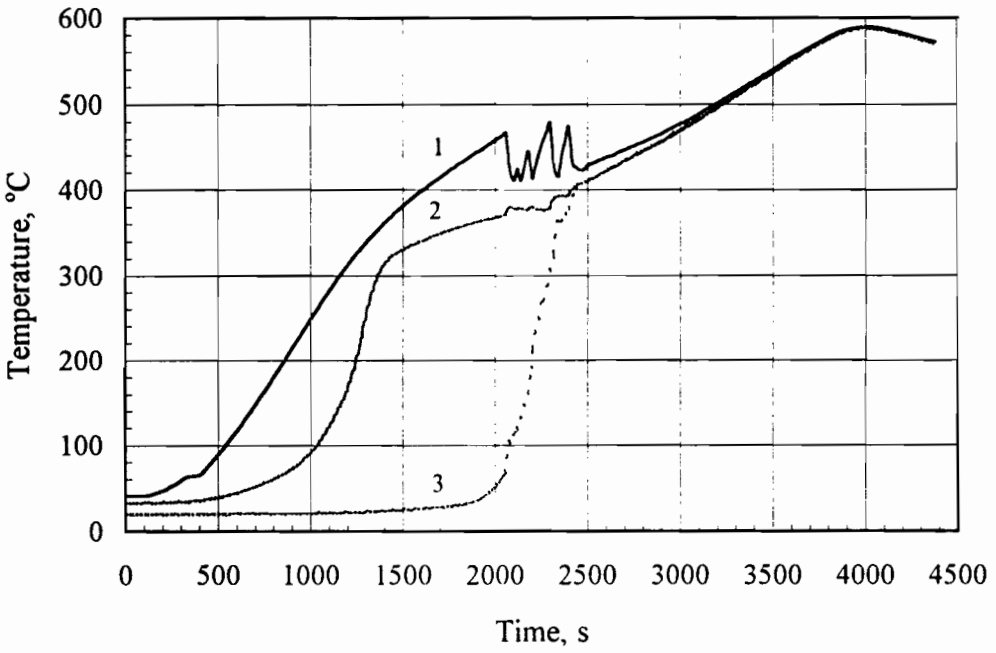

Figure 7.3 Transient temperature profile at a low heating rate

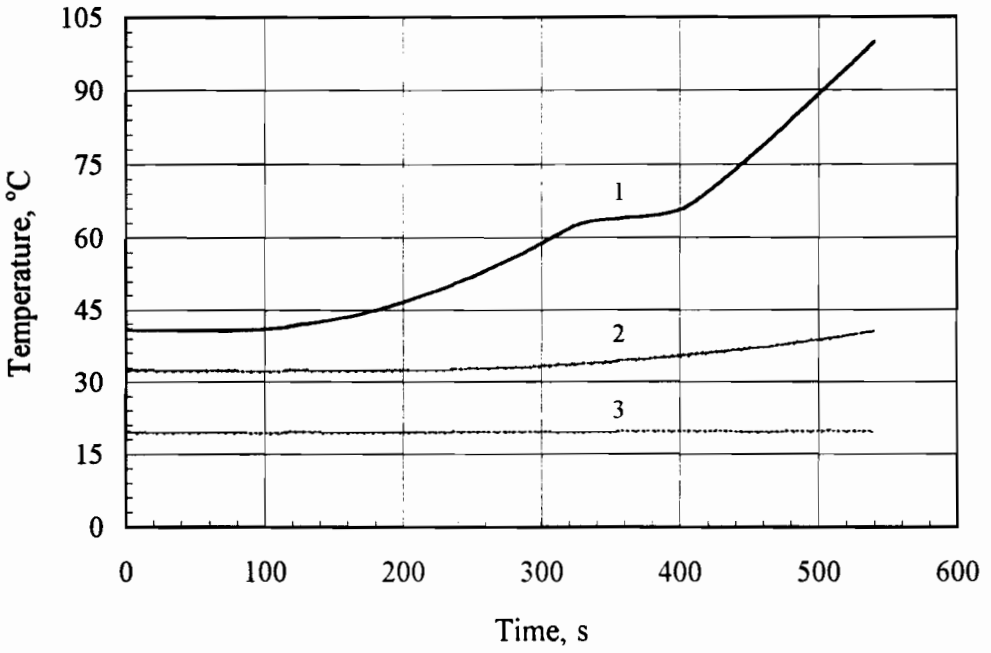

Figure 7.4 Transient temperature profile at a low heating rate showing the melting point of potassium

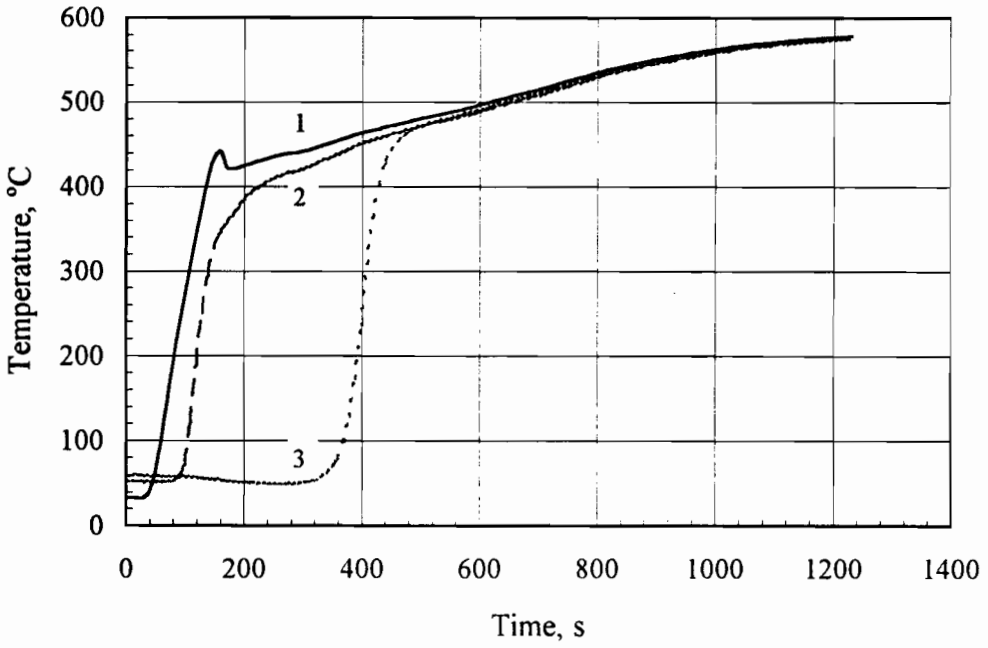

Figure 7.5 Transient temperature profile at a high heating rate

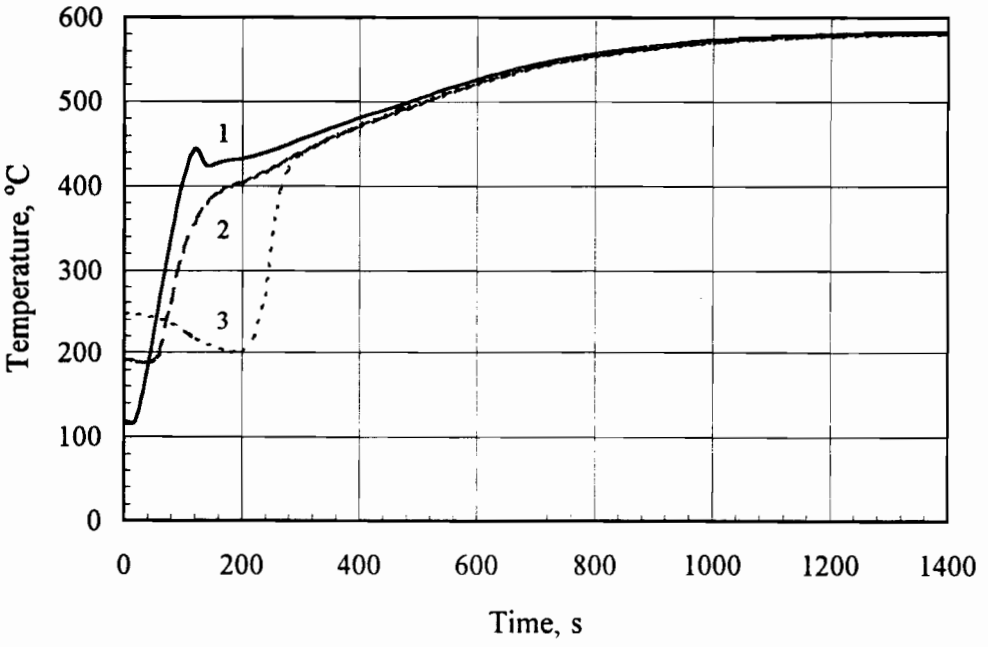

Figure 7.6 Transient temperature profile at a high heating rate and high initial pipe temperature

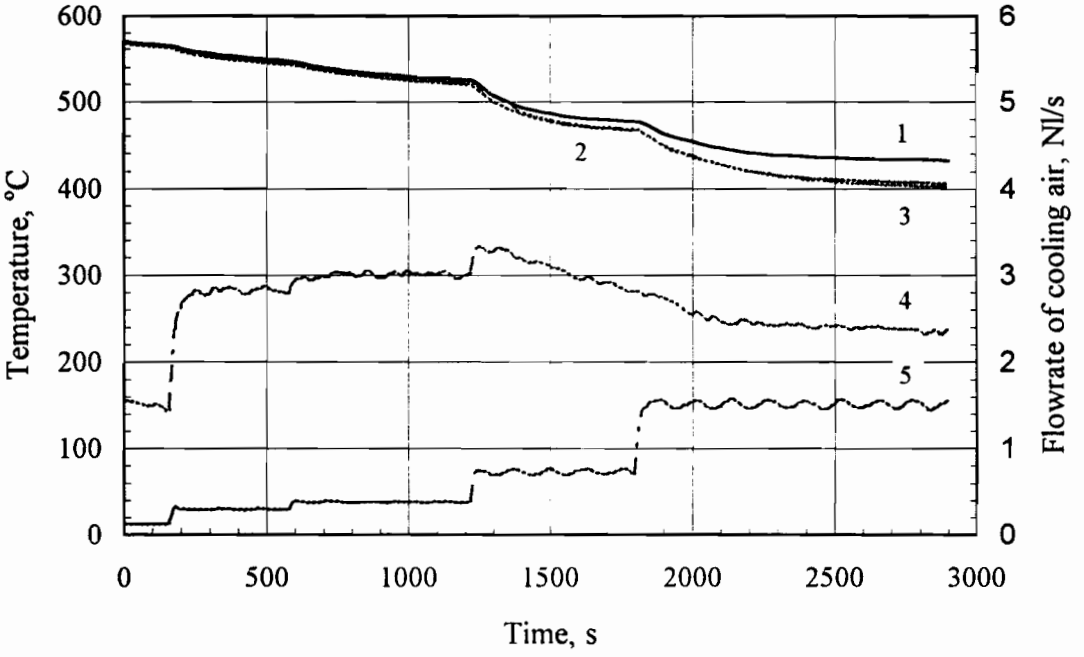

Figure 7.7 Temperature and flowrate profiles at different steady-states

The other test was conducted at a high heating rate which was obtained by positioning the heat pipe cooled injection lance in a hot furnace environment. Figures 7.5 and 7.6 show the temperature profiles for the high heating rate with different initial pipe temperatures. Curves 1 to 3 in Figures 7.5 and 7.6 represent the corresponding curves shown in Figure 7.3. For the high heating rate, the thermocouples were positioned at the same locations as they were at the low heating rate. It should be noted that at the high heating rate the temperature stabilizer operated very effectively and quickly stabilized the heat pipe operation at an early point in the heating procedure. Only one attempt was required to achieve stable operation.

7.2.2 Performance of the Heat Pipe at Steady-State Conditions

The performance of the new generation heat pipe cooled injection lances under steady-state conditions was also investigated. Figure 7.7 shows the transient to steady state temperature profiles for several different cooling air flow rates in the jacket while the furnace temperature was about 825°C. In Figure 7.7, curves 1 to 3 represent the temperatures in the liquid pool, in the evaporator, and in the condenser, respectively.

Curve 4 represents the outlet temperature of the cooling air. Curve 5 represents the flowrate of cooling air. At the higher end of the operating temperature range, the temperature differences between the liquid pool, the evaporator, and the condenser are within a few degrees. At the lower end of the operating temperature range, the temperature differences are within 15°C. The results show that the entire heat pipe worked as well as expected. They also show that the operating temperature responded quickly to changes in the flowrate of cooling air. It indicates that the control function of the heat pipe cooled injection lance worked properly. By adjusting the flowrate of cooling air, the operating temperature can be readily controlled.

Figure 7.7 also indicates that the lowest operating temperature for the heat pipe cooled injection lance is about 440°C. Below that temperature, the temperatures in the liquid pool, evaporator section, and condenser section will start to deviate significantly from each other.

7.3 Laboratory Tests with the Blowing of Reagent

Many pyrometallurgical operations may benefit by using this new generation of heat pipe cooled injection lances. In this study the processes of steelmaking, copper converting, and silver refining were used to investigate heat pipe cooled injection lances[83-89].

The common feature of all three processes was the need to top inject oxygen into each of the melts to promote selective oxidation. The difference between them was the characteristics of the oxide products and more specifically the gaseous products. In the steelmaking test, the oxidation results in the evolution of CO gas, which is flammable. In the copper converting test, the oxidation results in SO_2 gas, which is non-flammable. In the silver refining test, the oxidation results in PbO, which is liquid under normal operating conditions. This means that there is no major off-gas being generated during silver refining. Thus, the three distinct processes cover a broad range of operations.

Unless indicated specifically, the final version of heat pipe cooled injection lance, as described in the last section, was used in all the tests as described in the following sections.

Figure 7.8 illustrates a schematic diagram of the setup for testing the lance in a pyrometallurgical environment. All tests were conducted in an induction furnace fitted with an alumina crucible measuring 140 mm in internal diameter and 260 mm in depth. The size and nature of the charge was dictated by the process that was to be studied. The position of the lance and the oxygen gas flowrate were varied.

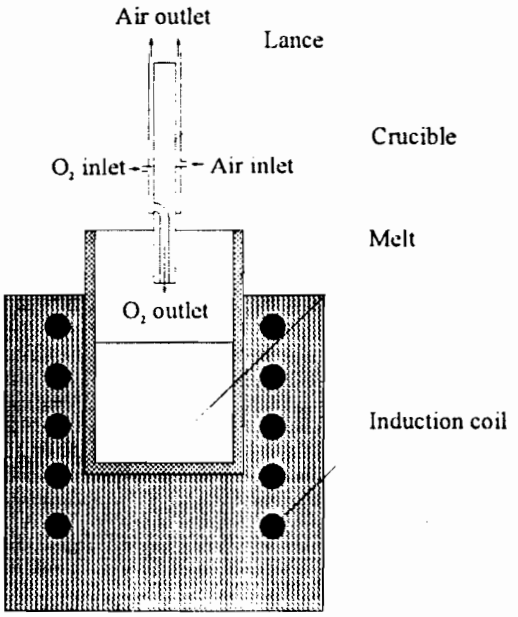

Figure 7.8 Schematic diagram of the experimental setup of the laboratory-scale heat pipe cooled injection lance in an induction furnace

7.3.1 Steelmaking Test

In the area of steelmaking, both the EAF (electric arc furnace) process and BOF process are potential candidates for this technology. While BOF's present a formidable challenge, electric furnaces are much more hospitable and thus the likely target for the implementation of this technology in the near future. Tests to date in the laboratory have focused on oxygen lancing to decarburize steel. While the tests to be described in a subsequent section clearly demonstrate the viability of a heat pipe cooled injection lance to cope with steelmaking environments, plant trials will be needed to resolve any scale-up difficulties.

A series of tests have been carried out using different versions of the heat pipe cooled injection lances that were developed throughout this study to inject oxygen into the melts. A sampling of the results that were obtained is outlined in the following paragraphs.

Example 1:

A heat pipe cooled injection lance designed according to the embodiments of the present improvements with the exception of the temperature stabilizer was used to make steel from pig iron initially containing 4.1%C (by weight). The lance was 50 cm in total length with 20 cm of uncovered evaporator length, a 10 cm long preheating jacket and a 20 cm

long cooling jacket. The heat pipe body was 25.4 mm in outer diameter with a wall thickness of 1.65 mm. Both jackets were affixed to the outer heat pipe wall to create a gap of 1.5 mm in width for both the air and oxygen. The central conduit connecting the preheating jacket and the nozzle was 6.35 mm in outer diameter with a wall thickness of 0.89 mm. Two wraps of 100 mesh screen were embedded on the inner surface of the outer wall of the pipe. The pipe was charged with 17 grams of sodium, evacuated and sealed. All materials of construction were 304 stainless steel with the exception of the leading face of the lance which was made of nickel 200.

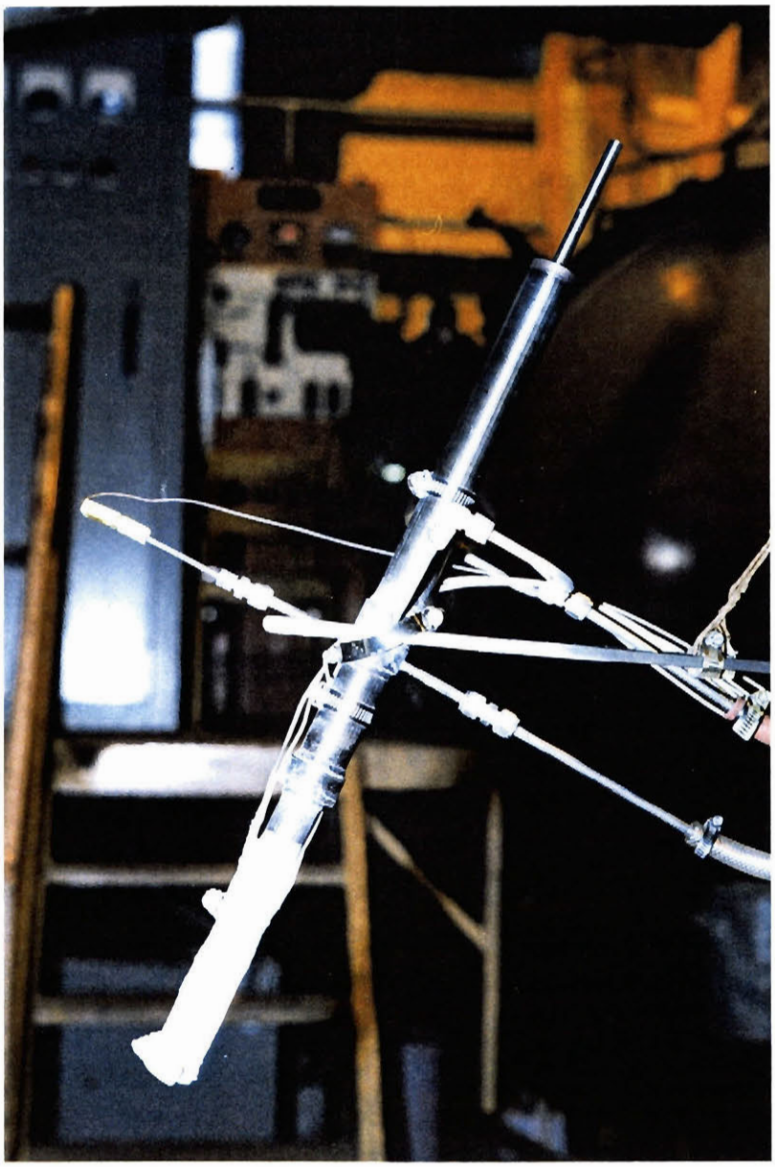

Figure 7.9 A view of the heat pipe cooled injection lance prior to the test

The test to be described was conducted on an inclined system. To illustrate the capabilities of the heat pipe cooled injection lance, it is best to consider the series of photographs shown as Figures 7.9 to 7.15. Figure 7.9 shows a view of the heat pipe cooled injection lance prior to the test. The angle of inclination of about 30° from the vertical is clearly visible. The lance was lowered over the melt and oxygen injection initiated. A view of the lance during the blow is shown in Figure 7.10. Note the intense CO flame emanating from the upper half of the mouth of the crucible. Upon terminating the blow, the lance was raised and appeared as shown in Figure 7.11. It will be noted that the leading end of the lance was coated by a relatively hot accretion - the thickest portion being on the topside. After the accretion had cooled off, the lower section of the lance appeared as shown in Figure 7.12. A frontal view of the buildup on the lance tip is shown in Figure 7.13. The accretion was removed by knocking it free to expose the lance body as shown in Figure 7.14. A frontal view of the lance after the accretion was removed is shown in Figure 7.15. Note the excellent physical condition of both the leading end and the nozzle.

Figure 7.10 A view of the lance during the blow

During the test, a series of temperatures were monitored with thermocouples strapped onto the outer body of the lance. For the sake of simplicity only 4 temperature curves are shown in Figure 7.16. Curves 1 and 2 represent the topside and underside shell temperatures, respectively, at the leading end of the heat pipe cooled injection lance. Curves 3 and 4 represent the topside and underside shell temperatures, respectively, at a displacement of 10 cm from the leading end. Curve 5 depicts the flowrate of the oxygen reagent. Both curves 1 and 3, which represent the topside temperatures, produced on average, readings that were somewhat higher than the corresponding underside values. This was a result of the blowing orientation by which the reaction front was projected ahead of the lance with the CO flame being of greater intensity on the topside as shown in the photograph in Figure 7.12. Heat fluxes in excess of 1 MW/m^2 were readily dissipated during the blow by the leading end of the lance[83]. The heat fluxes were estimated with the mathematical model that is described in the next chapter.

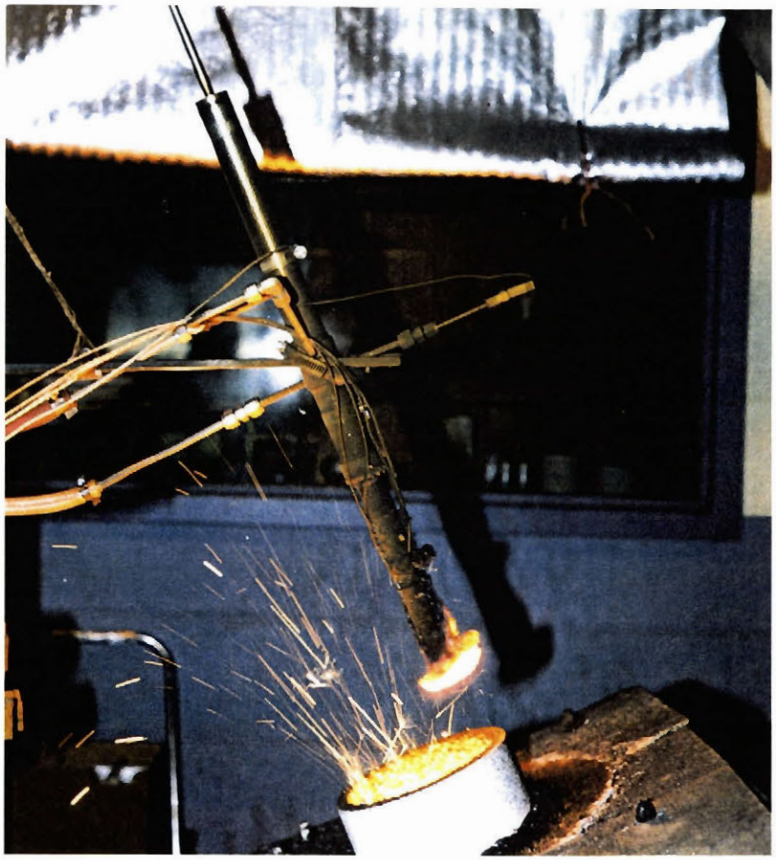

Figure 7.11 Leading end of the lance coated by a relatively hot accretion

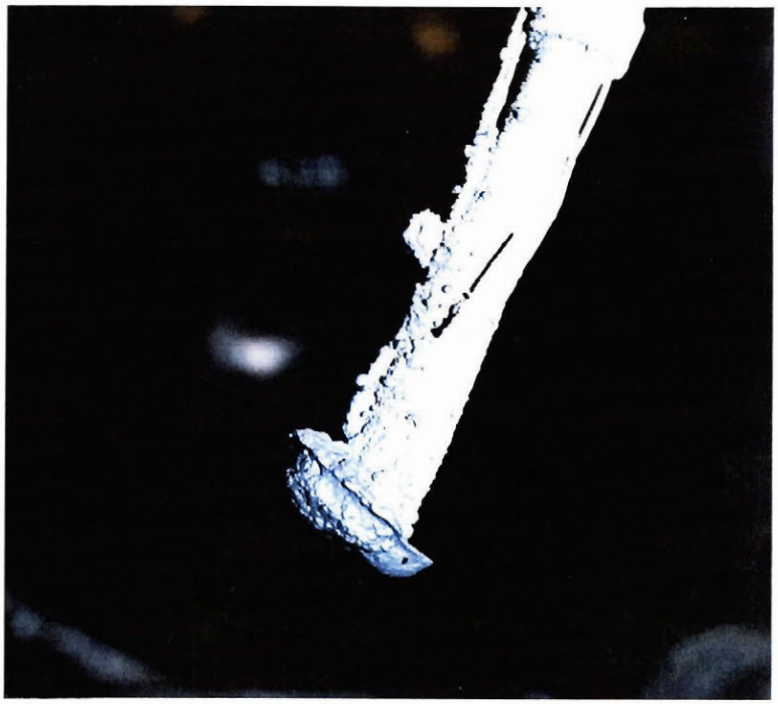

Figure 7.12 Lower section of the lance after the accretion cooled off

Figure 7.13 A frontal view of the buildup on the lance tip

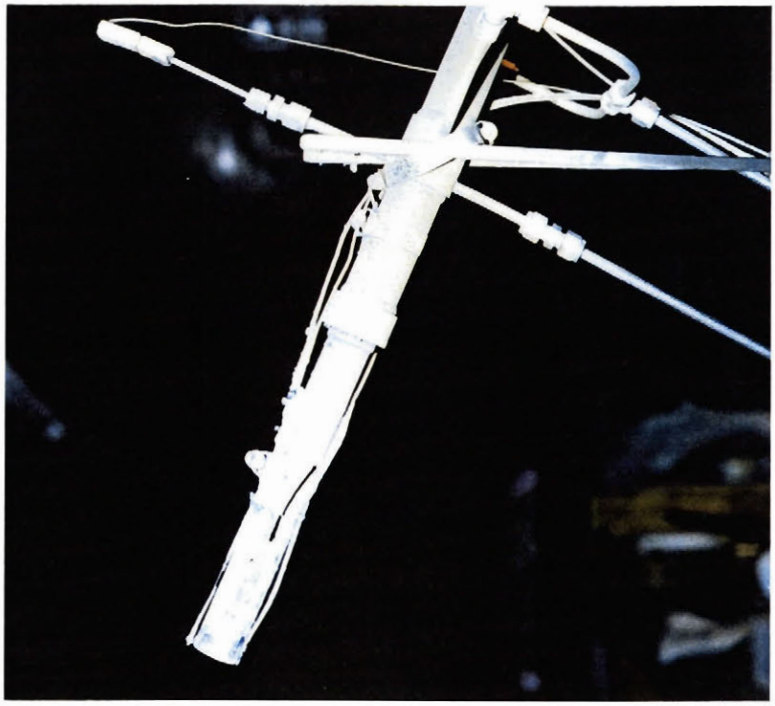

Figure 7.14 Lower section of lance without accretion

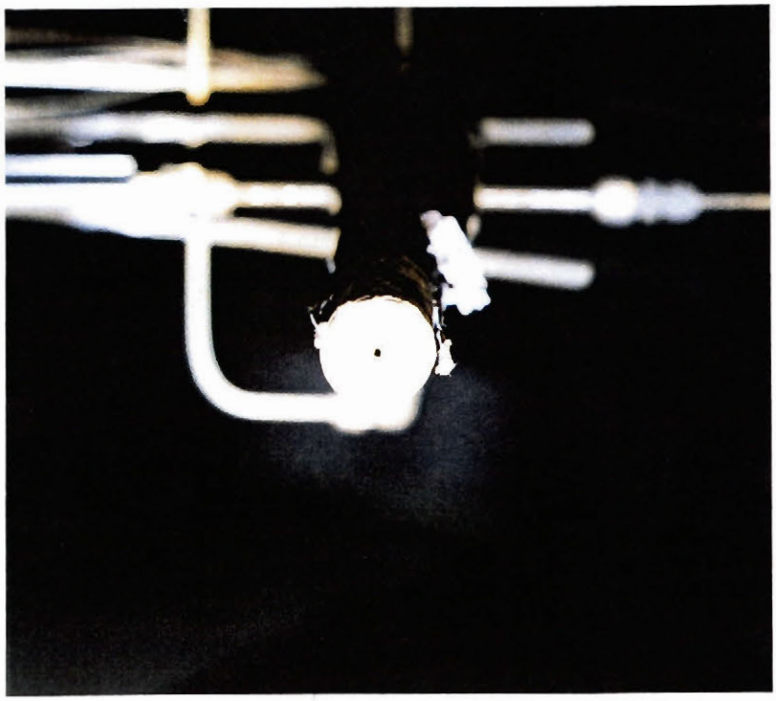

Figure 7.15 A frontal view of the lance after the accretion was removed

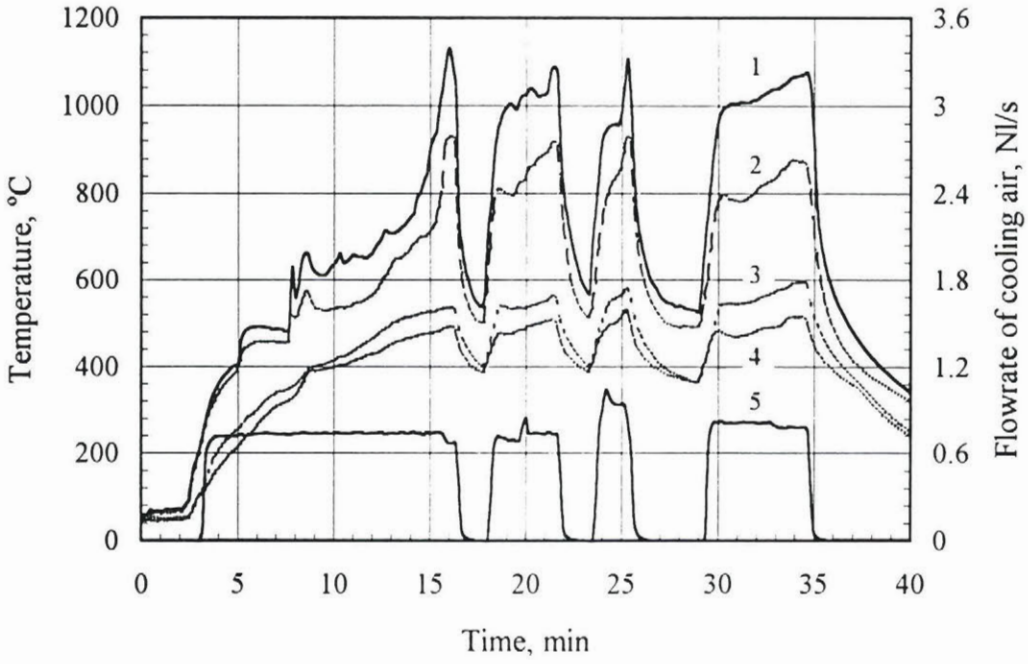

Figure 7.16 Temperature response curves on lance body during steelmaking

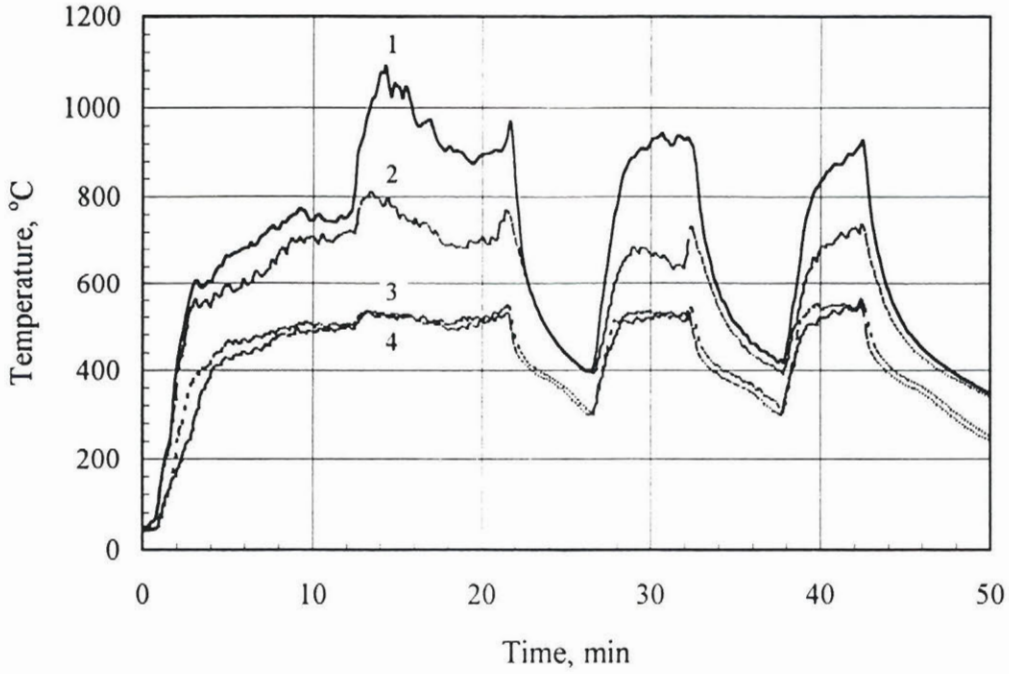

Figure 7.17 Temperature response curves on inclined lance body during steelmaking

The blowing of oxygen was stopped on 3 separate occasions because of excessive foaming of the slag. On the fourth occasion the test was terminated, the carbon content being less than 0.5%. Oxygen utilization efficiencies based on the cumulative oxidation of carbon to CO and of CO to CO_2 approached 100%.

Example 2:

The same heat pipe cooled lance as used in Example 1 was used for this test. A charge of 12 kg of pig iron was melted in a 14 cm diameter alumina crucible in an induction furnace. Once at the desired temperature of 1250°C, The crucible was tipped to 30° from the vertical. The lance was positioned, also at the angle of 30°, such that the nozzle was 7 cm from the melt surface. Oxygen reagent was blown at a rate of 0.3 Nl/s into the melt through the 2 mm nozzle. Thermocouples strapped onto the body of the lance and on the base monitored the temperatures, as shown in Figure 7.17. Blowing of reagent was continued for a total of 30 minutes after which time the melt carbon concentration had been reduced to less than 1% C.

During the test the lance body was found to be uniform in temperature but dependent on heat flux with fluctuations occurring only in time. A maximum temperature of 1080°C was recorded at the outside surface of the tip of the lance where incipient heat fluxes were highest. The lance operating temperature was readily adjusted by varying the flow rate of cooling air through the coolant jacket. For example, a flow rate of 1 Nl/s of air reduced the temperature by slightly more than 50°C. At the end of the blow which lasted about 25 minutes, the melt temperature was about 1600°C. As the lance operated at a relatively low temperature with the working fluid averaging about 560°C, an accretion formed on the leading face of the lance and on the lower body of the evaporator. Once the accretion was removed at the end of the test, the nozzle and leading face were found to be in excellent condition with no signs of wear or attack. The lance was reused on a number of occasions with identical results.

It should be noted that the flowrate of oxygen has a significant impact on the environment temperature in the furnace, and thus on the operating temperature of the heat pipe cooled injection lance. As shown in Figures 7.16 and 7.17, the different oxygen flowrates (more than 0.6 Nl/s in example 1, and 0.3 Nl/s in example 2) resulted in higher temperatures on the lance tip and lance body in example 1 than those in example 2. This was caused by the faster reduction rate and higher heat generation rate in example 1 than in example 2.

In fact, this lance is now used on a weekly basis in an undergraduate course in metallurgical engineering to acquaint the students with the steelmaking process (i.e. decarburization). To date over 20 tests have been conducted - the reproducibility of the

tests is excellent. Moreover, the lance is still in excellent condition.

Example 3:

In the test to be described, the final version of the heat pipe cooled injection lance that incorporated the features as described at the beginning of this chapter was used. The lance was positioned vertically, and the lance nozzle was 75 mm above the initial melt surface. Oxygen was blown at an average rate of 0.3 Nl/s into the melt which at the start consisted of 9.75 kg of Sorelmetal (4.1% C) and was 1350°C in temperature. Three thermocouples were positioned in the thermocouple well to monitor the performance of the lance. Thermocouple #1 was right at the bottom of the upper liquid pool, thermocouple #2 was 100 mm above the nozzle, and thermocouple #3 was 150 mm below the top cap. Thermocouple #4 was used to measure the outlet temperature of the cooling air. The flowrate of cooling air, curve 5 in Figure 7.18, was recorded, and the flowrate of oxygen was kept constant at 0.3 Nl/s. Figure 7.18 shows the four temperature curves and the flowrate curve of cooling air. During the blowing time shown in Figure 7.18, temperatures #1 and #2 were relatively constant which means the heat pipe worked well. It is evident from temperature #3 that the lance was operated at its lower operating range. The heat extraction rate at peak by the cooling air was about 600 W.

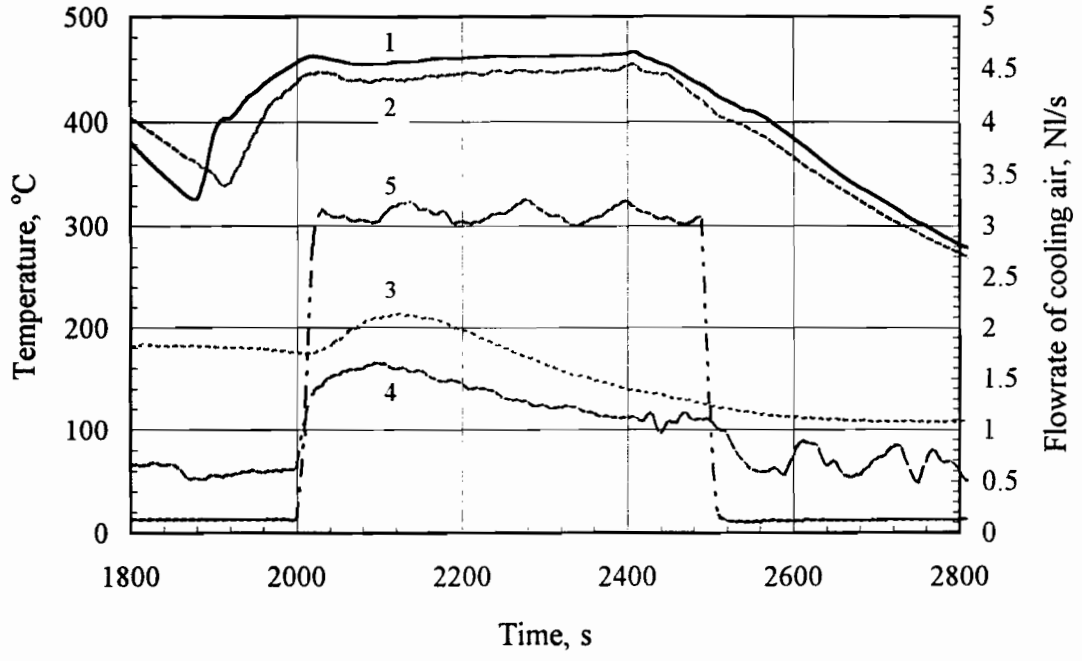

Figure 7.18 Temperature and flowrate profiles on the final version lance during steelmaking

One should also note that the rate of heat extraction began a gradual decline after it peaked. This was the result of increasing thermal resistance on the evaporator that was caused by the growth of an accretion layer. In such tests this is a natural evolution wherein the rate of heat extraction attains a peak early in the blow and subsequently declines. Accretion formation is a positive development that aids in protecting the lance.

7.3.2 Copper Converting Test

Another area of potential significance for heat pipe cooled injection lances is the converting of copper matte (consisting typically of approximately 85% Cu_2S) into metallic copper. While several converting processes are currently in use, the Mitsubishi process which relies strictly on top lancing is an obvious choice for adopting heat pipe cooled lancing technology. Laboratory testing of copper matte converting will now be described.

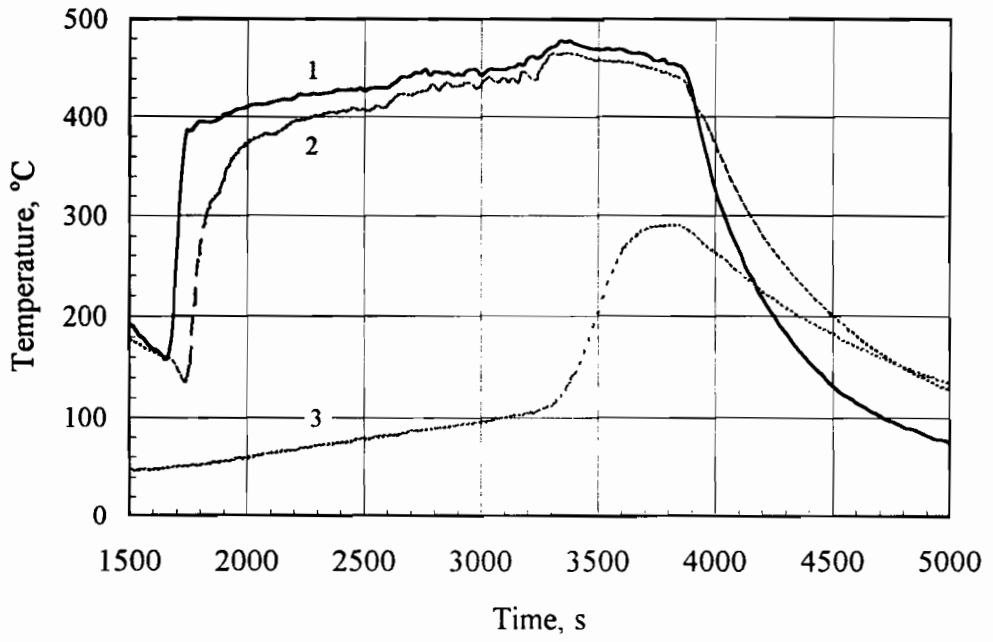

Figure 7.19 Temperature profiles on the final version lance during copper converting

Example:

The next set of trials to be discussed dealt with the converting of copper matte, which is predominantly Cu_2S, to metallic copper by the injection of pure oxygen. While pure

oxygen is never solely injected in commercial practice, it was used in the laboratory to demonstrate the versatility of the lance. The results from only one test will be reported, however, it should be noted that more than 10 tests were actually performed. The test to be described involved the use of the final version of the heat pipe cooled injection lance in the vertical position. The lance nozzle was positioned 30 mm above the melt surface. The charge consisted of 9.5 kg of Noranda reactor matte (approximately 70% Cu). Oxygen was blown into the melt at an average rate of 0.35 Nl/s.

Figure 7.19 shows three temperature curves. Thermocouples #1 to #3 were in the thermocouple well and were 10, 110 and 360 mm up from the leading end of the lance. As shown in Figure 7.19, temperatures #1 and #2 were relatively constant and close to each other, which means the heat pipe worked well. The heat extraction rate was obviously smaller than that of the steelmaking tests because cooling air was not required for the copper matte converting trials. As with the steelmaking trials, an accretion formed on the lance tip, however, its thickness was in general substantially less.

7.3.3 Silver Refining Test

The last system to be tested in the laboratory involved the selective oxidation of lead in a cupel to recover the precious metals - the bulk being silver. Even though top lancing has seen limited implementation to date, the AUSMELT Corp. has been a strong proponent of top lancing and has been chosen to design several new silver refining operations that will be based on top injection.

Example:

The final set of trials (6 tests were conducted in total) to be discussed involved the refining of silver by the selective oxidation of lead and other constituents. The results from one test follow. The feed material comprising about 85% Pb and 10% Ag was supplied by Brunswick Mining and Smelting. A charge of 11.34 kg of alloy was melted and heated to about 1300°C in the same induction furnace used for the other trials. The lance was positioned vertically, the lance tip was positioned 60 mm above the melt surface, and oxygen was blown at rates ranging between 0.25 and 0.35 Nl/s.

Figure 7.20 shows three temperature curves. Thermocouples #1 to #3 were position at the same locations as in copper converting test. As shown in Figure 7.20, the difference between temperatures #1 and #2 was about 100°C, and temperature #3 never exceeded 100°C during the entire operation. This indicates that the heat which needed to be dissipated from the nozzle was so small that the vapor of working substance did not even move over the second thermocouple. Of the three types of tests, this is the one which

required the lowest amount of heat dissipation.

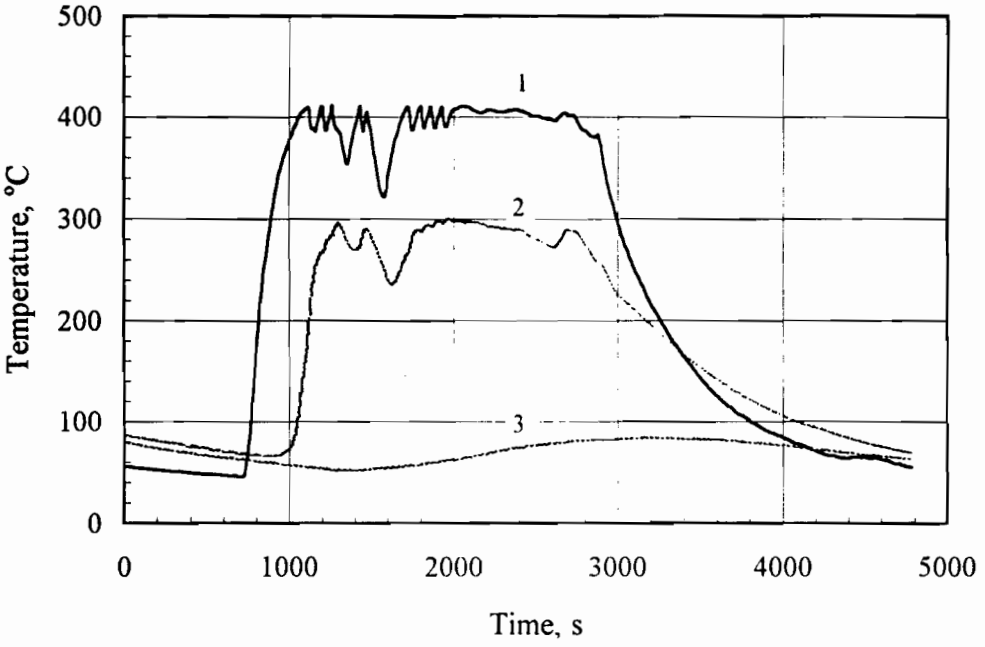

Figure 7.20 Temperature profiles on the final version lance during silver refining

7.4 Hot Simulation of the Oxygen Injection Tests

The behavior of the final version of the heat pipe cooled injection lance in steelmaking, copper converting, and silver refining tests was also evaluated in hot furnace environments created by an electric furnace with no molten bath, no cooling air flowing through the jacket, and no reagent blowing through the reagent conduit. The purpose behind these tests was to assess qualitatively whether the induction field present when the smelting systems were tested had any influence on the measured temperatures in the lance.

First, the furnace was heated up to 925°C, then the lance from the leading end to 40 mm up was exposed in the hot furnace environment. Three thermocouples were positioned at the same locations as in copper converting and silver refining tests. Figure 7.21 shows the three resulting temperature curves, which are very similar to the results from the copper converting test. Another similar result is shown in Figure 7.22 with the furnace at 975°C and 30 mm in the hot furnace environment.

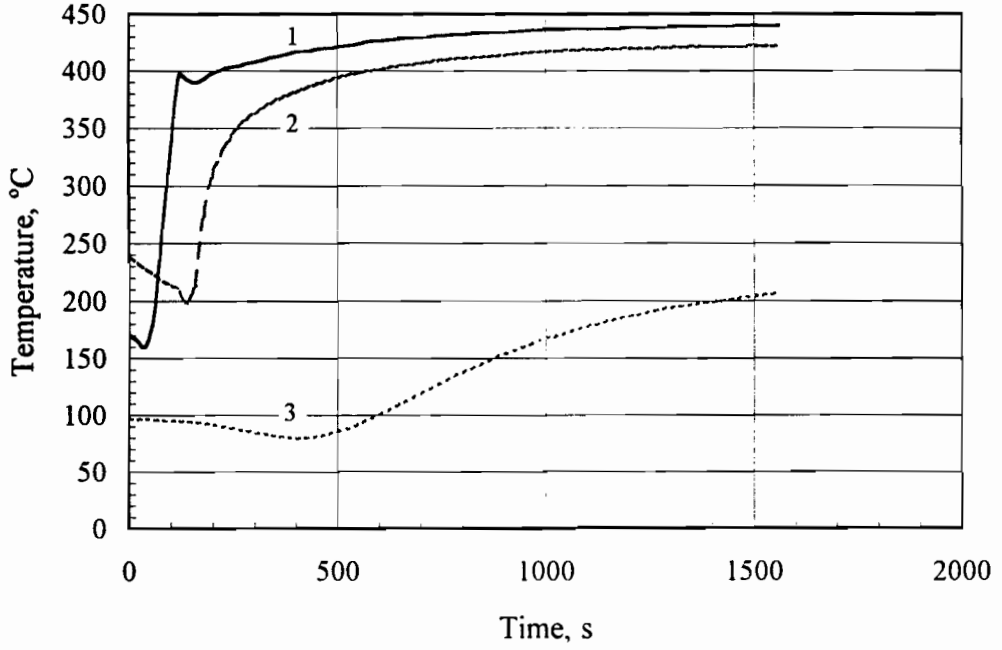

Figure 7.21 Temperature profiles during hot simulation with 40 mm evaporator

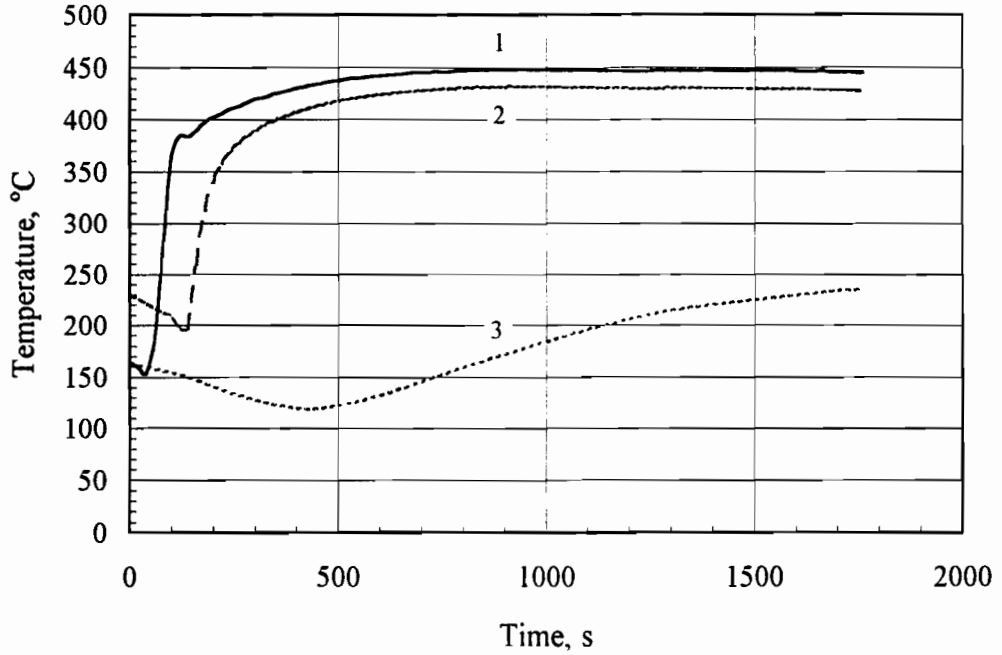

Figure 7.22 Temperature profiles during hot simulation with 30 mm evaporator

The hot furnace simulation tests confirmed that the induction field has only a minor influence on the measured temperature. The temperature measurements of the lance in all three metallurgical processes represent real phenomena. Since temperature #3 was always much lower than the two others in all three processes, it indicates that the lance was over designed for the given conditions that were applied in the laboratory.

Given that cooling air was not used in the copper and silver tests, one can readily conclude that the oxygen reagent was sufficient to adequately cool the lance system. Thus, this lance can be shorten by a considerable amount. The steelmaking tests, on the other hand, required a fair amount of cooling. One can then conclude that the lance was adequately sized for this application. Since the lance was designed for steelmaking, the conclusions drawn from the tests are consistent with the assumptions that were originally made.

CHAPTER 8

MATHEMATICAL MODELING OF HEAT PIPE COOLED INJECTION LANCES

In this chapter a mathematical model of the heat pipe cooled injection lance is presented. The results from the mathematical model will be compared to those of some of the experiments.

8.1 Introduction

A PC-based software package, henceforth referred to as HEATPIPE 1.0, was developed in a previous study to model steady-state variable-conductance heat pipe operation assuming the flat front hypothesis[78]. The user inputs the specifications of the pipe geometry and boundary conditions, as well as the physical properties of the working substance, reagent and air. The program then iteratively solves the governing equations and outputs the unknown operating variables including temperatures and heat fluxes.

Based on the modifications made in this study, a new version of the mathematical model for heat pipe cooled injection lances, HEATPIPE 2.0, was proposed, formulated, and tested. HEATPIPE 2.0 was designed specifically for modeling steady-state operation of the new generation of heat pipe cooled injection lances.

There are two major differences between HEATPIPE 1.0 and HEATPIPE 2.0.

Firstly, HEATPIPE 2.0 was designed for a heat pipe which has no inert gas in the pipe. Secondly, HEATPIPE 2.0 has more flexibility when considering different boundary conditions on the condenser section. Both forced cooling and free convection/radiation are valid boundary conditions for HEATPIPE 2.0. The preheating of oxygen on the condenser is also a valid boundary condition.

8.2 Mathematical Model

This section consists of assumptions used in the model, model construction, variables and equations, input, computation, and output.

8.2.1 Assumptions

The basic principal of the numerical approach to a heat transfer problem is the replacement of the differential equation for the continuous temperature distribution in a heat conducting solid by a finite difference equation which must be satisfied at only certain points in the solid.

A relatively simple 2-D heat transfer model was developed in this study. Several key assumptions of this model are 1) the entire mass of working substance including the liquid and vapor phases is at one uniform temperature and 2) axial wall-conduction is ignored.

The mathematical model assumes that only heat transfer normal to the surfaces of the containers is considered. Because of the super conductivity of the heat pipe, temperature differences along the longitudinal axis are, in general, very small.

8.2.2 Model Construction

HEATPIPE 2.0 was formulated for modeling only steady-state operation of the new generation of heat pipe cooled lances, because the transient-state is not considered as important as the steady-state case and because the transient state would unduly complicate the modeling with little to be gained.

HEATPIPE 2.0 executes air-cooled heat pipe modeling according to user-specified inputs. These inputs include specifications of the geometry and composition of the heat pipe. Axially, the pipe is divided into seven nodes. Users can define how many nodes should be used as the evaporator section, adiabatic section, and condenser section, and the dimensions of each node. The layout of the axial nodes is illustrated in Figure 8.1. An

additional node to the above axial nodes is the node at lance tip, which is illustrated in Figure 8.2. Radially, the pipe is divided into ten nodes. The layout of the radial notes is illustrated in Figures 8.3 and 8.4, respectively.

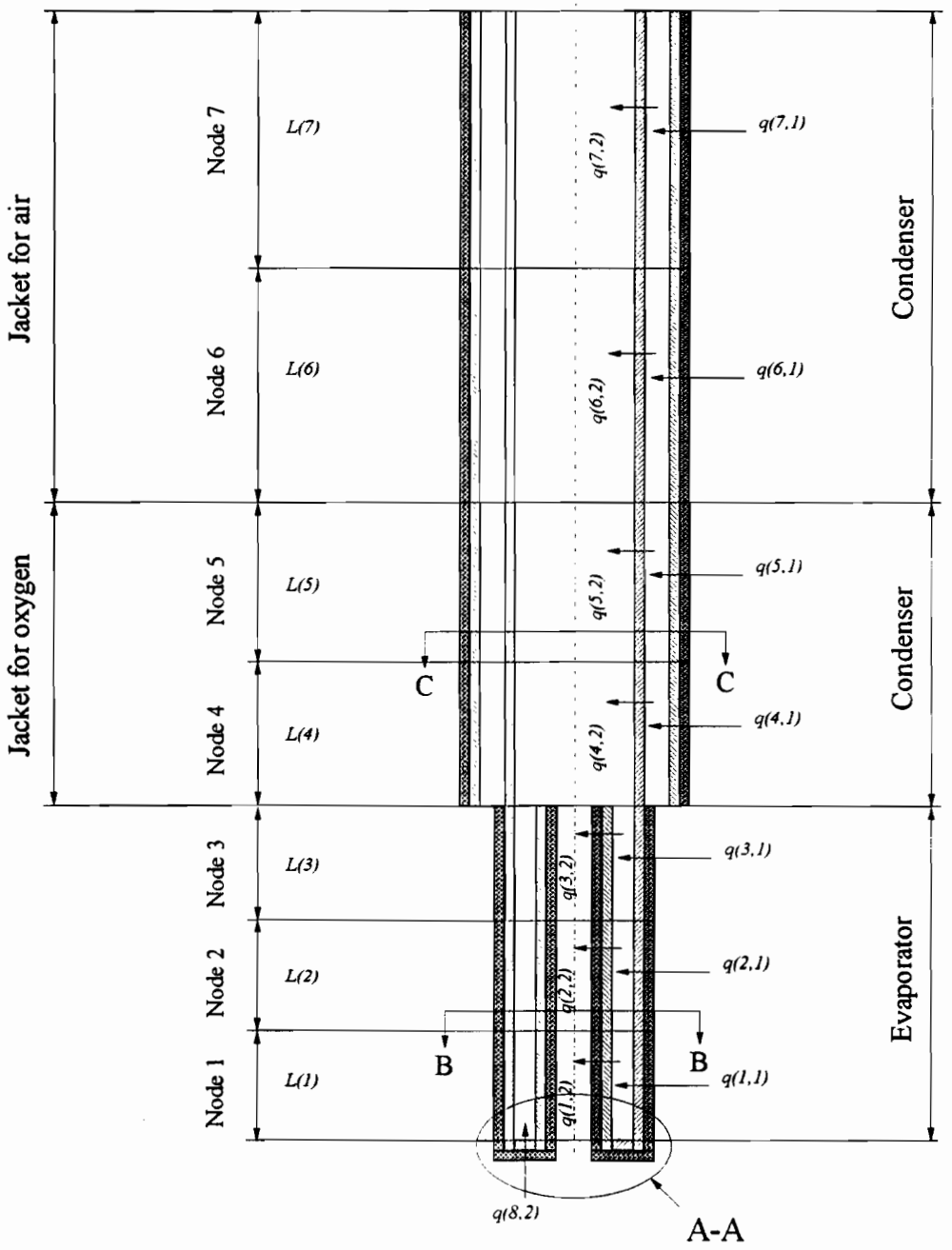

Figure 8.1 Schematic diagram of the model

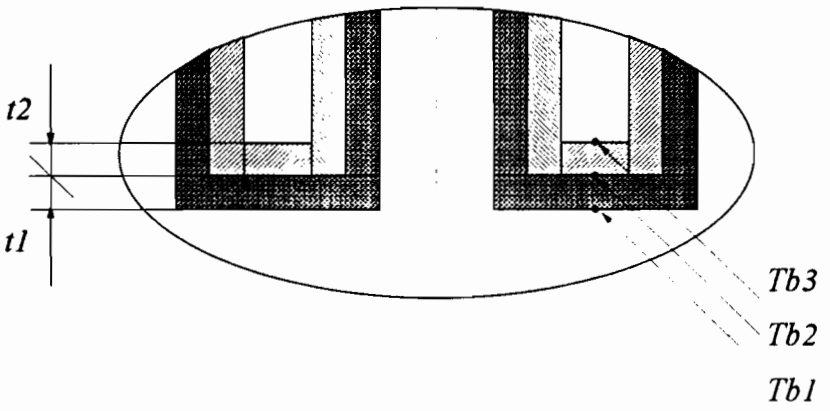

Figure 8.2 Section A-A of the model

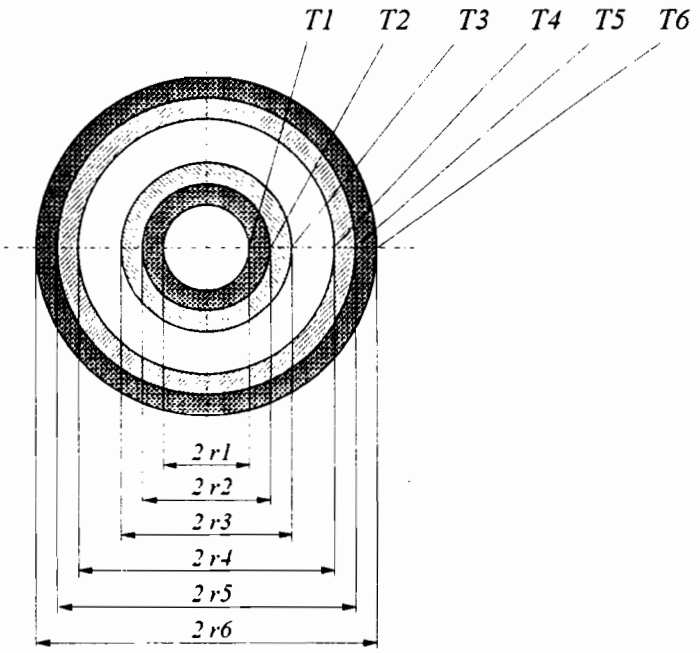

Figure 8.3 Section B-B of the model

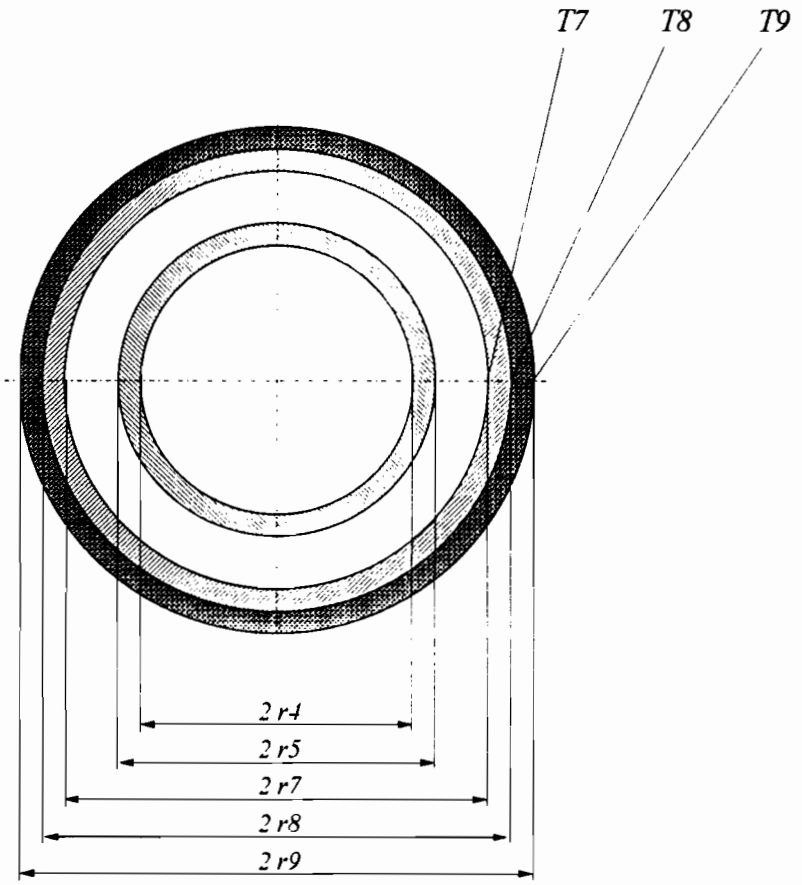

Figure 8.4 Section C-C of the model

8.2.3 Variables, Equations, and HEATPIPE 2.0

HEATPIPE 2.0 solves a system of 64 equations and 64 variables by use of the Newton-Rapheson matrix method[79].

The number of variables is determined by the number of the nodes and the nature of the model. All the 64 variables, as well as their descriptions and units are listed in Table 8.1. Of these variables, 49 of them are temperature variables, the rest are heat energy variables. Meanwhile, all the governing equations for the entire collection of modes are listed in Table 8.2.

Table 8.1 Variables employed in HEATPIPE 2.0 model

Variables	Description	No.
q(i,1), for i = 1, ···, 3	energy transfer from environment to working substance, ith node, W.	3
q(i,1), for i = 4, ···, 7	energy transfer from environment to jacket shells, ith node, W.	4
q(i,2), for i = 1, ···, 3	energy expelled from working substance to reagent gas, ith node, W.	3
q(i,2), for i = 4, ···, 7	energy transfer from environment, cooling air and reagent to working substance, ith node, W.	4
q(8,2)	energy transfer from environment (lance tip) to working substance, W.	1
T(i,1), for i = 1, ···, 3	temperature of insulating material on inner wall of reagent conduit, ith node, °C.	3
T(i,2), for i = 1, ···, 3	temperature of inner wall of reagent conduit, ith node, °C.	3
T(i,3), for i = 1, ···, 3	temperature of outer wall of reagent conduit, ith node, °C.	3
T(i,4), for i = 1, ···, 7	temperature of inner wall of heat pipe shell, ith node, °C.	7
T(i,5), for i = 1, ···, 7	temperature of outer wall of heat pipe shell, ith node, °C.	7
T(i,6), for i = 1, ···, 3	temperature of outer wall of protective coating on heat pipe, ith node, °C.	3
T(i,7), for i = 4, ···, 7	temperature of inner wall of air or reagent jacket, ith node, °C.	4
T(i,8), for i = 4, ···, 7	temperature of outer wall of air or reagent jacket, ith node, °C.	4
T(i,9), for i = 4, ···, 7	temperature of outer wall of protective coating on jackets, ith node, °C.	4
T(i,10), for i = 1, ···, 5	bulk temperature of reagent gas, ith node, °C.	5
T(i,10), for i = 6, 7	bulk temperature of cooling air, ith node, °C.	2
Tb1	temperature of lower surface of protective coating on bottom cap, °C.	1
Tb2	temperature of lower surface of bottom cap, °C.	1
Tb3	temperature of upper surface of bottom cap, °C.	1
Tws	temperature of working substance, °C.	1
Variables	total	64

Table 8.2 Equations employed in HEATPIPE 2.0 model

1. $q_{i,1}$ from environment to outer coating, node i, $i=1, 3$

$$q_{i,1} = 2\pi\, r_{i,6}\, l_i\, [h_{i,6}(Tamb_i - T_{i,6}) + \sigma\, eF(Tamb_i^4 - T_{i,6}^4)] \tag{8.1}$$

2. $q_{i,1}$ through outer coating, node i, $i=1, 3$

$$q_{i,1} = 2\pi\, l_i\, k5 \ln\left(\frac{r_{i,6}}{r_{i,5}}\right)(T_{i,6} - T_{i,5}) \tag{8.2}$$

3. $q_{i,1}$ through outer pipe shell, node i, $i=1,3$

$$q_{i,1} = 2\pi\, l_i\, k4 \ln\left(\frac{r_{i,5}}{r_{i,4}}\right)(T_{i,5} - T_{i,4}) \tag{8.3}$$

4. $q_{i,1}$ from outer pipe shell to working substance, node i, $i=1, 3$

$$q_{i,1} = 2\pi\, r_{i,4}\, l_i\, h_{i,4}(T_{i,4} - Tws) \tag{8.4}$$

5. $q_{i,2}$ from working substance to inner pipe shell, node i, $i=1, 3$

$$q_{i,2} = 2\pi\, r_{i,3}\, l_i\, h_{i,3}(Tws - T_{i,3}) \tag{8.5}$$

6. $q_{i,2}$ through reagent conduit, node i, $i=1, 3$

$$q_{i,2} = 2\pi\, l_i\, k2 \ln\left(\frac{r_{i,3}}{r_{i,2}}\right)(T_{i,3} - T_{i,2}) \tag{8.6}$$

7. $q_{i,2}$ through insulating materials in reagent conduit, node i, $i=1,3$

$$q_{i,2} = 2\pi\, l_i\, k1 \ln\left(\frac{r_{i,2}}{r_{i,1}}\right)(T_{i,2} - T_{i,1}) \tag{8.7}$$

8. $q_{i,2}$ into reagent gas, node i, $i=1, 3$

$$q_{i,2} = 2\pi\, r_{i,1}\, l_i\, h_{i,1}(T_{i,1} - T_{i,10}) \tag{8.8}$$

9. $q_{i,1}$ from environment to outer coating, node i, $i=4, 7$

$$q_{i,1} = 2\pi\, r_{i,9}\, l_i\, [h_{i,9}(Tamb_i - T_{i,9}) + \sigma\, eF(Tamb_i^4 - T_{i,9}^4)] \tag{8.9}$$

10. $q_{i,1}$ through outer coating, node i, $i=4, 7$

$$q_{i,1} = 2\pi\, l_i\, k8\, ln\left(\frac{r_{i,9}}{r_{i,8}}\right)(T_{i,9} - T_{i,8}) \tag{8.10}$$

11. $q_{i,1}$ through air cooling jacket and reagent preheating jacket, node i, $i=4, 7$

$$q_{i,1} = 2\pi\, l_i\, k7\, ln\left(\frac{r_{i,8}}{r_{i,7}}\right)(T_{i,8} - T_{i,7}) \tag{8.11}$$

12. $q_{i,1}$ into reagent gas or air in jackets and outer pipe shell, node i, $i=4, 7$

$$q_{i,1} = 2\pi\, r_{i,7}\, l_i\, [h_{i,7}(T_{i,7} - T_{i,10}) + \sigma\, eF(T_{i,7}^4 - T_{i,5}^4)] \tag{8.12}$$

13. $q_{i,2}$ from reagent gas or air in jackets and jacket shells, node i, $i=4, 7$

$$q_{i,2} = 2\pi\, r_{i,5}\, l_i\, [h_{i,5}(T_{i,10} - T_{i,5}) + \sigma\, eF(T_{i,7}^4 - T_{i,5}^4)] \tag{8.13}$$

14. $q_{i,2}$ through outer pipe shell, node i, $i=4,7$

$$q_{i,2} = 2\pi\, l_i\, k4\, ln\left(\frac{r_{i,5}}{r_{i,4}}\right)(T_{i,5} - T_{i,4}) \tag{8.14}$$

15. $q_{i,2}$ from outer pipe shell to working substance, node i, $i=4, 7$

$$q_{i,2} = 2\pi\, r_{i,4}\, l_i\, h_{i,4}(T_{i,4} - Tws) \tag{8.15}$$

16. $q_{8,2}$ from environment to outer coating, node 8 (lance tip)

$$q_{8,2} = \pi(r_4^2 - r_3^2)[h_{8,1}(Tamb_8 - Tb1) + \sigma\, eF(T_{8,amb}^4 - Tb1^4)] \tag{8.16}$$

17. $q_{8,2}$ through outer coating, node 8 (lance tip)

$$q_{8,2} = \frac{\pi(r_4^2 - r_3^2)k5(Tb1 - Tb2)}{t1} \tag{8.17}$$

18. $q_{8,2}$ through outer pipe shell, node 8 (lance tip)

$$q_{8,2} = \frac{\pi(r_4^2 - r_3^2)k9(Tb2 - Tb3)}{t2} \tag{8.18}$$

19. $q_{8,2}$ from outer pipe shell to working substance, node 8 (lance tip)

$$q_{8,2} = \pi (r_4^2 - r_3^2) h_{8,3} (Tb3 - Tws) \tag{8.19}$$

20. Reagent gas heat accumulation, node *i*, *i=1, 3*

$$q_{i,2} = \pi r_{i,1}^2 \rho_r v_r C_{p,r} (T_{i,10} - T_{i+1,10}) - \pi r_{i,1}^2 v_r \frac{inletp(1) - 101300}{\sum_{i=1}^{5} l_i} \tag{8.20}$$

21. Reagent gas heat accumulation, node *i*, *i=4*

$$q_{i,2} = \pi (r_{i,6}^2 - r_{i,5}^2) \rho_r v_r C_{p,r} (T_{i,10} - T_{i+1,10}) - \pi (r_{i,6}^2 - r_{i,5}^2) v_r \frac{inletp(1) - 101300}{\sum_{i=1}^{5} l_i} \tag{8.21}$$

22. Reagent gas heat accumulation, node *i*, *i=5*

$$q_{i,2} = \pi (r_{i,6}^2 - r_{i,5}^2) \rho_r v_r C_{p,r} (T_{i,10} - T_{in}(1)) - \pi (r_{i,6}^2 - r_{i,5}^2) v_r \frac{inletp(1) - 101300}{\sum_{i=1}^{5} l_i} \tag{8.22}$$

23. Cooling air heat accumulation, node *i*, *i=6*

$$q_{i,2} = \pi (r_{i,6}^2 - r_{i,5}^2) \rho_a v_a C_{p,a} (T_{i,10} - T_{in}(2)) - \pi (r_{i,6}^2 - r_{i,5}^2) v_a \frac{inletp(2) - 101300}{l_6 + l_7} \tag{8.23}$$

24. Cooling air heat accumulation, node *i*, *i=7*

$$q_{i,2} = \pi (r_{i,6}^2 - r_{i,5}^2) \rho_a v_a C_{p,a} (T_{i,10} - T_{i-1,10}) - \pi (r_{i,6}^2 - r_{i,5}^2) v_a \frac{inletp(2) - 101300}{l_6 + l_7} \tag{8.24}$$

25. Working substance q balance

$$\sum_{i=1}^{3} q_{i,1} + \sum_{i=1}^{8} q_{i,2} = 0 \tag{8.25}$$

HEATPIPE 2.0 has been written in FORTRAN for MS-DOS PCs. The code of HEATPIPE 2.0 is listed in Appendix I. The serial numbers of all the variables are listed in Appendix II.

8.2.4 Input

59 parameters need to be put into the input file. The following is a list with a number used in one input file, the parameter used in the program, and the meaning and unit of that parameter.

Values	*Parameters*	*Descriptions*
1	*relax*	*relax number.*
10	*maxcycle*	*maximum number of cycles.*
0.5	*thresh*	*thresh number.*
0.0021999	*r1*	*inner radius of insulating material in oxygen conduit (m).*
0.0022000	*r2*	*inner radius of oxygen conduit (m).*
0.0032000	*r3*	*outer radius of oxygen conduit (m).*
0.0110000	*r4*	*inner radius of heat pipe shell (m).*
0.0127000	*r5*	*outer radius of heat pipe shell (m).*
0.0127001	*r6*	*outer radius of coating material on heat pipe shell (m).*
0.0142240	*r7*	*inner radius of oxygen or air jacket (m).*
0.0158750	*r8*	*outer radius of oxygen or air jacket (m).*
0.0158751	*r9*	*outer radius of coating material on jackets (m).*
0.001	*l11*	*length of node 1 (m).*
0.007	*l22*	*length of node 2 (m).*
0.012	*l33*	*length of node 3(m).*
0.080	*l45*	*length of nodes 4 and 5 (m).*
0.070	*l67*	*length of nodes 6 and 7 (m).*
0.0000001	*t1*	*thickness of build up on bottom cap (m).*
0.005	*t2*	*thickness of bottom cap (m).*
1900	*Tamb11*	*ambient temperature applied to node 1 (°C).*
1300	*Tamb22*	*ambient temperature applied to node 2 (°C).*
300	*Tamb33*	*ambient temperature applied to node 3 (°C).*
20	*Tamb45*	*ambient temperature applied to nodes 4 and 5 (°C).*
20	*Tamb67*	*ambient temperature applied to nodes 6 and 7 (°C).*
1900	*Tamb88*	*ambient temperature applied to node 8 (°C).*
20	*Tin(1)*	*inlet temperature of reagent (°C).*
101300	*inletp(1)*	*inlet pressure of reagent (N/m^2).*
1.43	*dg(1)*	*density of reagent (kg/m^3).*
0.9159	*hcg(1)*	*heat capacity of reagent(kJ/kg-°C).*

0.3	*flowrate(1)*	*flow rate of reagent (l/s).*
20	*Tin(2)*	*inlet temperature of air (°C).*
101300	*inletp(2)*	*inlet pressure of air (N/m^2).*
1.2923	*dg(2)*	*density of air (kg/m^3).*
1.0057	*hcg(2)*	*heat capacity of air (kJ/kg-°C).*
3.000	*flowrate(2)*	*flow rate of air (l/s).*
2	*k1*	*thermal conductivity of insulating materials in reagent conduit (W/m-°C).*
15	*k2*	*thermal conductivity of reagent conduit (W/m-°C).*
15	*k4*	*thermal conductivity of heat pipe shell (W/m-°C).*
2	*k5*	*thermal conductivity of build-up on lance body (W/m-°C).*
15	*k7*	*thermal conductivity of air cooling jacket and reagent preheating jacket (W/m-°C).*
2	*k8*	*thermal conductivity of coating on two jackets (W/m-°C).*
70	*k9*	*thermal conductivity of bottom cap (W/m-°C).*
50	*h1*	*heat transfer coefficient on the inner surface of reagent conduit (W/m^2-°C).*
100000	*h3*	*heat transfer coefficient on the outer surface of reagent conduit (W/m^2-°C).*
100000	*h41*	*heat transfer coefficient on the inner surface of heat pipe shell at node 1 (W/m^2-°C).*
100000	*h42*	*heat transfer coefficient on the inner surface of heat pipe shell at node 2 (W/m^2-°C).*
100000	*h43*	*heat transfer coefficient on the inner surface of heat pipe shell at node 3 (W/m^2-°C).*
100000	*h447*	*heat transfer coefficient on the inner surface of heat pipe shell at nodes 4 to 7 (W/m^2-°C).*
50	*h51*	*heat transfer coefficient on the outer surface of heat pipe shell in reagent preheating section (W/m^2-°C).*
180	*h52*	*heat transfer coefficient on the outer surface of heat pipe shell in air cooling section (W/m^2-°C).*
30	*h6*	*heat transfer coefficient on the outer surface of build-up in the evaporator section (W/m^2-°C).*
50	*h71*	*heat transfer coefficient on the inner surface of reagent preheating jacket (W/m^2-°C).*
180	*h72*	*heat transfer coefficient on the inner surface of air cooling*

		jacket (W/m^2-°C).
30	*h9*	*heat transfer coefficient on the outer surface of the coating on reagent preheating and air cooling jackets (W/m^2-°C).*
30	*h10*	*heat transfer coefficient on the outer surface of the build-up on bottom cap (W/m^2-°C).*
100000	*h11*	*heat transfer coefficient on the inner surface of bottom cap (W/m^2-°C).*

8.2.5 Computation

Matrix operations are performed through Gauss-Jordan elimination. Initial guesses for the iterative solution are produced automatically by the program. During the iterative process. the user is updated on the solution process with each successive iteration. Normally, solution convergence requires 3 to 5 iterations. The following is the information displayed on the screen during a computation.

```
maxcycle=            0
errorsum= 1050757.823940454000000
maxdiff=  703715.366553268400000
maxcycle=            1
errorsum=     435.748461604195000
maxdiff=      134.502838509771000
maxcycle=            2
errorsum=      60.517425043997330
maxdiff=        7.178004735590794
maxcycle=            3
errorsum=       1.033784710029467
maxdiff=  9.957720385513041E-002
Stop - Program terminated
```

8.2.6 Output

The file name of the output data is called *output.dat*. The format of *output.dat* is presented as follows:

q(1,1), q(2,1), ·····, q(7,1)

$q(1,2)$, $q(2,2)$, ·····, $q(7,2)$, $q(8,2)$

$T(7,1)$, $T(7,2)$, ·····, $T(7,10)$
$T(6,1)$, $T(6,2)$, ·····, $T(6,10)$
$T(5,1)$, $T(5,2)$, ·····, $T(5,10)$
$T(4,1)$, $T(4,2)$, ·····, $T(4,10)$
$T(3,1)$, $T(3,2)$, ·····, $T(3,10)$
$T(2,1)$, $T(2,2)$, ·····, $T(2,10)$
$T(1,1)$, $T(1,2)$, ·····, $T(1,10)$

$Tb1$, $Tb2$, $Tb3$, Tws

The units for all q_s are Watts, and the units for all the temperatures are Celsius.

8.3 Evaluation of Model Results

For a heat pipe cooled injection lance, the most important parameter is the operating temperature of the lance. Generally, the lower the operating temperature is, the longer the life of the lance will be. Therefore, it is a basic requirement for the model to be able to generate the operating temperature of the lance.

Meanwhile, the operating temperature of the lance is a function of the flowrate of cooling air. In reality, the operating temperature can be adjusted by changing the flowrate of cooling air. The more heat that is dissipated by the cooling air, the lower the operating temperature will be. Therefore, the heat extraction rate of cooling air is another important parameter. Since the flowrate of cooling air is an input parameter, the heat extraction rate by the cooling air is a function of the outlet temperature of the cooling air. Therefore, the operating temperature of the heat pipe and the outlet temperature of cooling air were evaluated.

Of the boundary conditions required by the mathematical model, one is the heat transfer coefficient between the cooling air and the heat pipe. Basically, the accuracy of the mathematical model is dependent on the accuracy of the value of this heat transfer coefficient. In this section, the heat transfer coefficient on the condenser was obtained from indirect measurement, as shown in Section 4.3.2. In general, the heat transfer coefficient can be estimated based on empirical data.

Example 1:

In Table 4.2, the operating temperatures and the outlet temperatures of the cooling air were measured for three different flowrates of cooling air. The heat transfer coefficient was computed based on the measurements. The same boundary conditions as well as the physical properties of cooling air and reagent, the flowrate of cooling air, thermal conductivities, heat transfer coefficients, and so on, were used as input for HEATPIPE 2.0. The simulation results from the mathematical model are listed in Tables 8.3 and 8.4.

Table 8.3 Comparison between measured and computed operating temperature

Flowrate of cooling air, Nl/s	Measured operating temperature, °C	Computed operating temperature, °C	Difference °C
0.657	546.3	554.9	-8.6
1.413	502.9	491.4	11.5
2.367	423.7	428.5	-4.8

The maximum error between the measured and computed operating temperature is 1.5%, and the maximum error between the measured and computed outlet temperature is 3.5% based on the absolute Kelvin temperature scale.

Table 8.4 Comparison between measured and computed outlet temperature

Flowrate of cooling air, Nl/s	Measured outlet temperature of cooling air, °C	Computed outlet temperature of cooling air, °C	Difference °C
0.657	363.4	351.1	12.3
1.413	300.3	280.4	19.9
2.367	233.1	223.1	10.0

Example 2:

As mentioned in Section 7.4, the behavior of the heat pipe cooled injection lance in the steelmaking, copper converting, and silver refining tests was simulated in hot furnace

environments created by an electric furnace with no molten bath, no cooling air flowing through the jacket, and no reagent blowing through the reagent conduit. Comparable temperature profiles as obtained in steelmaking, copper converting, and silver refining trials were recreated in hot furnace environments. It was concluded, as has already been stated, that the heat pipe cooled injection lance was over designed for those kinds of conditions. In this section, the mathematical model is used to draw an independent conclusion.

The same boundary conditions were applied to the model, which means that the evaporator was about 40 mm long and it was exposed to 925°C in the hot furnace environment. The computed operating temperature for this case was 396°C. When the evaporator was about 30 mm long and it was exposed to 925°C in the hot furnace environment, the computed operating temperature for this case was 383°C. As shown in Section 7.2, the minimum operating temperature for the final heat pipe cooled injection lance was 440°C. For both cases mentioned above, the computed operating temperatures are less than 440°C, which means that for the real system the condenser was only partially active at 440°C. In effect, the lower portion of the condenser was at 440°C while the upper regions were at temperatures substantially below 440°C. Thus, for operating temperatures as generated by the model of less than 440°C, the heat pipe does not operate 'isothermally'. Therefore, the same conclusion can be drawn that the heat pipe cooled injection lance was over designed for those kinds of conditions.

According to the results from both examples, it can be concluded that the mathematical model is reliable, and the results are relatively accurate. It can be a strong tool in further developing this technology and bringing this technology to a commercial level in the near future.

8.4 Simulating Performance of Lances in Real Processes

The performance of the heat pipe cooled injection lance in the steelmaking experiment as presented in example 3 of Section 7.3.1 is simulated with HEATPIPE 2.0. The boundary conditions and results follow.

The boundary conditions for the simulation are listed in Section 8.2.4. The same boundary conditions were used as in Reference 78 except the parameters which did not exist in the Reference. The total active length of the heat pipe cooled injection lance was estimated to be 350 mm based on the location of thermocouple 3 and its reading during the experiment as presented in Figure 7.18. The heat transfer coefficient between the

cooling air and the surface of the jacket was estimated to be 180 W/m^2-°C based on the information presented in Table 4.2.

The simulation results are presented in Appendix III. The operating temperature of the heat pipe was 469.5°C. The temperature gradient through the 5 mm nickel tip was 71.7°C, while when exposed to the same hot environment the temperature gradient through 1.65 mm of heat pipe wall was 117.7°C. The temperature profile from the computed simulation is presented in Figure 8.5. In the air cooling jacket, cool air was heated up to 120.3°C. In the reagent preheating jacket, oxygen was heated up to 265.2°C. Because the outlet temperature of oxygen on the nozzle is 272.6°C, oxygen is only heated up by 7.3°C in the central conduit. This insures that the mass balance of the working fluid is upheld. In Table 8.5, a comparison between the measured and computed operating temperatures is made, while Table 8.6, a comparison between the measured and computed outlet temperatures of the cooling air is made. The maximum error between the measured and computed operating temperature is 2.8%, and the maximum error between the measured and computed outlet temperature is 7.6% based on the absolute Kelvin temperature scale. On the lance tip, the amount of heat applied on it was 353.3 W. Since the area of the lance tip was 351.9×10^{-6} m^2, the heat flux dissipated on the lance tip was about 1.004 MW/m^2.

Table 8.5 ***Comparison between measured and computed operating temperature in steelmaking***

Flowrate of cooling air, Nl/s	Measured operating temperature, °C	Computed operating temperature, °C	Difference °C
3.0	450	470	-20

Table 8.6 ***Comparison between measured and computed outlet air temperature in steelmaking***

Flowrate of cooling air, Nl/s	Measured outlet temperature of cooling air, °C	Computed outlet temperature of cooling air, °C	Temperature difference, °C
3.0	150	120	30

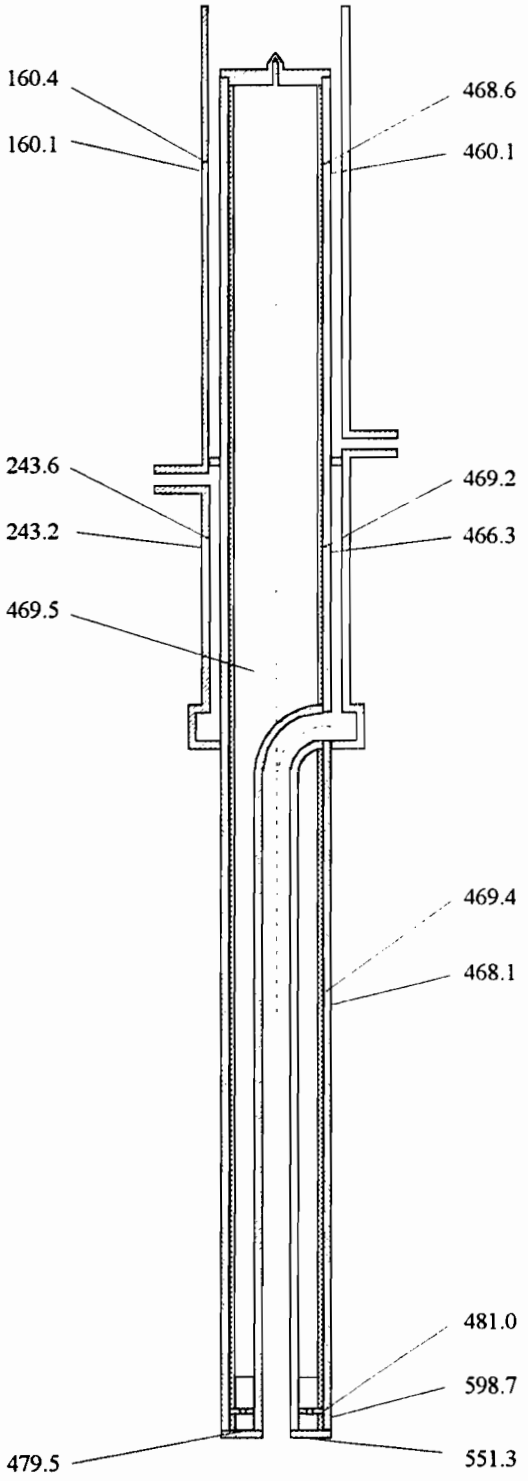

Figure 8.5 Temperature profile from computed simulation

The discrepancies between measured and computed results can be ascribed to the uncertainties in estimating boundary conditions. It is virtually impossible to fully and accurately describe the system as it exists during a blow. Some variability in the results is characteristic of the system.

As has been shown, HEATPIPE 2.0 is a reliable mathematical model for simulating heat pipe cooled injection lances. Therefore, for any project that is related to the scale up of heat pipe cooled injection lances, HEATPIPE 2.0 can be used during the design stage.

In formulating the boundary conditions for the mathematical model, one of the biggest unknowns is the configuration of buildup on the lance. In reality, this depends on the environment that the lance is in, and it is also a function of operating temperature of the heat pipe.

CHAPTER 9

CONCLUSIONS

In the present work, heat pipes and heat pipe cooled injection lances were investigated by conducting both fundamental and experimental studies in combination with mathematical modeling. Based on the results and discussions presented in Chapter 4 to 8, the following conclusions can be drawn.

1. The effects of wick structure on the performance of a gravity-assisted heat pipe were studied. For high temperature applications of a gravity-assisted heat pipe, wick structure plays a very important role on redistributing working fluid over the entire evaporator section. Without a proper wick structure installed in the gravity-assisted heat pipe it may not be possible to ensure that the working fluid covers and protects the entire evaporator section. Therefore, in a heat pipe or heat pipe cooled injection lance, a wick has to be applied.
2. The influence of the inert gas zone in a variable-conductance heat pipe on the overall performance was examined. For the situation that the temperature in the inert gas zone is lower than the melting point of working fluid, all the working fluid tends to condense and freeze in the inert gas zone over some period of time. This causes the evaporator of the heat pipe to be dried out and the pipe to fail. Under this circumstance, the variable-conductance heat pipe cannot be applied. All the non-condensable gases should be taken out from the heat pipe.
3. The role of forced convection cooling as applied to the condenser section of the heat

pipe was investigated. An air cooling jacket on the condenser section is recommended. With a suitable cooling jacket in place it is possible to operate the heat pipe at the lowest temperature for a given set of conditions. Given that lance life is directly correlated to the operating temperature, enhanced cooling can greatly prolong the life of the heat pipe cooled injection lance.

4. The superheat in the liquid pool of working fluid in a gravity-assisted heat pipe was studied. A method of reducing the superheat in the liquid pool was proposed, and tested. It has been demonstrated that by using the proposed method (i.e. placing a temperature stabilizer in the liquid pool) the superheat in the pool can be reduced by more than 75%. Thus, the evaporator, and, in particular, the lance nozzle can be cooled more efficiently.
5. A mass balance of the working fluid in the annular heat pipe cooled injection lance as proposed in prior studies was carried out. It was discovered that for a sizable heat pipe cooled injection lance there is a large possibility of creating a mass imbalance of working fluid. The consequences of this mass imbalance is the generation of a dry region in the evaporator section, called a hot-ring, and the premature failure of this dry region. A number of methods for preventing the mass imbalance have been proposed. One specific method was applied successfully to the new generation of heat pipe cooled injection lances developed in this study
6. A new generation of heat pipe cooled injection lances featuring all the improvements made in this study has been detailed. A number of heat pipe cooled injection lances were tested in hot furnace environments and three different pyrometallurgical processes in the laboratory. This new lance was shown to be durable under extremely harsh conditions. The lance tip was capable of dissipating localized heat fluxes exceeding 1 MW/m^2. It was also shown that given the low operating temperature of the lance, an accretion layer forms on a portion of the evaporator. This protective layer is of great benefit in prolonging lance life.
7. A mathematical model for the final configuration of the new generation of heat pipe cooled injection lances was formulated, and tested.

STATEMENT OF ORIGINALITY AND CONTRIBUTION TO KNOWLEDGE

The results obtained in this work are of industrial as well as academic interest, and include the following original contributions.

1. For the first time heat pipe cooled injection lances were investigated systematically. A new generation of heat pipe cooled injection lances has been proposed, designed, fabricated and tested successfully.
2. It has been demonstrated experimentally that the hot-spot phenomenon can be a problem for thermosyphons when alkali metals are chosen as working fluids. The formation of hot-spots on the evaporator of a vertical alkali metal thermosyphon is inevitable for high temperature applications. Installing wick structure in the thermosyphon is an easy, effective, and reliable way of preventing the formation of hot-spots on the evaporator. It has been shown that heat pipes are more suitable for high temperature applications than wickless heat pipes (thermosyphons).
3. Variable-conductance heat pipes have certain advantages overcoming the difficulty of startup from the frozen state over basic heat pipes. However, when an alkali metal with a melting point that is higher than ambient temperature is chosen as the working fluid in a variable-conductance heat pipe, most of the working fluid will eventually freeze in the inert gas section and cause the heat pipe to stop operating. The solution for the problem of working fluid freeze-up is to eliminate all inert gases from the heat pipe.
4. Forced-convection cooling on the condenser provides the possibility of controlling the heat pipe operating temperature at any desired level. By using the heat flux transformation property of heat pipes, it is possible to use air as a cooling medium when the ratio between the area of the condenser and the area of evaporator is big enough. Air cooling on the condenser offers several advantages over a self-cooled system and a water-cooled system.
5. A method was developed for dramatically reducing the temperature difference between the liquid temperature and the saturation temperature by implementing the temperature stabilizer. Installation of a temperature stabilizer in the pool of the working fluid is one of

the best ways for reducing the difference between the liquid temperature and the saturation temperature. All aspects of the temperature stabilizer were novel to this work. In fact the term, temperature stabilizer, originates from this study.

6. It has been shown in this study that a large (i.e. scaled up) annular heat pipe cooled injection lance may encounter the problem of a hot-ring (another term that originated from this study) caused by the mass imbalance of working fluid. The hot-ring phenomenon was recreated successfully on a laboratory scale annular heat pipe cooled injection lance. Several possible solutions to avoid the hot-ring problem on the annular heat pipe cooled lance have been proposed. One solution (i.e. reagent preheating jacket has been stressed in this study.

REFERENCES

1. Volkwin Köster, Günter Paul, and Jobst Weber, "Lance Manipulator for Oxygen Carbon Injection in Steelmaking," Steel Technology International, London, Ed. P.H. Scholes, pp. 91-92, 1992.
2. N. Rymarchyk Jr. and J.R. Paules, "Electric Furnace Lance Maintenance - A Critical Process," Iron & Steelmaker, Vol 23, No. 3, pp. 79-82, 1996.
3. G. Savard and R. Lee, "Improvements in Metallurgical Process," French Patent, Patent No. 1,450,718, 18, July, 1966.
4. K. Brotzmann, "The Bottom Blown Oxygen Converter - A New Method for Steelmaking," Technik und Forschung, Vol. 41, pp. 718-720, 1968, BISI Translation No. 7255.
5. G. Savard and R. Lee, "Submerged Oxygen Injection for Pyrometallurgy," Proceeding of Savard-Lee International Symposium on Bath Smelting, TMS, Warrendale, Pa, pp. 645-660.
6. P.J. Mackey, and J.K. Brimacombe, "Savard and Lee - Transforming the Metallurgical Landscape," Proceeding of Savard-Lee International Symposium on Bath Smelting, TMS, Warrendale, Pa, pp. 3-29, 1992.
7. J.G. Whellock, "Metallurgical Lance and Method of Cooling the Lance," U.S Patent 5,350,158, September, 27, 1994.
8. J.M. Floyd, "Sirosmelt - The Emerging Role of New Bath Smelting Technology in Non-Ferrous Metals Production," Proceeding of Savard-Lee International Symposium on Bath Smelting, TMS, Warrendale, Pa, pp. 103-123, 1992.
9. J.M. Floyd and D.S. Conochie, "Sirosmelt - The First Ten Years," The AusIMM Melbourne Branch Symposium on Extraction Metallurgy," 1984.
10. A. Chatterjee, C. Mariquie, and P. Nilles, "Overview of Present Status of Oxygen Steelmaking and Its Expected Future Trends," Ironmaking and Steelmaking, Vol. 11, pp. 117-131, 1984.
11. T. Suzuki, "The Mitsubishi Process, Operation of Semi-Commercial Plant," The Future of Copper Pyrometallurgy, The Chilean Institute of Mining Engineers, Santiago, Chile, pp. 107-119, 1974.
12. Canadian Patent 952319, 1974.

13. P.D. Dunn, and D.A. Reay, "Heat Pipes," 4th ed., Pergamon Press, Oxford, 1994.
14. C.C. Silverstein, "Design and Technology of Heat Pipes for Cooling and Heat Exchange," Hemisphere Publishing Corporation, Washington, DC, 1992.
15. A. Faghri, "Heat Pipe Science and Technology," Taylor & Francis, Washington, DC, 1995.
16. Peterson, "An Introduction to Heat Pipes," John Wiley & Sons, Inc., New York, 1994.
17. R.S. Gaugler, "Heat Transfer Device," U.S. Patent No. 2,350,348, June, 1944.
18. G.M. Grover, "Evaporation-Condensation Heat Transfer Device," U.S. Patent No. 3,229,759, January, 1964.
19. K.R. Chun, "Some Experiments on Screen Wick Dry-out Limits," ASME, J. Heat Transfer, Vol. 94, No. 1, pp. 46-, 1972.
20. H. Noda, K. Yoshioka, and T. Hamatake, "An Experimental Study on the Permeability of Screen Wicks," JSME International Journal, Series B, Vol. 36, No. 2, pp. 357-363, 1993.
21. C.L. Tien, and A.R. Rohani, "Analysis of the Effects of Vapor Pressure Drop on Heat Pipe Performance," International Journal of Heat and Mass Transfer, Vol. 17, pp. 61-67, 1974.
22. C.A. Busse, and R.I. Loehrke, "Subsonic Pressure Recovery in Cylindrical Condensers," Journal of Heat Transfer, Vol. 111, pp. 533-537, 1989.
23. C.A. Busse, "Theory of the Ultimate Heat Transfer Limit of Cylindrical Heat Pipes," Int. J. Heat Mass Transfer, Vol. 16. pp. 169-186. 1973.
24. T.P. Cotter, "Theory of Heat Pipes," LA-3246-MS, Los Alamos Scientific Laboratory, Los Alamos, New Mexico, 1965.
25. J.E. Kemme, "Ultimate Heat-Pipe Performance," IEEE Transactions on Electron Devices, Vol 16, No, 8, pp. 717-723, 1969.
26. C.C. Silverstein, "Correlation of Heat Pipe Heat Transport Limits with Vapor Pressure," AIAA-85-0939, 1985.
27. C.L. Tien, and K.S. Chung, "Entrainment Limits in Heat Pipes," AIAA Journal, Vol. 17, No, 6, 1979.
28. C.C Silverstein, "Correlation of Heat Pipe Heat Transport Limits with Vapor Pressure," AIA-85-0949, 1985.
29. J.E. Kemme, "Vapor Flow Considerations in Conventional and Gravity-Assist Heat Pipes," Proceedings of 2nd International Heat Pipe Conference, Vol. 1, pp. 11-22, 1976.
30. W.M. Rosenhow, and P. Griffith, "Correlation of Maximum Heat Flux Data for

Boiling of Saturated Liquids," A.S.M.E. - A.I.C.E. Heat Transfer Symposium, Loiisville, Ky, 1955.

31. B.F. Caswell, and R.E. Balzhieser, "The Critical Heat Flux for Boiling Metal Systems," Chemical Engineering Progress Symposium, Series of Heat Transfer, Los Angeles, No. 64, Vol. 62, pp. 41-46, 1966.
32. G.V. Ratiani, and I.G. Shekriladze, "Study of the Process of Fully Developed Boiling of Liquids," Heat Transfer-Soviet Research, Vol. 4, No. 4. 1972.
33. J.E. Deverall, and E.S. Keddy, "Helical Wick Structures for Gravity-Assist Heat Pipes," Proceedings of the Second International Heat Pipe Conference, Bologna, Italy, 1976, pp. 3-10.
34. F.C. Prenger, E.S. Keddy and J.T. Sena, "Performance Characteristics of Gravity-Assisted Potassium Heat Pipes," Journal of Spacecraft and Rockets, Vol. 23, No. 4, pp. 407-410, 1986.
35. C.A. Busse, and J.E. Kemme, "Dry-out Phenomena in Gravity-Assist Heat Pipes With Capillary Flow," Int. J. Heat Mass Transfer, Vol 23, pp. 643-654, 1980.
36. F.C. Prenger, "Performance Limits of Gravity-Assisted Heat Pipes," Proceedings of the Fifth International Heat Pipe Conference, Tsukuba, Japan, 1984, pp. 1-9.
37. F.C. Prenger, and J.E. Kemme, "Performance Limits of Gravity Assist Heat Pipes with Simple Wick Structures," Proceedings of the Forth International Heat Pipe Conference, London, England, 1981, pp. 137-146.
38. J.E Kemme, E.S. Keddy, and J.R. Phillips, "Performance Characteristics of Liquid-Metal Heat Pipes for Space and Terrestrial Investigations," Proceedings of the Third International Heat Pipe Conference, Palo Alto, CA, 1978, pp. 260-367.
39. I.C. Bilegan, and D. Fetcu, Proceedings of the Forth International Heat Pipe Conference, London, England, 1981, pp. 89-95.
40. M. Akyurt, Solar Energy, No. 32, pp. 125-135, 1984.
41. S. Seshan, and D. Vijayalakshmi, "Heat Pipes - Concepts, Materials, and Applications," Energy Convers. Mgmt, Vol. 26, No. 1, pp. 1-9, 1986.
42. C.J. Savage and J.P. Mathieu, Proceedings of the Forth International Heat Pipe Conference, London, England, pp. 619-, 1981.
43. A.A. Rohani, and C.L. Tien, "Steady Two-Dimensional Heat and Mass Transfer in the Vapor-Gas Region of a Gas loaded Heat Pipe," Journal of Heat Transfer, Vol, 95, pp. 377-382, 1972.
44. K. Hijakata, S.J. Chen, and C.L. Tien, "Noncondensable Gas Effect on Condensation in a Two-phase Closed Thermo-syphon," International Journal of Heat Transfer, Vol. 27, pp. 1319-1325, 1984.

45. R.P. Bobco, "Variable Conductance Heat Pipe Performance Analysis: Zero-to-Full Load," Journal of Thernophysics, Vol. 3, No. 1, 1989.
46. V.H. Gray, ASME Paper No. 69-HT-19, 1969.
47. F. Polasek, Proceedings of the Forth International Heat Pipe Conference, 1973.
48. W.B. Veltkamp, L.R. Wolff, J.M.W.M. Schoonen, R. Bakker, M.P.A. Houtermans, and A.M. de Pijper, "Design and Testing of a Heat Pipe Cooled Thermionic Energy Converter," Proceedings of the Intersociety Energy Conversion Engineering Conference, pp. 1171-1175, 1990.
49. T. Osakabe, et al, "Application of heat pipe to audio amplifier," Advances in Heat Pipe Technology, Proceedings of 4th International Heat Pipe Conference, 1981.
50. M.S. El-Genk, and J.T. Seo, "Study of the SP-100 Radiator Heat Pipes Response to External Thermal Exposure," Journal of Propulsion and Power, Vol. 6, No. 1, pp. 69-77, 1990.
51. D.R. Adkins, "Design Considerations for Heat-Pipe Solar Receivers," Journal of Solar Energy Engineering, Transaction of the ASME, Vol. 112, No. 3, pp. 169-176, 1990.
52. C.E. Andaka, D.A. Wolf, and R.B. Diver, "Design, Fabrication, and Testing of a 30 kW_t Screen-Wick Heat-Pipe Solar Receiver," Proceedings of the Intersociety Energy Conversion Engineering Conference, Vol. 5, pp. 185-190, 1992.
53. V. Trujillo, E. Keddy, and M. Merrigan, "Design and Demonstration of a High-Temperature, Deployable, Membrane Heat-Pipe Radiator Element," Proceedings of the Intersociety Energy Conversion Engineering Conference, Vol. 4, pp. 1891-1895, 1990.
54. M.A. Merrigan, "Heat Pipe Design for Space Power Heat Rejection Applications," Proceedings of the Intersociety Energy Conversion Engineering Conference, pp. 1993-1998, 1990.
55. D.R Adkins, and K.S. Rawlinson, "Design, Fabrication and Testing of a 15-kW Gas-Fired Liquid-Metal Evaporator," Proceedings of the Intersociety Energy Conversion Engineering Conference, Vol. 5, pp. 191-199, 1992.
56. M. Terpstra, and J.G. Van Veen, "Heat Pipes: Construction and Application - A Study of Patents and Patent Applications," Elsevier Applied Science, London, 1987.
57. I. Sauciuc, A. Akbarzadeh, and P. Johnson, "Temperature control using variable conductance closed two-phase heat pipe," International Communications in Heat & Mass Transfer. Vol. 23, No. 3, pp. 427-433, 1996.
58. J.C. Ralph, and G. Chaffey, "Tests on an Electrically Heated Heat Pipe for

Temperature Control of Irradiation Experiments in the UK Prototype Fast Reactor," Proceedings of the Intersociety Energy Conversion Engineering Conference, Vol. 5, pp. 2473-2478, 1986.

59. L.R. Grzyll, "Investigation of Heat Pipe Working Fluids for Thermal Control of the Sodium/Sulfur Battery," Proceedings of the Intersociety Energy Conversion Engineering Conference, pp. 390-394, 1990.
60. J. Winship, "Die casting sharpens its edge," American Machinist, Vol. 118, pp. 77-78, 1974.
61. D.A. Reay, "Heat Pipes - a New Die casting Aid," Proceedings of the 1st National Die casters Conference, Birmingham Exhibition Centre, 1977.
62. D.A. Reay, Foundry Trade, J. Vol. 143, pp. 1161-, 1977.
63. F. Mucciardi, "Cooling in the Hot Rolling of Steel Products," 35th MWSP Conference Proceeding, ISS-AIME, Vol. 31, pp. 289-295, 1994.
64. K.G. Bullerschen, and H. Wilhelmi, "Cooling of Arc Furnace Electrodes with Heat Pipe," Chem. Eng. Technol., Vol. 14, pp. 45-53, 1991.
65. E. Mast, F. Mucciardi, and M. Brown, "Self Cooling Lance or Tuyere," U.S. Patent No. 5,310,166, 1994.
66. T.P. Cotter, "Heat Pipe Start-up Dynamics," Proc. Thermionics Conversion Specialist Conf., Palo Alto, CA, 1967.
67. W.J. Bowman and J.E. Hitchcock, "Transient Compressible Heat Pipe vapor dynamics," National Heat Transfer Conference, Houston, TX, HTD-96, Vol. 1, pp. 329-337, 1988.
68. F. Issacci, I. Catton and N.M. Ghoniem, "Vapor Dynamics of Heat Pipe Startup," ASME J. Heat Transfer, No. 113, pp. 985-994, 1991.
69. M.N. Ivanovsky, V.P. Sorokin, and I.V. Yagodkin, "The Physical Principles of Heat Pipes," Oxford University Press, New York, 1982.
70. D. Tilton, J. Johnson, J. Gottschlich, and S. Iden, "Transient Response of a Liquid-Metal Heat Pipe," Air Force Wright Aeronautical Laboratory Report, AFWALTR-86-2037, Wright Patterson AFB, OH, 1986.
71. W.S. Chang, and G.T. Colwell, "Mathematical Modeling of the Transient Operating Characteristics of a Low-Temperature Heat Pipe," Numerical Heat Transfer, Vol. 8, pp. 169-186, 1985.
72. K.B. Narayana, "Vapor Flow Characteristics of Slender Cylindrical Heat Pipe - A Numerical Approach," Numerical Heat Transfer, Vol. 10, pp. 79-93, 1986.
73. A. Faghri, and M.M. Chen, "A Numerical Analysis of the Effects of Conjugate Heat Transfer, Vapor Compressibility and Viscous Dissipation in Heat Pipes,"

Numerical Heat Transfer, Part A, Vol. 16, pp. 389-405, 1989.

74. Y. Cao and A. Faghri, "Transient Two-Dimensional Compressible Analysis for High-Temperature Heat Pipes with Pulsed Heat Input," Numerical Heat Transfer, Part A, Vol. 18, pp. 483-502, 1990.
75. J. Kay, and F. Mucciardi, "A Computational Investigation of a Heat Pipe Injection Lance," Steel Research, Vol. 66, No. 1, pp. 8-13, 1995.
76. A. Faghri, "Vapor Flow Analysis in a Double-Walled Concentric Heat Pipe," Numerical Heat Transfer, Vol. 10, pp. 583-595, 1986.
77. P. Botos, "The Heat Pipe Injection Lance," M. Eng. Thesis, McGill University, 1992.
78. J. Kay, "A Computational and Experimental Investigation of a Heat Pipe Lance," M. Eng. Thesis, McGill University, 1994.
79. W.H. Press, "Numerical Recipes in FORTRAN," 2nd Ed., Cambridge University Press, 1992.
80. O.E. Dwyer, "On Incipient-Boiling wall Superheats in Liquid Metals," Int. J. Heat Mass Transfer, Vol. 12, pp. 1403-1419, 1969.
81. J.C. Chen, "Incipient Boiling Superheats in Liquid Metals," Trans. Am. Soc. Mech. Engrs, J. Heat Transfer C, Vol. 90, pp. 303-312, 1968.
82. R.E. Holtz, and R. M. Singer, "On the Initiation of Pool Boiling in Sodium," Paper presented at the Tenth National Heat Transfer Conference, Philadelphia, Pa., August, 1968.
83. F. Mucciardi, N. Jin, and J. Kay, "A Cooling of Lances - A New Perspective", I&SM, September, 1994, pp. 39-47.
84. F. Mucciardi, and N. Jin, "Innovations in Top Blowing and Continuous Casting", Proc. of CIM Conference, August, 1996.
85. F. Mucciardi, and N. Jin, "Improved Control - Top Blowing Processes", Proc. of CIM Conference, August, 1995.
86. N. Jin, "Inclined Heat Pipe Lance for Gas Injection", The 78th ISS Steelmaking Conference, April, 1995.
87. F. Mucciardi, and N. Jin, "A Cooling of Lances - A New Perspective", The 78th ISS Steelmaking Conference, April, 1995.
88. F. Mucciardi, N. Jin, and J. Kay, "A New Generation of Top-Blowing Injection Lances", Proc. of CIM Conference, August, 1994.
89. F. Mucciardi, N. Jin, and J. Kay, "The Cooling of BOF Steelmaking Lances", Steelmaking Conference Proceedings, ISS, v77, 1994, pp. 209-216.

APPENDICES

Appendix I

Program for the modeling of heat pipe cooled injection lances

```
PROGRAM lengine1


      DOUBLEPRECISION maxdiff,errorsum

      INTEGER i,j,k,maxcycle

      REAL *8 relax,thresh,

c
c  input data
c

     & r1,r2,r3,r4,r5,r6,r7,r8,r9,l11,l22,l33,l45,l67,t1,t2,
     & Tamb11,Tamb22,Tamb33,Tamb45,Tamb67,Tamb88,k1,k2,k4,k5,k7,k8,k9,
     & h1,h3,h41,h42,h43,h447,h51,h52,h6,h71,h72,h9,h10,h11,
     & Tin(2),inletp(2),hcg(2),dg(2),flowrate(2),

c
c  constant
c

     & denom(2),pgrad(2),totpdif(2),c1(2),
     & sigma,pi,

c
c  processing data
c
```

```
     & r(7,9),l(7),ll,Tamb(8),h(8,9),e(8,9),f(8,9),
     & k12(8),k23(8),k45(8),k56(8),k78(8),k89(8),
     & s(64),a(64,64),

c
c  variables
c

     & q1(7),q2(8),T(7,10),Tb(3),Tws

c
c  set up READ WRITE files...
c

      OPEN (7,FILE='input.dat', STATUS='old')
      OPEN (8,FILE='guess.dat', STATUS='old')
      OPEN (9,FILE='check.dat', STATUS='unknown')

c
c   read input data from file 7 which contains parameters
c

      READ (7,*) relax
      READ (7,*) maxcycle
      READ (7,*) thresh
      READ (7,*) r1
      READ (7,*) r2
      READ (7,*) r3
      READ (7,*) r4
      READ (7,*) r5
      READ (7,*) r6
      READ (7,*) r7
      READ (7,*) r8
      READ (7,*) r9
      READ (7,*) l11
      READ (7,*) l22
      READ (7,*) l33
      READ (7,*) l45
      READ (7,*) l67
```

```
READ (7,*) t1
READ (7,*) t2
READ (7,*) Tamb11
READ (7,*) Tamb22
READ (7,*) Tamb33
READ (7,*) Tamb45
READ (7,*) Tamb67
READ (7,*) Tamb88
READ (7,*) Tin(1)
READ (7,*) inletp(1)
READ (7,*) dg(1)
READ (7,*) hcg(1)
READ (7,*) flowrate(1)
READ (7,*) Tin(2)
READ (7,*) inletp(2)
READ (7,*) dg(2)
READ (7,*) hcg(2)
READ (7,*) flowrate(2)
READ (7,*) k1
READ (7,*) k2
READ (7,*) k4
READ (7,*) k5
READ (7,*) k7
READ (7,*) k8
READ (7,*) k9
READ (7,*) h1
READ (7,*) h3
READ (7,*) h41
READ (7,*) h42
READ (7,*) h43
READ (7,*) h447
READ (7,*) h51
READ (7,*) h52
READ (7,*) h6
READ (7,*) h71
READ (7,*) h72
READ (7,*) h9
READ (7,*) h10
READ (7,*) h11
```

```
      CLOSE(7)

c
c  read guess data from file 8
c

      DO j=1,7
          READ (8,*) q1(j)
      END DO
      DO j=1,8
          READ (8,*) q2(j)
      END DO
      DO j=1,7
          DO k=1,10
              READ (8,*) T(j,k)
              T(j,k)=T(j,k)+273
          END DO
      END DO
      DO j=1,3
          READ (8,*) Tb(j)
          Tb(j)=Tb(j)+273
      END DO
      READ (8,*) Tws
      Tws=Tws+273

      CLOSE(8)

      DO j=1,7
          WRITE (9,*) q1(j)
      END DO
      DO j=1,8
          WRITE (9,*) q2(j)
      END DO
      DO j=1,7
          DO k=1,10
              WRITE (9,*) T(j,k)
          END DO
      END DO
      DO j=1,3
          WRITE (9,*) Tb(j)
```

```
END DO
WRITE (9,*) Tws

i=0
sigma=5.67e-8
pi=3.1415926535

DO j=1,7
    r(j,1)=r1
    r(j,2)=r2
    r(j,3)=r3
    r(j,4)=r4
    r(j,5)=r5
    r(j,6)=r6
    r(j,7)=r7
    r(j,8)=r8
    r(j,9)=r9
END DO

l(1)=l11
l(2)=l22
l(3)=l33
l(4)=l45/2
l(5)=l(4)
l(6)=l67/2
l(7)=l(6)
ll=l11+l22+l33+l45

Tin(1)=Tin(1)+273
Tin(2)=Tin(2)+273

Tamb(1)=Tamb11+273
Tamb(2)=Tamb22+273
Tamb(3)=Tamb33+273
Tamb(4)=Tamb45+273
Tamb(5)=Tamb45+273
Tamb(6)=Tamb67+273
Tamb(7)=Tamb67+273
Tamb(8)=Tamb88+273
```

```
DO j=1,8
    DO k=1,9
        h(j,k)=0.0
        e(j,k)=0.8
        f(j,k)=1.0
    END DO
END DO

DO j=1,3
    h(j,1)=h1
    h(j,3)=h3
    h(j,6)=h6
END DO
h(1,4)=h41
h(2,4)=h42
h(3,4)=h43

DO j=4,5
    h(j,4)=h447
    h(j,5)=h51
    h(j,7)=h71
    h(j,9)=h9
END DO

DO j=6,7
    h(j,4)=h447
    h(j,5)=h52
    h(j,7)=h72
    h(j,9)=h9
END DO

h(8,1)=h10
h(8,3)=h11

DO j=1,7
    f(j,7)=r5/r7
END DO

DO j=1,8
    k12=0
```

```
    k23=0
    k45=0
    k56=0
    k78=0
    k89=0
END DO

DO j=1,3
    k12(j)=k1
    k23(j)=k2
END DO
DO j=1,7
    k45(j)=k4
    k56(j)=k5
    k78(j)=k7
    k89(j)=k8
END DO
k12(8)=k1
k23(8)=k9

WRITE (9,*) r
WRITE (9,*) l
WRITE (9,*) h
WRITE (9,*) e
WRITE (9,*) f
WRITE (9,*) k12
WRITE (9,*) k23
WRITE (9,*) k45
WRITE (9,*) k56
WRITE (9,*) k78
WRITE (9,*) k89

denom(1)=hcg(1)*dg(1)*flowrate(1)
pgrad(1)=MAX((inletp(1)-101300)/(111+122+133+45),0)
totpdif(1)=MAX(inletp(1)-101300,0)
c1(1)=flowrate(1)*pgrad(1)/(Tin(1)/inletp(1))

denom(2)=hcg(2)*dg(2)*flowrate(2)
pgrad(2)=MAX((inletp(2)-101300)/167,0)
totpdif(2)=MAX(inletp(2)-101300,0)
```

```
      c1(2)=flowrate(2)*pgrad(2)/(Tin(2)/inletp(2))

c
c   main loop
c

      maxdiff=10000
      errorsum=10000

      DO 200, WHILE (((i-1).LT.maxcycle).AND.(maxdiff.GT.thresh).AND.
     +            (errorsum.LT.9000000000000.0))
      i=i+1

c
c  initialize matrices
c

      DO 35, j=1,64
          s(j)=0.0
          DO 33, k=1,64
              a(j,k)=0.0
33        CONTINUE
35    CONTINUE

c
c  evaporator section
c

      s(1)=-q1(1)+2*pi*r(1,6)*l(1)*(h(1,6)*(Tamb(1)-T(1,6))+
     &sigma*e(1,6)*f(1,6)*(Tamb(1)**4-T(1,6)**4))
      a(1,1)=-1
      a(1,39)=-2*pi*r(1,6)*l(1)*(h(1,6)+sigma*e(1,6)*f(1,6)*4*T(1,6)**3)

      s(2)=-q1(2)+2*pi*r(2,6)*l(2)*(h(2,6)*(Tamb(2)-T(2,6))+
     &sigma*e(2,6)*f(2,6)*(Tamb(2)**4-T(2,6)**4))
      a(2,2)=-1
      a(2,40)=-2*pi*r(2,6)*l(2)*(h(2,6)+sigma*e(2,6)*f(2,6)*4*T(2,6)**3)

      s(3)=-q1(3)+2*pi*r(3,6)*l(3)*(h(3,6)*(Tamb(3)-T(3,6))+
     &sigma*e(3,6)*f(3,6)*(Tamb(3)**4-T(3,6)**4))
```

```
a(3,3)=-1
a(3,41)=-2*pi*r(3,6)*l(3)*(h(3,6)+sigma*e(3,6)*f(3,6)*4*T(3,6)**3)

s(4)=-q1(1)+2*pi*l(1)*k56(1)/log(r(1,6)/r(1,5))*(T(1,6)-T(1,5))
a(4,1)=-1
a(4,39)=2*pi*l(1)*k56(1)/log(r(1,6)/r(1,5))
a(4,32)=-2*pi*l(1)*k56(1)/log(r(1,6)/r(1,5))

s(5)=-q1(2)+2*pi*l(2)*k56(2)/log(r(2,6)/r(2,5))*(T(2,6)-T(2,5))
a(5,2)=-1
a(5,40)=2*pi*l(2)*k56(2)/log(r(2,6)/r(2,5))
a(5,33)=-2*pi*l(2)*k56(2)/log(r(2,6)/r(2,5))

s(6)=-q1(3)+2*pi*l(3)*k56(3)/log(r(3,6)/r(3,5))*(T(3,6)-T(3,5))
a(6,3)=-1
a(6,41)=2*pi*l(3)*k56(3)/log(r(3,6)/r(3,5))
a(6,34)=-2*pi*l(3)*k56(3)/log(r(3,6)/r(3,5))

s(7)=-q1(1)+2*pi*l(1)*k45(1)/log(r(1,5)/r(1,4))*(T(1,5)-T(1,4))
a(7,1)=-1
a(7,32)=2*pi*l(1)*k45(1)/log(r(1,5)/r(1,4))
a(7,25)=-2*pi*l(1)*k45(1)/log(r(1,5)/r(1,4))

s(8)=-q1(2)+2*pi*l(2)*k45(2)/log(r(2,5)/r(2,4))*(T(2,5)-T(2,4))
a(8,2)=-1
a(8,33)=2*pi*l(2)*k45(2)/log(r(2,5)/r(2,4))
a(8,26)=-2*pi*l(2)*k45(2)/log(r(2,5)/r(2,4))

s(9)=-q1(3)+2*pi*l(3)*k45(3)/log(r(3,5)/r(3,4))*(T(3,5)-T(3,4))
a(9,3)=-1
a(9,34)=2*pi*l(3)*k45(3)/log(r(3,5)/r(3,4))
a(9,27)=-2*pi*l(3)*k45(3)/log(r(3,5)/r(3,4))

s(10)=-q1(1)+2*pi*r(1,4)*l(1)*h(1,4)*(T(1,4)-Tws)
a(10,1)=-1
a(10,25)=2*pi*r(1,4)*l(1)*h(1,4)
a(10,64)=-2*pi*r(1,4)*l(1)*h(1,4)

s(11)=-q1(2)+2*pi*r(2,4)*l(2)*h(2,4)*(T(2,4)-Tws)
a(11,2)=-1
```

```
a(11,26)=2*pi*r(2,4)*l(2)*h(2,4)
a(11,64)=-2*pi*r(2,4)*l(2)*h(2,4)

s(12)=-q1(3)+2*pi*r(3,4)*l(3)*h(3,4)*(T(3,4)-Tws)
a(12,3)=-1
a(12,27)=2*pi*r(3,4)*l(3)*h(3,4)
a(12,64)=-2*pi*r(3,4)*l(3)*h(3,4)

s(13)=-q2(1)+2*pi*r(1,3)*l(1)*h(1,3)*(Tws-T(1,3))
a(13,8)=-1
a(13,64)=2*pi*r(1,3)*l(1)*h(1,3)
a(13,22)=-2*pi*r(1,3)*l(1)*h(1,3)

s(14)=-q2(2)+2*pi*r(2,3)*l(2)*h(2,3)*(Tws-T(2,3))
a(14,9)=-1
a(14,64)=2*pi*r(2,3)*l(2)*h(2,3)
a(14,23)=-2*pi*r(2,3)*l(2)*h(2,3)

s(15)=-q2(3)+2*pi*r(3,3)*l(3)*h(3,3)*(Tws-T(3,3))
a(15,10)=-1
a(15,64)=2*pi*r(3,3)*l(3)*h(3,3)
a(15,24)=-2*pi*r(3,3)*l(3)*h(3,3)

s(16)=-q2(1)+2*pi*l(1)*k23(1)/log(r(1,3)/r(1,2))*(T(1,3)-T(1,2))
a(16,8)=-1
a(16,22)=2*pi*l(1)*k23(1)/log(r(1,3)/r(1,2))
a(16,19)=-2*pi*l(1)*k23(1)/log(r(1,3)/r(1,2))

s(17)=-q2(2)+2*pi*l(2)*k23(2)/log(r(2,3)/r(2,2))*(T(2,3)-T(2,2))
a(17,9)=-1
a(17,23)=2*pi*l(2)*k23(2)/log(r(2,3)/r(2,2))
a(17,20)=-2*pi*l(2)*k23(2)/log(r(2,3)/r(2,2))

s(18)=-q2(3)+2*pi*l(3)*k23(3)/log(r(3,3)/r(3,2))*(T(3,3)-T(3,2))
a(18,10)=-1
a(18,24)=2*pi*l(3)*k23(3)/log(r(3,3)/r(3,2))
a(18,21)=-2*pi*l(3)*k23(3)/log(r(3,3)/r(3,2))

s(19)=-q2(1)+2*pi*l(1)*k12(1)/log(r(1,2)/r(1,1))*(T(1,2)-T(1,1))
a(19,8)=-1
```

```
      a(19,19)=2*pi*l(1)*k12(1)/log(r(1,2)/r(1,1))
      a(19,16)=-2*pi*l(1)*k12(1)/log(r(1,2)/r(1,1))

      s(20)=-q2(2)+2*pi*l(2)*k12(2)/log(r(2,2)/r(2,1))*(T(2,2)-T(2,1))
      a(20,9)=-1
      a(20,20)=2*pi*l(2)*k12(2)/log(r(2,2)/r(2,1))
      a(20,17)=-2*pi*l(2)*k12(2)/log(r(2,2)/r(2,1))

      s(21)=-q2(3)+2*pi*l(3)*k12(3)/log(r(3,2)/r(3,1))*(T(3,2)-T(3,1))
      a(21,10)=-1
      a(21,21)=2*pi*l(3)*k12(3)/log(r(3,2)/r(3,1))
      a(21,18)=-2*pi*l(3)*k12(3)/log(r(3,2)/r(3,1))

      s(22)=-q2(1)+2*pi*r(1,1)*l(1)*h(1,1)*(T(1,1)-T(1,10))
      a(22,8)=-1
      a(22,16)=2*pi*r(1,1)*l(1)*h(1,1)
      a(22,54)=-2*pi*r(1,1)*l(1)*h(1,1)

      s(23)=-q2(2)+2*pi*r(2,1)*l(2)*h(2,1)*(T(2,1)-T(2,10))
      a(23,9)=-1
      a(23,17)=2*pi*r(2,1)*l(2)*h(2,1)
      a(23,55)=-2*pi*r(2,1)*l(2)*h(2,1)

      s(24)=-q2(3)+2*pi*r(3,1)*l(3)*h(3,1)*(T(3,1)-T(3,10))
      a(24,10)=-1
      a(24,18)=2*pi*r(3,1)*l(3)*h(3,1)
      a(24,56)=-2*pi*r(3,1)*l(3)*h(3,1)


c
c     condenser section
c

      s(25)=-q1(4)+2*pi*r(4,9)*l(4)*(h(4,9)*(Tamb(4)-T(4,9))+
     &sigma*e(4,9)*f(4,9)*(Tamb(4)**4-T(4,9)**4))
      a(25,4)=-1
      a(25,50)=-2*pi*r(4,9)*l(4)*
     &(h(4,9)+sigma*e(4,9)*f(4,9)*4*T(4,9)**3)

      s(26)=-q1(5)+2*pi*r(5,9)*l(5)*(h(5,9)*(Tamb(5)-T(5,9))+
```

```
&sigma*e(5,9)*f(5,9)*(Tamb(5)**4-T(5,9)**4))
 a(26,5)=-1
 a(26,51)=-2*pi*r(5,9)*l(5)*
&(h(5,9)+sigma*e(5,9)*f(5,9)*4*T(5,9)**3)

 s(27)=-q1(6)+2*pi*r(6,9)*l(6)*(h(6,9)*(Tamb(6)-T(6,9))+
&sigma*e(6,9)*f(6,9)*(Tamb(6)**4-T(6,9)**4))
 a(27,6)=-1
 a(27,52)=-2*pi*r(6,9)*l(6)*
&(h(6,9)+sigma*e(6,9)*f(6,9)*4*T(6,9)**3)

 s(28)=-q1(7)+2*pi*r(7,9)*l(7)*(h(7,9)*(Tamb(7)-T(7,9))+
&sigma*e(7,9)*f(7,9)*(Tamb(7)**4-T(7,9)**4))
 a(28,7)=-1
 a(28,53)=-2*pi*r(7,9)*l(7)*
&(h(7,9)+sigma*e(7,9)*f(7,9)*4*T(7,9)**3)

 s(29)=-q1(4)+2*pi*l(4)*k89(4)/log(r(4,9)/r(4,8))*(T(4,9)-T(4,8))
 a(29,4)=-1
 a(29,50)=2*pi*l(4)*k89(4)/log(r(4,9)/r(4,8))
 a(29,46)=-2*pi*l(4)*k89(4)/log(r(4,9)/r(4,8))

 s(30)=-q1(5)+2*pi*l(5)*k89(5)/log(r(5,9)/r(5,8))*(T(5,9)-T(5,8))
 a(30,5)=-1
 a(30,51)=2*pi*l(5)*k89(5)/log(r(5,9)/r(5,8))
 a(30,47)=-2*pi*l(5)*k89(5)/log(r(5,9)/r(5,8))

 s(31)=-q1(6)+2*pi*l(6)*k89(6)/log(r(6,9)/r(6,8))*(T(6,9)-T(6,8))
 a(31,6)=-1
 a(31,52)=2*pi*l(6)*k89(6)/log(r(6,9)/r(6,8))
 a(31,48)=-2*pi*l(6)*k89(6)/log(r(6,9)/r(6,8))

 s(32)=-q1(7)+2*pi*l(7)*k89(7)/log(r(7,9)/r(7,8))*(T(7,9)-T(7,8))
 a(32,7)=-1
 a(32,53)=2*pi*l(7)*k89(7)/log(r(7,9)/r(7,8))
 a(32,49)=-2*pi*l(7)*k89(7)/log(r(7,9)/r(7,8))

 s(33)=-q1(4)+2*pi*l(4)*k78(4)/log(r(4,8)/r(4,7))*(T(4,8)-T(4,7))
 a(33,4)=-1
 a(33,46)=2*pi*l(4)*k78(4)/log(r(4,8)/r(4,7))
```

```
 a(33,42)=-2*pi*l(4)*k78(4)/log(r(4,8)/r(4,7))

 s(34)=-q1(5)+2*pi*l(5)*k78(5)/log(r(5,8)/r(5,7))*(T(5,8)-T(5,7))
 a(34,5)=-1
 a(34,47)=2*pi*l(5)*k78(5)/log(r(5,8)/r(5,7))
 a(34,43)=-2*pi*l(5)*k78(5)/log(r(5,8)/r(5,7))

 s(35)=-q1(6)+2*pi*l(6)*k78(6)/log(r(6,8)/r(6,7))*(T(6,8)-T(6,7))
 a(35,6)=-1
 a(35,48)=2*pi*l(6)*k78(6)/log(r(6,8)/r(6,7))
 a(35,44)=-2*pi*l(6)*k78(6)/log(r(6,8)/r(6,7))

 s(36)=-q1(7)+2*pi*l(7)*k78(7)/log(r(7,8)/r(7,7))*(T(7,8)-T(7,7))
 a(36,7)=-1
 a(36,49)=2*pi*l(7)*k78(7)/log(r(7,8)/r(7,7))
 a(36,45)=-2*pi*l(7)*k78(7)/log(r(7,8)/r(7,7))

 s(37)=-q1(4)+2*pi*r(4,7)*l(4)*(h(4,7)*(T(4,7)-T(4,10))+
&sigma*e(4,7)*f(4,7)*(T(4,7)**4-T(4,5)**4))
 a(37,4)=-1
 a(37,42)=2*pi*r(4,7)*l(4)*(h(4,7)+sigma*e(4,7)*f(4,7)*4*T(4,7)**3)
 a(37,57)=-2*pi*r(4,7)*l(4)*h(4,7)
 a(37,35)=-2*pi*r(4,7)*l(4)*sigma*e(4,7)*f(4,7)*4*T(4,5)**3

 s(38)=-q1(5)+2*pi*r(5,7)*l(5)*(h(5,7)*(T(5,7)-T(5,10))+
&sigma*e(5,7)*f(5,7)*(T(5,7)**4-T(5,5)**4))
 a(38,5)=-1
 a(38,43)=2*pi*r(5,7)*l(5)*(h(5,7)+sigma*e(5,7)*f(5,7)*4*T(5,7)**3)
 a(38,58)=-2*pi*r(5,7)*l(5)*h(5,7)
 a(38,36)=-2*pi*r(5,7)*l(5)*sigma*e(5,7)*f(5,7)*4*T(5,5)**3

 s(39)=-q1(6)+2*pi*r(6,7)*l(6)*(h(6,7)*(T(6,7)-T(6,10))+
&sigma*e(6,7)*f(6,7)*(T(6,7)**4-T(6,5)**4))
 a(39,6)=-1
 a(39,44)=2*pi*r(6,7)*l(6)*(h(6,7)+sigma*e(6,7)*f(6,7)*4*T(6,7)**3)
 a(39,59)=-2*pi*r(6,7)*l(6)*h(6,7)
 a(39,37)=-2*pi*r(6,7)*l(6)*sigma*e(6,7)*f(6,7)*4*T(6,5)**3

 s(40)=-q1(7)+2*pi*r(7,7)*l(7)*(h(7,7)*(T(7,7)-T(7,10))+
&sigma*e(7,7)*f(7,7)*(T(7,7)**4-T(7,5)**4))
```

```
 a(40,7)=-1
 a(40,45)=2*pi*r(7,7)*l(7)*(h(7,7)+sigma*e(7,7)*f(7,7)*4*T(7,7)**3)
 a(40,60)=-2*pi*r(7,7)*l(7)*h(7,7)
 a(40,38)=-2*pi*r(7,7)*l(7)*sigma*e(7,7)*f(7,7)*4*T(7,5)**3

 s(41)=-q2(4)+2*pi*r(4,5)*l(4)*(h(4,5)*(T(4,10)-T(4,5))+
&sigma*e(4,5)*f(4,5)*(T(4,7)**4-T(4,5)**4))
 a(41,11)=-1
 a(41,57)=2*pi*r(4,5)*l(4)*h(4,5)
 a(41,35)=-2*pi*r(4,5)*l(4)
&*(h(4,5)+sigma*e(4,5)*f(4,5)*4*T(4,5)**3)
 a(41,42)=2*pi*r(4,5)*l(4)*sigma*e(4,5)*f(4,5)*4*T(4,7)**3

 s(42)=-q2(5)+2*pi*r(5,5)*l(5)*(h(5,5)*(T(5,10)-T(5,5))+
&sigma*e(5,5)*f(5,5)*(T(5,7)**4-T(5,5)**4))
 a(42,12)=-1
 a(42,58)=2*pi*r(5,5)*l(5)*h(5,5)
 a(42,36)=-2*pi*r(5,5)*l(5)*
&(h(5,5)+sigma*e(5,5)*f(5,5)*4*T(5,5)**3)
 a(42,43)=2*pi*r(5,5)*l(5)*sigma*e(5,5)*f(5,5)*4*T(5,7)**3

 s(43)=-q2(6)+2*pi*r(6,5)*l(6)*(h(6,5)*(T(6,10)-T(6,5))+
&sigma*e(6,5)*f(6,5)*(T(6,7)**4-T(6,5)**4))
 a(43,13)=-1
 a(43,59)=2*pi*r(6,5)*l(6)*h(6,5)
 a(43,37)=-2*pi*r(6,5)*l(6)*
&(h(6,5)+sigma*e(6,5)*f(6,5)*4*T(6,5)**3)
 a(43,44)=2*pi*r(6,5)*l(6)*sigma*e(6,5)*f(6,5)*4*T(6,7)**3

 s(44)=-q2(7)+2*pi*r(7,5)*l(7)*(h(7,5)*(T(7,10)-T(7,5))+
&sigma*e(7,5)*f(7,5)*(T(7,7)**4-T(7,5)**4))
 a(44,14)=-1
 a(44,60)=2*pi*r(7,5)*l(7)*h(7,5)
 a(44,38)=-2*pi*r(7,5)*l(7)*
&(h(7,5)+sigma*e(7,5)*f(7,5)*4*T(7,5)**3)
 a(44,45)=2*pi*r(7,5)*l(7)*sigma*e(7,5)*f(7,5)*4*T(7,7)**3

 s(45)=-q2(4)+2*pi*l(4)*k45(4)/log(r(4,5)/r(4,4))*(T(4,5)-T(4,4))
 a(45,11)=-1
 a(45,35)=2*pi*l(4)*k45(4)/log(r(4,5)/r(4,4))
```

```
a(45,28)=-2*pi*l(4)*k45(4)/log(r(4,5)/r(4,4))

s(46)=-q2(5)+2*pi*l(5)*k45(5)/log(r(5,5)/r(5,4))*(T(5,5)-T(5,4))
a(46,12)=-1
a(46,36)=2*pi*l(5)*k45(5)/log(r(5,5)/r(5,4))
a(46,29)=-2*pi*l(5)*k45(5)/log(r(5,5)/r(5,4))

s(47)=-q2(6)+2*pi*l(6)*k45(6)/log(r(6,5)/r(6,4))*(T(6,5)-T(6,4))
a(47,13)=-1
a(47,37)=2*pi*l(6)*k45(6)/log(r(6,5)/r(6,4))
a(47,30)=-2*pi*l(6)*k45(6)/log(r(6,5)/r(6,4))

s(48)=-q2(7)+2*pi*l(7)*k45(7)/log(r(7,5)/r(7,4))*(T(7,5)-T(7,4))
a(48,14)=-1
a(48,38)=2*pi*l(7)*k45(7)/log(r(7,5)/r(7,4))
a(48,31)=-2*pi*l(7)*k45(7)/log(r(7,5)/r(7,4))

s(49)=-q2(4)+2*pi*r(4,4)*l(4)*h(4,4)*(T(4,4)-Tws)
a(49,11)=-1
a(49,28)=2*pi*r(4,4)*l(4)*h(4,4)
a(49,64)=-2*pi*r(4,4)*l(4)*h(4,4)

s(50)=-q2(5)+2*pi*r(5,4)*l(5)*h(5,4)*(T(5,4)-Tws)
a(50,12)=-1
a(50,29)=2*pi*r(5,4)*l(5)*h(5,4)
a(50,64)=-2*pi*r(5,4)*l(5)*h(5,4)

s(51)=-q2(6)+2*pi*r(6,4)*l(6)*h(6,4)*(T(6,4)-Tws)
a(51,13)=-1
a(51,30)=2*pi*r(6,4)*l(6)*h(6,4)
a(51,64)=-2*pi*r(6,4)*l(6)*h(6,4)

s(52)=-q2(7)+2*pi*r(7,4)*l(7)*h(7,4)*(T(7,4)-Tws)
a(52,14)=-1
a(52,31)=2*pi*r(7,4)*l(7)*h(7,4)
a(52,64)=-2*pi*r(7,4)*l(7)*h(7,4)

c
c     lance tip section
```

```
c

      s(53)=-q2(8)+pi*(r4**2-r3**2)*(h(8,1)*(Tamb(8)-Tb(1))+
     &sigma*e(8,1)*f(8,1)*(Tamb(8)**4-Tb(1)**4))
      a(53,15)=-1
      a(53,61)=-pi*(r4**2-r3**2)*
     &(h(8,1)+sigma*e(8,1)*f(8,1)*4*Tb(1)**3)

      s(54)=-q2(8)+pi*(r4**2-r3**2)*k12(8)*(Tb(1)-Tb(2))/t1
      a(54,15)=-1
      a(54,61)=pi*(r4**2-r3**2)*k12(8)/t1
      a(54,62)=-pi*(r4**2-r3**2)*k12(8)/t1

      s(55)=-q2(8)+pi*(r4**2-r3**2)*k23(8)*(Tb(2)-Tb(3))/t2
      a(55,15)=-1
      a(55,62)=pi*(r4**2-r3**2)*k23(8)/t2
      a(55,63)=-pi*(r4**2-r3**2)*k23(8)/t2

      s(56)=-q2(8)+pi*(r4**2-r3**2)*h(8,3)*(Tb(3)-Tws)
      a(56,15)=-1
      a(56,63)=pi*(r4**2-r3**2)*h(8,3)
      a(56,64)=-pi*(r4**2-r3**2)*h(8,3)


c
c     heat acumulation
c

      s(57)=-q2(1)+denom(1)*(T(1,10)-T(2,10))+
     &l(1)*c1(1)*T(1,10)*(1/(101300))
      a(57,8)=-1
      a(57,54)=denom(1)+l(1)*c1(1)*(1/(101300))
      a(57,55)=-denom(1)

      s(58)=-q2(2)+denom(1)*(T(2,10)-T(3,10))+
     &l(2)*c1(1)*T(2,10)*(1/(101300+totpdif(1)*l(1)/ll))
      a(58,9)=-1
      a(58,55)=denom(1)+l(2)*c1(1)*(1/(101300+totpdif(1)*l(1)/ll))
      a(58,56)=-denom(1)
```

```
 s(59)=-q2(3)+denom(1)*(T(3,10)-T(4,10))+
&l(3)*c1(1)*T(3,10)*(1/(101300+totpdif(1)*
&(l(1)+l(2))/ll))
 a(59,10)=-1
 a(59,56)=denom(1)+
&l(3)*c1(1)*(1/(101300+totpdif(1)*(l(1)+l(2))/ll))
 a(59,57)=-denom(1)

 s(60)=q2(4)-q1(4)+denom(1)*(T(4,10)-T(5,10))+
&l(4)*c1(1)*T(4,10)*(1/(101300+totpdif(1)*
&(l(1)+l(2)+l(3))/ll))
 a(60,11)=1
 a(60,4)=-1
 a(60,57)=denom(1)+
&l(4)*c1(1)*(1/(101300+totpdif(1)*(l(1)+l(2)+l(3))/ll))
 a(60,58)=-denom(1)

 s(61)=q2(5)-q1(5)+denom(1)*(T(5,10)-Tin(1))+
&l(5)*c1(1)*T(5,10)*(1/(101300+totpdif(1)*
&(l(1)+l(2)+l(3)+l(4))/ll))
 a(61,12)=1
 a(61,5)=-1
 a(61,58)=denom(1)+
&l(5)*c1(1)*(1/(101300+totpdif(1)*(l(1)+l(2)+l(3)+l(4))/ll))

 s(62)=q2(6)-q1(6)+denom(2)*(T(6,10)-Tin(2))+
&l(6)*c1(2)*T(6,10)*(1/(101300+totpdif(2)*l(6)/(l(6)+l(7))))
 a(62,13)=1
 a(62,6)=-1
 a(62,59)=denom(2)+
&l(6)*c1(2)*(1/(101300+totpdif(2)*l(6)/(l(6)+l(7))))

 s(63)=q2(7)-q1(7)+denom(2)*(T(7,10)-T(6,10))+
&l(7)*c1(2)*T(7,10)*(1/(101300))
 a(63,14)=1
 a(63,7)=-1
 a(63,60)=denom(2)+l(7)*c1(2)*(1/(101300))
 a(63,59)=-denom(2)

 s(64)=q1(1)+q1(2)+q1(3)
```

```
     &-q2(1)-q2(2)-q2(3)+q2(4)+q2(5)+q2(6)+q2(7)+q2(8)
      a(64,1)=1
      a(64,2)=1
      a(64,3)=1
      a(64,8)=-1
      a(64,9)=-1
      a(64,10)=-1
      a(64,11)=1
      a(64,12)=1
      a(64,13)=1
      a(64,14)=1
      a(64,15)=1

c
c  check if all equations are under threshhold
c

      maxdiff=0
      errorsum=0
      DO k=1,64
          errorsum=errorsum+ABS(s(k))
          IF (ABS(s(k)).GT.ABS(maxdiff)) THEN
              nnn=nnn+1
              maxdiff=ABS(s(k))
              nn=k
          END IF
      END DO

      WRITE(*,*) "maxcycle=",i-1
      WRITE(*,*) "errorsum=",errorsum
      WRITE(*,*) "maxdiff=",maxdiff

c
c new system of output
c

      IF (errorsum.GT.9000000000000.0) THEN
          errorsum=   9999999999999.9
      END IF
```

```
      IF  (maxdiff.GT.9000000000000.0) THEN
          maxdiff=    9999999999999.9
      END IF

      IF ((maxdiff.LT.thresh).or.
     +         (errorsum.GT.9000000000000.0)) GOTO 100

c
c  call subroutine
c

      CALL gaussj(a,64,64,s,1,1)

c
c  set underelax. factor
c

      s=s/relax

c
c   update values
c

      n=0
      DO j=1,7
          n=n+1
          q1(j)=q1(j)-s(n)
      END DO

      DO j=1,8
          n=n+1
          q2(j)=q2(j)-s(n)
      END DO

      DO j=1,3
          DO k=1,3
              n=n+1
              T(k,j)=MAX(T(k,j)-s(n),0)
          END DO
      END DO
```

```
      DO j=4,5
          DO k=1,7
              n=n+1
              T(k,j)=MAX(T(k,j)-s(n),0)
          END DO
      END DO

      DO j=1,3
          n=n+1
          T(j,6)=MAX(T(j,6)-s(n),0)
      END DO

      DO j=7,9
          DO k=4,7
              n=n+1
              T(k,j)=MAX(T(k,j)-s(n),0)
          END DO
      END DO

      DO j=1,7
          n=n+1
          T(j,10)=MAX(T(j,10)-s(n),0)
      END DO

      Tb(1)=MAX(Tb(1)-s(61),0)
      Tb(2)=MAX(Tb(2)-s(62),0)
      Tb(3)=MAX(Tb(3)-s(63),0)
      Tws=MAX(Tws-s(64),0)

100   CONTINUE

200   CONTINUE

      IF (errorsum.GT.9000000000000.0) THEN
          i=maxcycle+1
      END IF

      OPEN (10,FILE='output.dat', STATUS='unknown')
```

```
c
c  Output
c

      WRITE (10,150) (q1(j),j=1,7)
150   FORMAT(7f7.1)
      WRITE (10,*) ' '

      WRITE (10,250) (q2(j),j=1,8)
250   FORMAT(8f7.1)
      WRITE (10,*) ' '

      DO j=1,7
              WRITE (10,300) (t(8-j,k)-273,k=1,10)
300           FORMAT(10f7.1)
      END DO
      WRITE (10,*) ' '

      WRITE (10,400) Tb(1)-273,Tb(2)-273,Tb(3)-273,Tws-273
400   FORMAT(10f7.1)

      CLOSE(10)

      STOP
      END
```

Appendix II

Variables and their serial numbers

1. q(1,1)
2. q(2,1)
3. q(3,1)
4. q(4,1)
5. q(5,1)
6. q(6,1)
7. q(7,1)
8. q(1,2)
9. q(2,2)
10. q(3,2)
11. q(4,2)
12. q(5,2)
13. q(6,2)
14. q(7,2)
15. q(8,2)
16. T(1,1)
17. T(2,1)
18. T(3,1)
19. T(1,2)
20. T(2,2)
21. T(3,2)
22. T(1,3)
23. T(2,3)
24. T(3,3)
25. T(1,4)
26. T(2,4)
27. T(3,4)
28. T(4,4)
29. T(5,4)
30. T(6,4)
31. T(7,4)
32. T(1,5)
33. T(2,5)
34. T(3,5)
35. T(4,5)
36. T(5,5)
37. T(6,5)
38. T(7,5)
39. T(1,6)
40. T(2,6)
41. T(3,6)
42. T(4,7)
43. T(5,7)
44. T(6,7)
45. T(7,7)
46. T(4,8)
47. T(5,8)
48. T(6,8)
49. T(7,8)
50. T(4,9)
51. T(5,9)
52. T(6,9)
53. T(7,9)
54. T(1,10)
55. T(2,10)
56. T(3,10)
57. T(4,10)
58. T(5,10)
59. T(6,10)
60. T(7,10)
61. Tb(1)
62. Tb(2)
63. Tb(3)
64. Twx

Appendix III

Simulation results of steelmaking test

79.7	150.4	-9.9	-26.2	-20.2	-6.2	-9.3			
0.1	1.0	1.7	-61.6	-79.5	-226.9	-202.7	353.3		
0.0	0.0	0.0	468.6	460.1	0.0	160.4	160.1	160.1	120.3
0.0	0.0	0.0	468.5	459.0	0.0	121.2	121.0	121.0	73.5
0.0	0.0	0.0	469.2	466.3	0.0	243.2	242.6	242.6	173.4
0.0	0.0	0.0	469.3	467.0	0.0	283.3	282.6	282.6	265.2
468.9	468.9	469.4	469.4	468.1	468.1	0.0	0.0	0.0	269.6
468.9	468.9	469.4	472.6	504.3	504.3	0.0	0.0	0.0	272.2
468.9	468.9	469.4	481.0	598.7	598.7	0.0	0.0	0.0	272.6
551.3	551.2	479.5	469.5						